

Stabilizer ground states: theory, algorithms and applications

Jiace Sun,¹ Lixue Cheng,^{1,2} and Shi-Xin Zhang³

¹*Division of Chemistry and Chemical Engineering,
California Institute of Technology, Pasadena, CA 91125, USA*^{*}

²*Microsoft Research AI4Science Lab, Berlin 10178, Germany*

³*Tencent Quantum Laboratory, Shenzhen 518057, China*

Stabilizer states have been commonly utilized in quantum information, quantum error correction, and quantum circuit simulation due to their simple mathematical structure. In this work, we apply stabilizer states to tackle quantum many-body problems and introduce the concept of stabilizer ground states. We establish an equivalence formalism for identifying stabilizer ground states of general Pauli Hamiltonians. Moreover, we also develop an exact and linear-scaled algorithm to obtain stabilizer ground states of 1D local Hamiltonians and thus free from discrete optimization. This proposed equivalence formalism and linear-scaled algorithm are not only applicable to finite-size systems, but also adaptable to infinite periodic systems. The scalability and efficiency of the algorithms are numerically benchmarked on different Hamiltonians. Finally, we demonstrate that stabilizer ground states are promising tools for not only qualitative understanding of quantum systems, but also cornerstones of more advanced quantum state ansatzes on both classical and quantum computers.

I. INTRODUCTION

Discovering the ground state of quantum Hamiltonians represents one of the significant quests in the domain of quantum many-body physics. However, the reality stands that exact computations of ground states are impractical in most cases due to the exponential growth of the Hilbert space dimension [1–6]. An arguably most commonly used approach is to construct a parameterized quantum state ansatz $|\psi(\theta)\rangle$ and employ the Rayleigh-Ritz principle [7] to approximate the ground state by minimizing the expectation energy $\langle\psi(\theta)|H|\psi(\theta)\rangle$, which can be evaluated on classical computers or quantum computers, and the latter is also known as variational quantum eigensolver (VQE) [8–10]. Various powerful variational ansatzes have been developed for both classical computers and quantum computers, including tensor network states [11–13], neural network quantum states (NQS) [14–19], and unitary coupled cluster (UCC) ansatz [20–22].

Despite these advancements, it is also desirable to construct ansatzes with simple structures, such as the well-known mean-field state [23, 24]. Mean-field states are widely used for not only qualitative analysis [25, 26] but also serving as the starting point of other advanced ansatzes. For example, the UCC ansatz builds on the mean-field ground state (also referred to as the Hartree-Fock state) [27, 28] with additional parameterized excitations $e^{\sum_i \theta_i (T_i - T_i^\dagger)}$, where each T_i is an excitation operator. Such mean-field ground state is also used similarly in many other ansatzes for classical simulations [29–31]. Nevertheless, mean-field states are oversimplified, and might not even be qualitatively correct for many systems, including topological systems [32, 33] and multireference systems [34, 35]. Therefore, ansatzes with both mathematical simplicity and physical expressivity are highly demanded.

During the development of quantum computing [36, 37] in recent decades, a new type of states called stabilizer states has gained significant attention. From one perspective, it is the set of quantum states “stabilized” by a maximum number of Pauli operators, which implies a polynomial-sized classical description [38, 39]. From another perspective, it is the set of quantum states reachable solely by Clifford operations, i.e., the combination of CNOT, Hadamard, and phase gates, which are the “easy-to-implement” gates in the fault-tolerant quantum computation (FTQC) era [40–42]. Compared with product states, stabilizer states are able to not only capture long-range area-law entanglement that is significant for understanding topological order and symmetry-protected topological states [43], but also support volume-law entanglement [44], which is a feature lacking in other ansatzes, such as matrix product states (MPS) [45]. Thanks to these features, Clifford operations and stabilizer states are utilized as important tools in the explorations of quantum information [46, 47], quantum dynamics [48–50], quantum error correction [51, 52], topological quantum computing [53], quantum circuit simulation [54–56], and quantum-classical hybrid algorithms [57–61].

With the polynomial-sized classical description and efficient implementation on quantum computers, stabilizer states naturally become a promising alternative to the mean-field states, facilitating the construction of more expressive

^{*} jsun3@caltech.edu.

quantum state ansatzes without complicating the energy evaluations. For example, stabilizer states have been used as initial states in VQE for enhanced accuracy. [57, 62, 63] However, the challenge lies in the absence of scalable and general algorithms for identifying the appropriate stabilizer state, typically the one with the minimum energy for a given Hamiltonian, which is defined as the stabilizer ground state in this work. Although several optimization-based methods have been proposed [62, 64], they are not guaranteed to reach the real minimum and are not scalable to large systems due to the intrinsic difficulty of discrete optimization and the $O(2^{(n+1)(n+2)/2})$ scaling of the number of n -qubit stabilizer states [65].

In this work, we provide a series of algorithms to identify the stabilizer ground state of different types of Hamiltonians. We start by theoretically establishing the equivalence between the stabilizer ground states and the closed maximum-commuting Pauli subsets (CMCS) for general Pauli Hamiltonians. We further present an exact and linear-scaled algorithm to find the stabilizer ground states of 1D local Hamiltonians. For properly defined sparse Hamiltonians, this exact 1D local algorithm is proved to be computationally efficient with a scaling of $O(n \exp(Ck \log k))$ with some constant C , where n is the number of qubits and k represents the locality. Additionally, we prove that stabilizer ground states of 1D local Hamiltonians can be prepared on quantum computers with fewer operations than general stabilizer states. Furthermore, we present that both the equivalence formalism for general Hamiltonians and the linear-scaled algorithm for 1D local Hamiltonians can be extended to infinite periodic systems. By numerical benchmarking on different systems with classical and quantum algorithms, we reveal that stabilizer ground states are promising tools for both qualitative understanding of quantum systems and serving as the starting point or initial states of advanced quantum state ansatzes on classical and quantum computers. We envision stabilizer ground states and the corresponding algorithms as a pivotal foundation for a wide range of interesting applications, and highlight the collective power of the theories, algorithms, and applications to advance the field of quantum physics.

This paper is organized as follows: We first introduce the notations and mathematical backgrounds of stabilizer states in Sec. II A. The equivalence between the stabilizer ground state and CMCS for general Hamiltonians is derived in Sec. II B, and the exact linear-scaled algorithm for the stabilizer ground states of 1D local Hamiltonians is further presented in Sec. II C. Sec. II D extends both the equivalence formalism for general Hamiltonians and the algorithm for 1D local Hamiltonians to infinite periodic systems. In Sec. II E, we discuss the advantages and potential applications of stabilizer ground states to both classical and quantum algorithms, along with a comparison with other approximated ground states. Secs. III A and III B benchmark the exact 1D local algorithm on example Hamiltonians by numerically verifying the computational scaling and comparing the performances with numerically optimized stabilizer ground states, respectively. In Sec. III C, we demonstrate the ability of stabilizer ground states to qualitatively describe topological systems. The power of stabilizer ground states as the cornerstone of advanced quantum state ansatzes is shown in Sec. III D and Sec. III E for classical algorithms and quantum algorithms, respectively. Finally, we draw conclusions and outline future directions for the development and applications of stabilizer ground states in Sec. IV.

II. THEORY

A. Notations and mathematical background of stabilizer groups

We first revisit the definitions and a few frequently used properties of Pauli operators and stabilizer groups [36, 51].

Let $\mathcal{P}_n = \pm\{I, X, Y, Z\}^{\otimes n}$ represent the set of Hermitian n -qubit Pauli operators. It is important to clarify that \mathcal{P}_n itself is not a group since \mathcal{P}_n does not include anti-Hermitian operators. For any two elements $P_i, P_j \in \mathcal{P}_n$, P_i and P_j either commute or anticommute. A Pauli operator Q commutes with a set of Pauli operators $\mathbf{P} = \{P_i\}$, denoted as $[Q, \mathbf{P}] = 0$, if $[Q, P] = 0$ for each $P \in \mathbf{P}$. We denote it as $[Q, \mathbf{P}] \neq 0$ if Q anticommutes with any $P \in \mathbf{P}$.

A stabilizer group \mathbf{S} is a subset of \mathcal{P}_n that forms a group and satisfies $-I \notin \mathbf{S}$. Any two elements P, Q in \mathbf{S} commute with each other, otherwise $PQPQ = -I$ violates the definition. $\langle \mathbf{P} \rangle = \langle P_1, \dots, P_l \rangle = \{\prod_{Q \in \mathbf{Q}} Q \mid \mathbf{Q} \subseteq \mathbf{P}\}$ is the stabilizer group generated by a set of Pauli operators $\mathbf{P} = \{P_{i=1}^l\}$, if $\langle \mathbf{P} \rangle$ satisfies the definition of stabilizer group. We say \mathbf{P} is a set of generators of the stabilizer group \mathbf{S} when $\mathbf{S} = \langle \mathbf{P} \rangle$. An n -qubit stabilizer group \mathbf{S} has at most n independent generators $\mathbf{g} = \{g_i\}$ and 2^n elements. If $|\mathbf{g}| = n$, \mathbf{S} is a full stabilizer group and we have either $P \in \mathbf{S}$ or $-P \in \mathbf{S}$ (denoted as $P \in \pm \mathbf{S}$) for any $[P, \mathbf{S}] = 0$, $P \in \mathcal{P}_n$.

We say state $|\psi\rangle$ is stabilized by $P \in \mathcal{P}_n$ if $P|\psi\rangle = |\psi\rangle$. We define the stabilizer group of a given $|\psi\rangle$ as $\text{Stab}(|\psi\rangle) = \{P \mid P|\psi\rangle = |\psi\rangle\}$, and $|\psi\rangle$ is a stabilizer state when $\text{Stab}(|\psi\rangle)$ is a full stabilizer group. The mapping $|\psi\rangle \rightarrow \text{Stab}(|\psi\rangle)$ from stabilizer states to full stabilizer groups is a one-to-one correspondence.

B. Stabilizer ground states of general Hamiltonians

In this section, we establish the equivalence between the stabilizer ground state and the closed maximally-commuting Pauli subset. Furthermore, we show that, for properly defined sparse Hamiltonian (which includes almost all common Hamiltonians), such equivalence implies a much cheaper algorithm to get the stabilizer state compared with the brute-force approach. We first define the stabilizer ground state of Hamiltonian H :

Definition 1. (*Stabilizer ground state*) The **stabilizer ground state** of a given Hamiltonian H is the stabilizer state $|\psi\rangle$ with the lowest energy expectation $\langle\psi|H|\psi\rangle$.

The number of n -qubit stabilizer states is $\mathcal{S}(n) = 2^n \prod_{i=1}^n (2^i + 1) \sim 2^{\frac{1}{2}(n+1)(n+2)}$, thus looping over all the stabilizer states is infeasible for large n [65]. To find the stabilizer ground state, Lemma 1 is first presented to determine the expectation value of a Pauli operator in a stabilizer state:

Lemma 1. (*Expectation values of stabilizer states*) For any n -qubit stabilizer state $|\psi\rangle$ and Pauli operator $P \in \mathcal{P}_n$, if $P \notin \pm \text{Stab}(|\psi\rangle)$, then $\langle\psi|P|\psi\rangle = 0$

Proof. Since $\text{Stab}(|\psi\rangle)$ is a full stabilizer group, there exists $Q \in \text{Stab}(|\psi\rangle)$ such that $\{P, Q\} = 0$. Thus

$$\langle\psi|P|\psi\rangle = \langle\psi|PQ|\psi\rangle = -\langle\psi|QP|\psi\rangle = -\langle\psi|P|\psi\rangle. \quad (1)$$

Therefore, $\langle\psi|P|\psi\rangle = 0$. \square

We further extend the concept of energy expectation associated with a stabilizer state to a (not necessarily full) stabilizer group:

Definition 2. (*Stabilizer group energies*) The energy of a stabilizer group \mathbf{S} for a given Pauli operator P or a Pauli Hamiltonian $H = \sum_{P \in \mathbf{P}} w_P P$ is defined by

$$E_{\text{stab}}(P, \mathbf{S}) = \begin{cases} \pm 1 & P \in \pm \mathbf{S} \\ 0 & \text{otherwise} \end{cases}, \quad (2)$$

$$E_{\text{stab}}(H, \mathbf{S}) = \sum_{P \in \mathbf{P}} w_P E_{\text{stab}}(P, \mathbf{S}).$$

The relationship of stabilizer state energies and stabilizer group energies can be given by:

Corollary 1. (*Stabilizer state energies are stabilizer group energies*) We denote $\tilde{\mathbf{P}} = \pm \mathbf{P} = \{\pm P | P \in \mathbf{P}\}$ for a set of Pauli operators \mathbf{P} . For a Hamiltonian $H = \sum_{P \in \mathbf{P}} w_P P$ and a stabilizer state $|\psi\rangle$, let stabilizer group $\mathbf{S} = \langle \text{Stab}(|\psi\rangle) \cap \tilde{\mathbf{P}} \rangle$, we have $\langle\psi|H|\psi\rangle = E_{\text{stab}}(H, \mathbf{S})$.

Corollary 1 implies that, the energy of a stabilizer state $|\psi\rangle$ depends only on $\text{Stab}(|\psi\rangle) \cap \tilde{\mathbf{P}} \subseteq \tilde{\mathbf{P}}$. Since the number of subsets of $\tilde{\mathbf{P}}$ is much less than $\mathcal{S}(n) \sim 2^{\frac{1}{2}(n+1)(n+2)}$ when $\tilde{\mathbf{P}}$ is sparse (see Definition 4 for rigorous definition), it gives a better way to determine the stabilizer ground state. Rigorously, we introduce the concept of closed commuting subsets as follows:

Definition 3. (*CCS*) We define the **closed commuting subsets** (CCS) induced by \mathbf{P} (or H) as

$$\mathcal{S}(\mathbf{P}) = \{\mathbf{Q} \subseteq \tilde{\mathbf{P}} | \mathbf{Q} = \langle \mathbf{Q} \rangle \cap \tilde{\mathbf{P}}, -I \notin \langle \mathbf{Q} \rangle\} \quad (3)$$

We note that $-I \notin \langle \mathbf{Q} \rangle$ implicitly indicates that $\langle \mathbf{Q} \rangle$ is a stabilizer group.

Physically $\mathbf{Q} = \langle \mathbf{Q} \rangle \cap \tilde{\mathbf{P}}$ is saying that, $\langle \mathbf{Q} \rangle$ is generated by elements in $\tilde{\mathbf{P}}$. The name ‘‘closed’’ means that \mathbf{Q} is closed under group multiplication operations within the range of $\tilde{\mathbf{P}}$. Thus $\{\langle \mathbf{Q} \rangle | \mathbf{Q} \in \mathcal{S}(\mathbf{P})\}$ is the full set of stabilizer groups generated by elements in $\tilde{\mathbf{P}}$, and $\mathcal{S}(\mathbf{P})$ is an equivalent approach to represent with the generators in $\tilde{\mathbf{P}}$ instead. (knowing either \mathbf{Q} or $\langle \mathbf{Q} \rangle$ immediately gives the other) As an example, we consider $\mathbf{P} = \{+Z_1, +Z_2, -X_1X_2\}$, then $\tilde{\mathbf{P}} = \{\pm Z_1, \pm Z_2, \pm X_1X_2\}$. Then $\mathcal{S}(\mathbf{P})$ includes $\emptyset, \{sZ_1\}, \{sZ_2\}, \{s_1Z_1, s_2Z_2\}, \{sX_1X_2\}$, where each s can be ± 1 independently. We now present Theorem 1, which states that the stabilizer ground state can be obtained by searching for $\mathbf{Q} \in \mathcal{S}(\mathbf{P})$ with the lowest $E_{\text{stab}}(H, \langle \mathbf{Q} \rangle)$. The proof is given in the Appendix V A.

Theorem 1. (*CMCS gives the stabilizer ground state*) Given a Hamiltonian $H = \sum_{P \in \mathbf{P}} w_P P$, then

$$E_{gs} = \min_{\mathbf{Q} \in \mathcal{S}(\mathbf{P})} E_{stab}(H, \langle \mathbf{Q} \rangle) \quad (4)$$

is the stabilizer ground state energy. Such \mathbf{Q} minimizes $E_{stab}(H, \langle \mathbf{Q} \rangle)$ is named as the **closed maximally-commuting subset** (CMCS) of $\tilde{\mathbf{P}}$ (or H). Additionally, for any $\mathbf{S} = \langle \mathbf{Q} \rangle$, $\mathbf{Q} \in \mathcal{S}(\mathbf{P})$ such that $E_{stab}(H, \mathbf{S}) = E_{gs}$, each stabilizer state $|\psi\rangle$ stabilized by \mathbf{S} is a (degenerate) stabilizer ground state.

Theorem 1 suggests that the stabilizer ground state of a Hamiltonian $H = \sum_{P \in \mathbf{P}} w_P P$ can be found by listing all elements of $\mathcal{S}(\mathbf{P})$, and thus the computational cost is scaled with $|\mathcal{S}(\mathbf{P})|$. However, the exact value of $|\mathcal{S}(\mathbf{P})|$ heavily depends on the form of the Hamiltonian, e.g. the commutation/anticommutation relations between the Pauli terms. We give a loose upper bound of $|\mathcal{S}(\mathbf{P})|$ as follows:

Lemma 2. (*Upper bound of CCS*) If \mathbf{P} is defined on at most n qubits, then $|\mathcal{S}(\mathbf{P})| \leq (n+1)|\tilde{\mathbf{P}}|^n$.

Proof. For any $\mathbf{Q} \in \mathcal{S}(\mathbf{P})$, $\langle \mathbf{Q} \rangle$ is constructed by at most n independent generators in $\tilde{\mathbf{P}}$. We simply select each generator one by one, each with at most $|\tilde{\mathbf{P}}|$ choices. Thus, we have $|\mathcal{S}(\mathbf{P})| \leq \sum_{l=0}^n |\tilde{\mathbf{P}}|^l \leq (n+1)|\tilde{\mathbf{P}}|^n$. \square

In fact, we will see that if $|\mathbf{P}|$ scales polynomial with n , $|\mathcal{S}(\mathbf{P})|$ will have a slower growing rate than the number of n -qubit stabilizer states $\mathcal{S}(n)$. Therefore we define the sparse Hamiltonians as follows:

Definition 4. (*Sparse Hamiltonians*) A n -qubit Pauli Hamiltonian $H = \sum_{P \in \mathbf{P}} w_P P$ is **sparse** if $|\mathbf{P}| \sim O(\text{poly}(n))$.

We note that almost all the common Hamiltonians are sparse Hamiltonians. Now we estimate $|\mathcal{S}(\mathbf{P})|$ of sparse Hamiltonians:

Corollary 2. (*Upper bound of CCS for sparse Hamiltonians*) For sparse Hamiltonians $H = \sum_{P \in \mathbf{P}} w_P P$, $|\mathcal{S}(\mathbf{P})| \sim \exp(Cn \log n)$ for some constant C .

For sparse Hamiltonians, although $|\mathcal{S}(\mathbf{P})|$ still increases exponentially with n , it is much smaller than the number of n -qubit stabilizer states $\mathcal{S}(n) \sim 2^{\frac{1}{2}(n+1)(n+2)}$. In fact, $|\mathcal{S}(\mathbf{P})| \sim \exp(Cn \log n)$ is also related to the computational scaling of the following algorithm for 1D local Hamiltonians.

C. Stabilizer ground states of 1D local Hamiltonians

In this section, we present an algorithm to determine the stabilizer ground state of a given n -qubit 1D local Hamiltonian with a $O(n)$ computational scaling. We refer to this algorithm as the **exact 1D local algorithm**. To illustrate the motivation of this algorithm, we first consider the constrained 1D classical Hamiltonians in Sec. II C 1 and introduce a state machine algorithm with a linear scaling to obtain the exact ground state. Then we build an exact mapping from the 1D local stabilizer ground state problem to the constrained 1D classical ground state problem in Sec. II C 2. We formally present the exact 1D local algorithm for stabilizer ground states in Secs. II C 3 and II C 4, and its computational complexity is discussed in Sec. II C 5.

1. A classical analogy: State machine algorithm for the constrained 1D classical ground state problem

We first consider a general 1D n -site, k -local classical Hamiltonian without constraints on a chain $\{\sigma_1, \dots, \sigma_n\}$ as:

$$H = \sum_{m=1}^n h_m(\sigma_m, \sigma_{m+1}, \dots, \sigma_{m+k-1}), \quad (5)$$

where each σ_i is a discrete variable which can take d distinct values, and h_i is an arbitrary discrete function. Here k -local means that each term acts on at most k continuous sites. The ground state of such Hamiltonian can be exactly determined by the following state machine algorithm with a computational complexity of $O(nd^{k+1})$. We introduce $s_m = (\sigma_m, \sigma_{m+1}, \dots, \sigma_{m+k-1})$, which combines k degree of freedoms (DOFs) as a single DOF with d^k possible values. The Hamiltonian can be written as the following 1-local form

$$H = \sum_{m=1}^n h_m(s_m), \quad (6)$$

with a disadvantage that different s_i are dependent. In other words, the coupling is transferred from the Hamiltonian to the valid state space. A key step in this algorithm is that, for a fixed s_m , the possible values of $\mathbf{s}_{\leq m} = \{s_1, \dots, s_m\}$ are now decoupled from $\mathbf{s}_{>m} = \{s_{m+1}, \dots, s_n\}$, i.e.,

$$\{\mathbf{s}|s_m\} = \{\mathbf{s}_{\leq m}|s_m\} \otimes \{\mathbf{s}_{>m}|s_m\} \quad (7)$$

where $\mathbf{s} = \{s_1, \dots, s_n\}$. This independence is because there is no overlap between $\mathbf{s}_{\leq m}$ and $\mathbf{s}_{>m}$ over $\{\sigma_i\}$ beyond $s_m = (\sigma_m, \sigma_{m+1}, \dots, \sigma_{m+k-1})$. We define the energy on $\mathbf{s}_{\leq m}$ as

$$E(\mathbf{s}_{\leq m}) = \sum_{i=1}^m h_i(s_i) \quad (8)$$

and the “conditioned ground state energy” $E_{\text{gs}}^{\leq m}(s_m)$ as

$$E_{\text{gs}}^{\leq m}(s_m) = \min_{\mathbf{s}'_{\leq m} \in \{\mathbf{s}_{\leq m}|s_m\}} E(\mathbf{s}'_{\leq m}). \quad (9)$$

One can similarly define $E_{\text{gs}}^{>m}(s_m)$ as well. Eq. (7) implies that the ground state can be found by solving the conditioned ground state energies $E_{\text{gs}}^{\leq m}(s_m)$ and $E_{\text{gs}}^{>m}(s_m)$ independently for each possible s_m and taking the minimum value of $E_{\text{gs}}^{\leq m}(s_m) + E_{\text{gs}}^{>m}(s_m)$ over all possible s_m . This reduces the computational complexity from $O(d^n)$ to $O(d^{n/2+k})$ by choosing $m \sim n/2$. One can recursively apply the same treatment to both parts of the chain in a divide and conquer fashion and finally reduce the computational cost to $O(d^{k \log n}) = O(n^{k \log d})$.

To further reduce the complexity to $O(nd^{k+1})$, which is the ideal complexity for this state machine algorithm, we need to make an analogy of $\{s_1, \dots, s_n\}$ to a non-probabilistic version of the Markov chain, since Eq. (7) implies that the past ($\mathbf{s}_{\leq m}$) and future ($\mathbf{s}_{>m}$) are independent given the present (s_m). In addition, $E_{\text{gs}}^{\leq m}(s_m)$, as a function defined on the “non-probabilistic Markov chain” s_m , has the property that, for given values of $E_{\text{gs}}^{\leq m}(s_m)$ for all s_m , $E_{\text{gs}}^{\leq m+1}(s_{m+1})$ for each s_{m+1} can be determined within $O(d^{k+1})$ time. This conclusion is proved by first noticing that

$$\begin{aligned} \{\mathbf{s}_{\leq m}|s_{m+1}\} &= \cup_{s_m} \{\mathbf{s}_{\leq m}|s_{m+1}, s_m\} \\ &= \cup_{s_m \in \{s'_m|s_{m+1}\}} \{\mathbf{s}_{\leq m}|s_m\} \\ &:= \cup_{s_m \in F_{\text{back}}(s_{m+1})} \{\mathbf{s}_{\leq m}|s_m\}. \end{aligned} \quad (10)$$

In the first line, all possible values of s_m are looped over to determine $\mathbf{s}_{\leq m}$. The shared sites $\sigma_{m+1}, \dots, \sigma_{m+k-1}$ in both s_{m+1} and s_m must have the same values, and this constraint is denoted as $s_m \in \{s'_m|s_{m+1}\}$ in the second line. If this constraint holds, we have $\{\mathbf{s}_{\leq m}|s_{m+1}, s_m\} = \{\mathbf{s}_{\leq m}|s_m\}$ due to the decoupling between $\mathbf{s}_{\leq m}$ and s_{m+1} for given s_m (see Eq. (7)). We also introduce a shorthand $F_{\text{back}}(s_{m+1})$ for $\{s'_m|s_{m+1}\}$ in the last line. For instance, the 2-local spin Hamiltonian, i.e., $k = 2$, $s_m = (\sigma_m, \sigma_{m+1})$, and $\sigma_i \in \{\uparrow, \downarrow\}$, has $F_{\text{back}}(\sigma_{m+1}, \sigma_{m+2}) = \{(\sigma_m, \sigma_{m+1})|\sigma_m \in \{\uparrow, \downarrow\}\}$. From Eq. (10), the recurrence relation between $E_{\text{gs}}^{\leq m}(s_m)$ and $E_{\text{gs}}^{\leq m+1}(s_{m+1})$ can be derived as

$$\begin{aligned} E_{\text{gs}}^{\leq m+1}(s_{m+1}) &= \min_{\mathbf{s}'_{\leq m+1} \in \{\mathbf{s}_{\leq m+1}|s_{m+1}\}} E(\mathbf{s}'_{\leq m+1}) \\ &= h_{m+1}(s_{m+1}) + \min_{\mathbf{s}'_{\leq m} \in \{\mathbf{s}_{\leq m}|s_{m+1}\}} E(\mathbf{s}'_{\leq m}) \\ &= h_{m+1}(s_{m+1}) + \min_{s_m \in F_{\text{back}}(s_{m+1})} E_{\text{gs}}^{\leq m}(s_m). \end{aligned} \quad (11)$$

For the above 2-local spin Hamiltonian example, Eq. (11) is equivalent to

$$E_{\text{gs}}^{\leq m+1}(\sigma_{m+1}, \sigma_{m+2}) = h_{m+1}(\sigma_{m+1}, \sigma_{m+2}) + \min_{\sigma_m \in \{\uparrow, \downarrow\}} E_{\text{gs}}^{\leq m}(\sigma_m, \sigma_{m+1}). \quad (12)$$

Thus, to obtain the ground state energy, we can sequentially build tables T_m for $m = 1, 2, \dots, n$ by Eq. (11) to record the values of $E_{\text{gs}}^{\leq m}(s_m)$ over all s_m , with the initial table T_1 as $E_{\text{gs}}^{\leq 1}(s_1) = h_1(s_1)$. The final ground state energy is expressed as

$$E_{\text{gs}} = \min_{s_n} E_{\text{gs}}^{\leq n}(s_n). \quad (13)$$

Since $F_{\text{back}}(s_{m+1})$ only has d elements (i.e. only σ_m can choose different values freely), and s_m has d^k choices, one can build T_{m+1} from T_m within $O(d^{k+1})$ time, so the final computational complexity is $O(nd^{k+1})$. The ground state \mathbf{s}^*

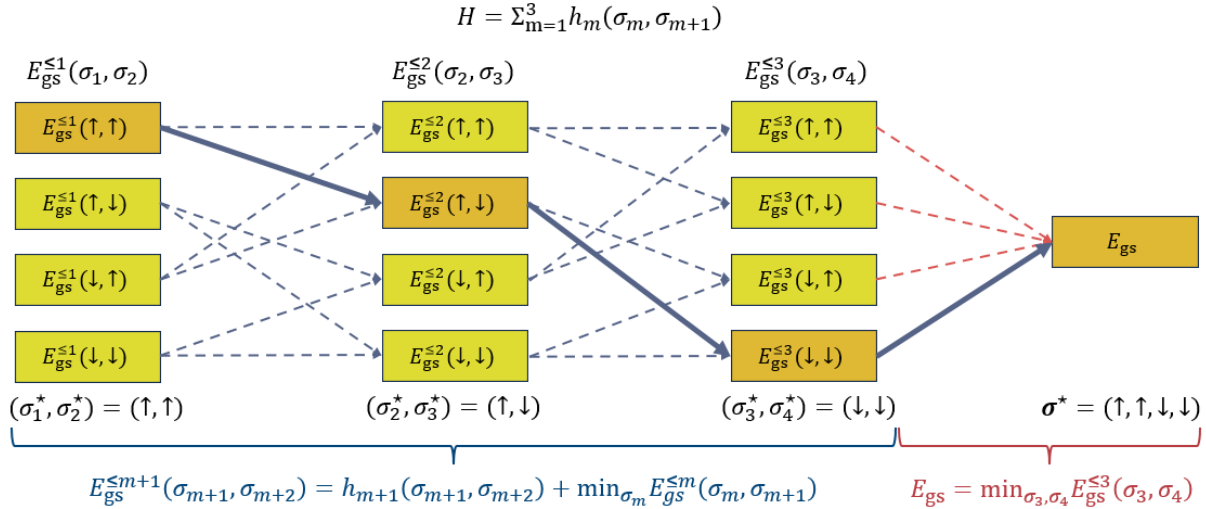


FIG. 1. State machine algorithm of the 1D local classical ground state problem illustrated by a 2-local spin Hamiltonian $H = \sum_{m=1}^3 h_m(\sigma_m, \sigma_{m+1})$. For illustration, we use σ instead of s everywhere. For each m we define the “conditioned ground state energy” $E_{\text{gs}}^{\leq m}(\sigma_m, \sigma_{m+1})$ (see Eq. (9)). $E_{\text{gs}}^{\leq 1}$ is simply h_1 , and $E_{\text{gs}}^{\leq m+1}$ can be determined from $E_{\text{gs}}^{\leq m}$ via Eq. 11. The final ground state is the minimum value of $E_{\text{gs}}^{\leq n}$ (see Eq. (13)). The ground state can be obtained by finding each $s_m = (\sigma_m, \sigma_{m+1})$ (orange blocks) that minimizes the RHS of Eq. (11) and Eq. (13).

(or σ^*) is achieved when each table T_m is built with $s_m = s_m^*$, where s_m^* minimizes the right hand side (RHS) of Eq. (11) ($m < n$) or Eq. (13) ($m = n$). A schematic workflow diagram of this algorithm using 2-local spin Hamiltonian example is shown in Fig. 1.

Although the constraints between s_m are local (s_m and $s_{m'}$ are independent if $|m - m'| \geq k$) in the above case, this approach also works for some special non-local constraints. An illustrative example is $H = \sum_{m=1}^n h_m(s_m)$, $s_m \in \{0, 1, \dots, d - 1\}$ with constraints $f_m(\sum_{i=1}^m s_i) \geq 0$ and $g_m(\sum_{i=m+1}^n s_i) \geq 0$ for each m , where the summation $\sum_{i=1}^m s_i$ and $\sum_{i=m+1}^n s_i$ are modulo d . We introduce a state machine

$$A_m = (s_m, \alpha_m = \sum_{i=1}^m s_i, \beta_m = \sum_{i=m+1}^n s_i), \quad (14)$$

which is a function of $s = \{s_1, \dots, s_n\}$. With a fixed $A_m = (s_m, \alpha_m, \beta_m)$, the constraints f_l and g_l with $l \leq m$ can be rewritten as

$$\begin{aligned} f_l\left(\sum_{i=1}^l s_i\right) &= f_l(\alpha_m - \tau_l(s_{\leq m})) \geq 0 \\ g_l\left(\sum_{i=l+1}^n s_i\right) &= g_l(\beta_m + \tau_l(s_{\leq m})) \geq 0, \end{aligned} \quad (15)$$

where $\tau_l(s_{\leq m}) = \sum_{i=l+1}^m s_i$. This implies that these two constraints act only on $s_{\leq m}$. Similarly, the constraints of $l > m$ act only on $s_{>m}$. Therefore, $s_{\leq m}$ and $s_{>m}$ are again decoupled given A_m , i.e.,

$$\{s|A_m\} = \{s_{\leq m}|A_m\} \otimes \{s_{>m}|A_m\}. \quad (16)$$

For a given A_m , $s_{\leq m}$ fully determines each $A_{l \leq m}$ as $A_l = (s_l, \alpha_m - \tau_l(s_{\leq m}), \beta_m + \tau_l(s_{\leq m}))$, and $s_{>m}$ similarly determines each $A_{l > m}$. Thus we conclude

$$\{A_1, \dots, A_n|A_m\} = \{A_1, \dots, A_m|A_m\} \otimes \{A_{m+1}, \dots, A_n|A_m\}, \quad (17)$$

which is a generalized form of Eq. (7). In fact, Eq. (7) can be viewed as a special case of Eq. (17) when $A_m = s_m$. Since A_m contains the information of s_m , we can rewrite $h_m(s_m)$ as $h'_m(A_m)$. To use the previous algorithm, we introduce a transition function

$$\begin{aligned} F(A_m) &= \{A_{m+1}|A_m\} \\ &= \{(s_{m+1}, \alpha_{m+1} = \alpha_m + s_{m+1}, \beta_{m+1} = \beta_m - s_{m+1})|f_{m+1}(\alpha_{m+1}) \geq 0, g_{m+1}(\beta_{m+1}) \geq 0\}, \end{aligned} \quad (18)$$

and thus $F_{\text{back}}(A_m) = \{A_{m-1} | A_m \in F(A_{m-1})\}$. We can then similarly define the “conditioned ground state energy” $E_{\text{gs}}^{\leq m}(A_m)$ and recursively construct the values for $m = 1, 2, \dots, n$ to determine the ground state. For this specific problem, A_m has d^3 choices, and $F(A_m)$ has d elements, so the computational complexity to obtain the ground state is $O(nd^4)$.

We further generalize the above solution of constrained 1D classical ground state problems. Without loss of generality, the input Hamiltonian can be assumed as 1-local since a k -local problem can always be rewritten as a 1-local problem. The key is to construct a state machine A_m that satisfies Eq. (17). Once we constructed such A_m , the ground state could be obtained by recursively building tables T_m that record each $E_{\text{gs}}^{\leq m}(A_m)$. Now we rigorously define a state machine as follows:

Definition 5. (State machine) Consider a classical system with single-site states s_1, \dots, s_n , where each of them can take some discrete values $s_i \in d_i$. The valid space \mathbf{D} is a subset of the full space $d_1 \otimes d_2 \otimes \dots \otimes d_n$ due to some constraints. A_m defined on \mathbf{D} is a **state machine** if (1) A_m contains information of s_m , i.e. there exists a **state function** $G(A_m(\mathbf{s})) = s_m$ for any $\mathbf{s} \in \mathbf{D}$, and (2) given A_m , the possible values of the left state machines A_1, \dots, A_m and the possible values of right state machines A_{m+1}, \dots, A_n are independent, i.e.

$$\{A_1, \dots, A_n | A_m\} = \{A_1, \dots, A_m | A_m\} \otimes \{A_{m+1}, \dots, A_n | A_m\}. \quad (19)$$

The corresponding **transition function** is defined as

$$F(A_m) = \{A_{m+1} | A_m\} \quad (20)$$

$$:= \{A_{m+1}(\mathbf{s}) | A_m(\mathbf{s}) = A_m, \mathbf{s} \in \mathbf{D}\}, \quad (21)$$

where the second line is a rigorous definition of $\{A_{m+1} | A_m\}$. The definitions of other expressions like $\{\dots | \dots\}$ are similar.

As mentioned previously, it can be understood as a non-probabilistic version of the Markov chain. We additionally require the existence of the state function G so that we could write $h_m(s_m)$ as $h_m(G(A_m))$ in the Hamiltonian. Now the above state machine algorithm of the constrained classical ground state problem can be generalized in the following theorem, and a schematic workflow is shown in Fig. 2.

Theorem 2. (State machine algorithm of the constrained classical ground state problem) If A_m is a state machine on $\mathbf{s} \in \mathbf{D}$ with the state function G and transition function F , then the ground state of Hamiltonian $H = \sum_{m=1}^n h_m(s_m)$ can be determined by

1. Construct $\mathcal{A}_1 = \{A_1(\mathbf{s}) | \mathbf{s} \in \mathbf{D}\}$ and $E_{\text{gs}}^{\leq 1}(A_1) = h_1(G(A_1))$ for all $A_1 \in \mathcal{A}_1$.
2. From $m = 1$ to $n - 1$, create $\mathcal{A}_{m+1} = \cup_{A_m \in \mathcal{A}_m} F(A_m)$ and

$$E_{\text{gs}}^{\leq m+1}(A_{m+1} \in \mathcal{A}_{m+1}) = h_{m+1}(G(A_{m+1})) + \min_{A_m \in F_{\text{back}}(A_{m+1})} E_{\text{gs}}^{\leq m}(A_m), \quad (22)$$

where $F_{\text{back}}(A_{m+1}) = \{A_m | A_{m+1} \in F(A_m)\}$.

3. The ground state energy is

$$E_{\text{gs}} = \min_{A_n \in \mathcal{A}_n} E_{\text{gs}}^{\leq n}(A_n). \quad (23)$$

4. To obtain the ground state \mathbf{s}^* , we find $\{A_1^*, \dots, A_n^*\}$ by

$$\begin{aligned} A_n^* &= \arg \min_{A_n \in \mathcal{A}_n} E_{\text{gs}}^{\leq n}(A_n), \\ A_m^* &= \arg \min_{A_m \in F_{\text{back}}(A_{m+1}^*)} E_{\text{gs}}^{\leq m}(A_m) \end{aligned} \quad (24)$$

for $m = 1, 2, \dots, n - 1$. Then the components of \mathbf{s}^* is $s_m^* = G(A_m^*)$ for $m = 1, 2, \dots, n$.

Proof. The Hamiltonian can be rewritten as $H = \sum_{m=1}^n h_m(G(A_m))$, thus the all derivations in the first k -local classical ground state problem still hold with all s_m changed to A_m . \square

We additionally note that, the algorithm in Theorem 2 is not automatically linearly-scaled, unless we can ensure that the evaluations of transition function F and the initial \mathcal{A}_1 can be done in a constant time.

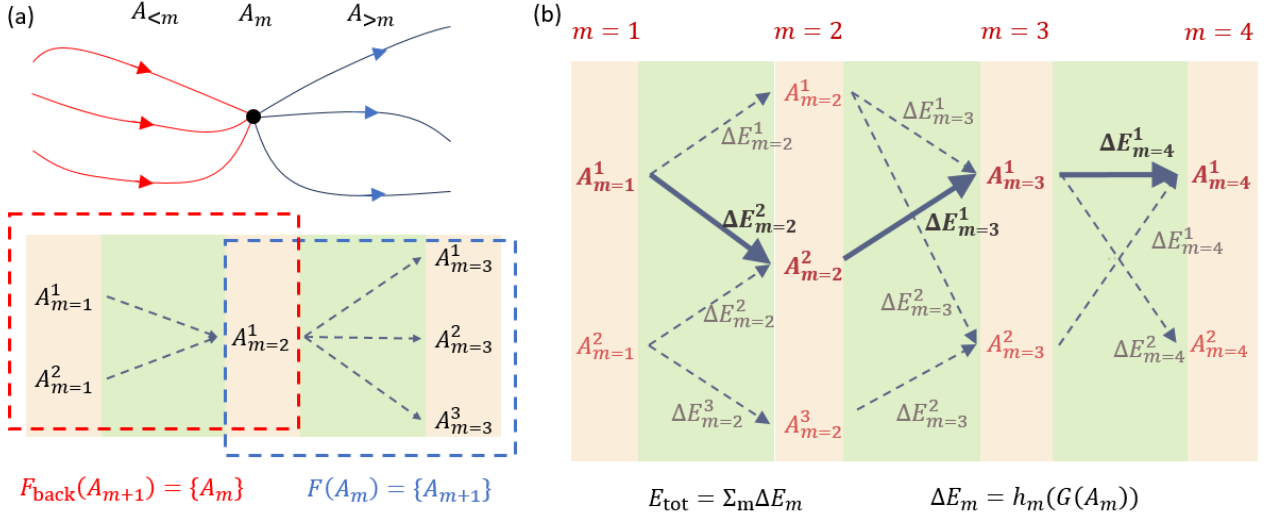


FIG. 2. (a) Schematic diagram of the state machine and transition function defined in Definition 5. Given A_m , the possible paths of $A_{<m} = \{A_1, \dots, A_{m-1}\}$ should be decoupled from the possible paths of $A_{>m} = \{A_{m+1}, \dots, A_n\}$. The transition function $F(A_m)$ gives the possible values of A_{m+1} given A_m , and $F_{\text{back}}(A_{m+1})$ gives the possible values of A_m given A_{m+1} . (b) Schematic diagram of the state machine algorithm in Theorem 2 to obtain the ground state of constrained 1D local classical Hamiltonians. The Hamiltonian is given by $H = \sum_{m=1}^n h_m(s_m)$ in some constrained space \mathbf{D} . Given a state machine A_m and transition function F satisfying Definition 5, we start from $A_1 \in \mathcal{A}_1$, and sequentially determine the possible values of $A_{m+1} \in F(A_m)$ for each A_m . (lines connecting A_m and A_{m+1} indicates that $A_{m+1} \in F(A_m)$) In this process, each A_m can generate multiple A_{m+1} , and each A_{m+1} can be generated from multiple A_m . The energy difference $\Delta E_m = h_m(G(A_m))$ is a function of A_m , where G is the state functions satisfying $G(A_m) = s_m$. By such construction, each path $\{A_1, \dots, A_n\}$ such that $A_{m+1} \in F(A_m)$, $m = 1, \dots, n-1$ uniquely maps a valid state $s \in \mathbf{D}$ via $s_m = G(A_m)$. To determine the ground state, we record the value of $E_{\text{gs}}^{\leq m}(A_m)$ for each A_m in a table starting from $E_{\text{gs}}^{\leq 1}(A_1) = h_1(A_1)$. Once we record all values of $E_{\text{gs}}^{\leq m}(A_m)$, the values of $E_{\text{gs}}^{\leq m+1}(A_{m+1})$ can be determined from Eq. (22). The final ground state is simply $E_{\text{gs}} = \min_{A_n} (E_{\text{gs}}^{\leq n}(A_n))$, and the ground state is the corresponding path $\{s_1^*, \dots, s_n^*\}$ (bold lines) such that each minimization in Eq. (22) and Eq. 23 is taken at $s_m = s_m^*$.

2. Mapping the stabilizer ground state problem to the constrained classical ground state problem

In this subsection, we show that the 1D local stabilizer ground state problem can be rigorously mapped to the constrained classical ground state problem considered in Sec. II C 1. we first define the 1D k -local Hamiltonian as follows:

Definition 6. (k-local Hamiltonians) A Hamiltonian $H = \sum_{P \in \mathbf{P}} w_P P$ is k -local if each $P \in \mathbf{P}$ is between qubit q_P^{first} to q_P^{last} that satisfies $q_P^{\text{last}} - q_P^{\text{first}} \leq k - 1$.

In the context of stabilizer ground states, we need to find suitable states with equivalent identities as s . According to Definition 5 and Theorem 2, the stabilizer ground state energy can be found via $E_{\text{gs}} = \min_{\mathbf{Q} \in \mathcal{S}(\mathbf{P})} E_{\text{stab}}(H, \langle \mathbf{Q} \rangle)$. In other words, $\mathcal{S}(\mathbf{P}) = \{\mathbf{Q} \subseteq \tilde{\mathbf{P}} | \mathbf{Q} = \langle \mathbf{Q} \rangle \cap \tilde{\mathbf{P}}, -I \notin \langle \mathbf{Q} \rangle\}$ serves as the state space \mathbf{D} , and each $\mathbf{Q} \in \mathcal{S}(\mathbf{P})$ is a state s . We find the equivalent identity of single-site states s_m as follows. We divide $\tilde{\mathbf{P}}$ onto sites m by the last non-identity qubit q_P^{last} for any $P \in \tilde{\mathbf{P}}$, and define $\tilde{\mathbf{P}}_I = \{P \in \tilde{\mathbf{P}} | q_P^{\text{last}} \in I\}$ for a given index set I . For index sets $\{m\}$, $\{i | a \leq i \leq b\}$, $\{i | i > m\}$, $\{i | i \geq m\}$, $\{i | i < m\}$, and $\{i | i \leq m\}$, we use shorthands $\tilde{\mathbf{P}}_m$, $\tilde{\mathbf{P}}_{a,b}$, $\tilde{\mathbf{P}}_{>m}$, $\tilde{\mathbf{P}}_{\geq m}$, $\tilde{\mathbf{P}}_{<m}$, and $\tilde{\mathbf{P}}_{\leq m}$, respectively. For example, $\tilde{\mathbf{P}}_{\leq m} = \{P \in \tilde{\mathbf{P}} | q_P^{\text{last}} \leq m\}$. According to the definition, we have $\tilde{\mathbf{P}} = \cup_{m=1}^n \tilde{\mathbf{P}}_m$. We also introduce similar shorthands for \mathbf{P}_I . Since $\mathbf{Q} \in \mathcal{S}(\mathbf{P})$ is a subset of $\tilde{\mathbf{P}}$, we have $\mathbf{Q} = \cup_{m=1}^n \mathbf{Q}_m$ with $\mathbf{Q}_m = \mathbf{Q} \cap \tilde{\mathbf{P}}_m$, and \mathbf{Q}_m is the equivalent identity of single-site states s_m . The constraint $\mathbf{Q} \in \mathcal{S}(\mathbf{P})$ is the equivalent relation of $s \in \mathbf{D}$. To give an example of the constraint, we consider $\mathbf{P} = \{Z_1, Z_2, Z_1 Z_2\}$, and correspondingly $\mathbf{P}_1 = \{Z_1\}$, $\mathbf{P}_2 = \{Z_2, Z_1 Z_2\}$. If $Z_1 \in \mathbf{Q}$ and $Z_2 \in \mathbf{Q}$ we must have $Z_1 Z_2 \in \mathbf{Q}$ as well, so $\mathbf{Q}_1 = \{Z_1\}$ and $\mathbf{Q}_2 = \{Z_2\}$ cannot hold simultaneously, although either of them can be taken if the other one is empty. Finally, the stabilizer

energy $E_{\text{stab}}(H, \langle \mathbf{Q} \rangle)$ for any $\mathbf{Q} \in \mathcal{S}(\mathbf{P})$ can also be written as the sum of local \mathbf{Q}_m :

$$\begin{aligned} E_{\text{stab}}(H, \langle \mathbf{Q} \rangle) &= \sum_{P \in \langle \mathbf{Q} \rangle \cap \mathbf{P}} w_P - \sum_{P \in \langle \mathbf{Q} \rangle \cap (-\mathbf{P})} w_{-P} \\ &= \sum_m \left(\sum_{Q \in \mathbf{Q}_m \cap \mathbf{P}_m} w_Q - \sum_{Q \in \mathbf{Q}_m \cap (-\mathbf{P}_m)} w_{-Q} \right) \\ &:= \sum_m h_m(\mathbf{Q}_m) \end{aligned} \quad (25)$$

In summary, the mapping from the 1D local stabilizer ground state problem to the 1D local constrained classical ground state problem is:

1. $\mathbf{Q}_m \rightarrow s_m$
2. $\{\mathbf{Q}_m | \mathbf{Q}_m \subseteq \tilde{\mathbf{P}}_m\} \rightarrow \mathbf{d}_m$
3. $\mathcal{S}(\mathbf{P}) \rightarrow \mathbf{D}$
4. $\mathbf{Q} \in \mathcal{S}(\mathbf{P}) \rightarrow \mathbf{s} \in \mathbf{D}$
5. $h_m(\mathbf{Q}_m) \rightarrow h_m(s_m)$

3. Construction of state machine A_m

In the previous section, we have already mapped the 1D local stabilizer ground state problem to a constrained classical ground state problem. Once we construct the state machine satisfying Definition 5, we can obtain the ground state by Theorem 2. We first introduce the projection operation as follow:

Definition 7. (Projection) We denote $\mathcal{P}_I = \pm\{I_i, X_i, Y_i, Z_i\}^{\otimes_{i \in I}}$, where i indicates the qubit index, and I stands for some index set. The **projection** of a set of Pauli operators \mathbf{P} to qubits I is $\mathbb{P}_I(\mathbf{P}) = \mathbf{P} \cap \mathcal{P}_I$. The notations of the index set I are the same with $\tilde{\mathbf{P}}_I$ in Sec. II C 2.

It is important to note that, if \mathbf{S} is a stabilizer group, $\mathcal{P}_I(\mathbf{S})$ is also a stabilizer group. Following the definition of state machine in Definition 5 and the mapping in Sec. II C 2, we hope to construct A_m on $\mathbf{Q} \in \mathcal{S}(\mathbf{P})$ satisfying Eq. (19). In the second example of Sec. II C 1, we first constructed A_m satisfying Eq. (16). In Appendix V B, we prove that Eq. (16) is a necessary condition of Eq. (19). According to the mapping $\mathbf{s} \rightarrow \mathbf{Q}$, Eq. (16) is

$$\{\mathbf{Q}|A_m\} = \{\mathbf{Q}_{\leq m}|A_m\} \otimes \{\mathbf{Q}_{>m}|A_m\}, \quad (26)$$

i.e., given A_m , $\mathbf{Q}_{\leq m}$ and $\mathbf{Q}_{>m}$ are decoupled. In Appendix V C, we derive

$$A_m(\mathbf{Q}) = (\mathbf{S}_{\text{proj}}^m(\mathbf{Q}_{\leq m}), \tilde{\mathbf{P}}_{\text{invalid}}^m(\mathbf{Q}_{\leq m}), \mathbf{S}_{\text{right}}^m(\mathbf{Q}_{\geq m})) \quad (27)$$

that satisfies Eq. (16) and further Eq. (19), where

$$\tilde{\mathbf{P}}_{\text{invalid}}^m(\mathbf{Q}_{\leq m}) = \{P \in \tilde{\mathbf{P}}_{>m} | [P, \mathbf{Q}_{\leq m}] \neq 0\}, \quad (28)$$

$$\mathbf{S}_{\text{proj}}^m(\mathbf{Q}_{\leq m}) = \mathbb{P}_{>m-k}(\langle \mathbf{Q}_{\leq m} \rangle), \quad (29)$$

$$\mathbf{S}_{\text{right}}^m(\mathbf{Q}_{\geq m}) = \mathbb{P}_{\leq m}(\langle \mathbf{Q}_{\geq m} \rangle). \quad (30)$$

A physical illustration is that, the coupling between $\mathbf{Q}_{\leq m}$ and $\mathbf{Q}_{>m}$ comes from (1) $[\mathbf{Q}_{>m}, \mathbf{Q}_{\leq m}] = 0$ since elements of a stabilizer group commute, and (2) group multiplication operations between $\mathbf{Q}_{\leq m}$ and $\mathbf{Q}_{>m}$ does not generate new elements in either $\tilde{\mathbf{P}}_{>m}$ and $\tilde{\mathbf{P}}_{\leq m}$. Given $A_m = (\mathbf{S}_{\text{proj}}^m, \tilde{\mathbf{P}}_{\text{invalid}}^m, \mathbf{S}_{\text{right}}^m)$, (1) is equivalent to $\tilde{\mathbf{P}}_{\text{invalid}}^m(\mathbf{Q}_{\leq m}) = \tilde{\mathbf{P}}_{\text{invalid}}^m$, and (2) is equivalent to $\mathbf{S}_{\text{proj}}^m(\mathbf{Q}_{\leq m}) = \mathbf{S}_{\text{proj}}^m$ (for the $\tilde{\mathbf{P}}_{>m}$ part) and $\mathbf{S}_{\text{right}}^m(\mathbf{Q}_{\geq m}) = \mathbf{S}_{\text{right}}^m$ (for the $\tilde{\mathbf{P}}_{\leq m}$ part), respectively. Thus, $\mathbf{Q}_{\leq m}$ and $\mathbf{Q}_{>m}$ are now decoupled.

Finally, by noticing

$$\mathbf{S}_{\text{right}}^m(\mathbf{Q}_{\geq m}) \cap \tilde{\mathbf{P}}_m = \mathbb{P}_{\leq m}(\langle \mathbf{Q}_{\geq m} \rangle) \cap \tilde{\mathbf{P}}_m = \mathbf{Q}_m, \quad (31)$$

the state function G is

$$G(A_m = (\mathbf{S}_{\text{proj}}^m, \tilde{\mathbf{P}}_{\text{invalid}}^m, \mathbf{S}_{\text{right}}^m)) = \mathbf{S}_{\text{right}}^m \cap \tilde{\mathbf{P}}_m. \quad (32)$$

Therefore, the state machine for the 1D local stabilizer ground state problem is

Corollary 3. (State machine of the 1D local stabilizer ground state problem) A_m defined in Eq. (27) is a state machine of the state space $\mathcal{S}(\mathbf{P})$. The state function G is given in Eq. (32).

4. Construction of transition function F

After defining the state machine in Corollary 3, we need to further derive the transition function $F(A_m) = \{A_{m+1}(\mathbf{Q})|A_m = A_m(\mathbf{Q}), \mathbf{Q} \in \mathcal{S}(\mathbf{P})\}$ in order to use Theorem 2. A naive strategy is looping over all $\mathbf{Q} \in \mathcal{S}(\mathbf{P})$ and calculating each $A_m(\mathbf{Q})$ and $A_{m+1}(\mathbf{Q})$, however its computational complexity is still exponential. Our strategy is introduced as follows with a linear complexity. We first notice that both $\mathbf{S}_{\text{proj}}^{m+1}$ and $\tilde{\mathbf{P}}_{\text{invalid}}^{m+1}$ can be obtained from A_m and $\mathbf{S}_{\text{right}}^{m+1}$ as:

$$\mathbf{S}_{\text{proj}}^{m+1}(\mathbf{S}_{\text{proj}}^m, \mathbf{Q}_{m+1}) = \langle \mathbb{P}_{>m-k+1}(\mathbf{S}_{\text{proj}}^m(\mathbf{Q}_{\leq m})), \mathbf{Q}_{m+1} \rangle, \quad (33)$$

$$\tilde{\mathbf{P}}_{\text{invalid}}^{m+1}(\tilde{\mathbf{P}}_{\text{invalid}}^m, \mathbf{Q}_{m+1}) = \{P \in \tilde{\mathbf{P}}_{\geq m+1}^m | P \in \tilde{\mathbf{P}}_{\text{invalid}}^m(\mathbf{Q}_{\leq m}) \text{ or } [P, \mathbf{Q}_{m+1}] \neq 0\}, \quad (34)$$

where $\mathbf{Q}_{m+1} = \mathbf{S}_{\text{right}}^{m+1} \cap \tilde{\mathbf{P}}_{m+1}$ is determined by $\mathbf{S}_{\text{right}}^{m+1}$. The derivations can be found in Appendix V C. For given A_m and $\mathbf{S}_{\text{right}}^{m+1}$, A_{m+1} is determined via Eq. (33) and Eq. (34), and we denote it as

$$A_{m+1} = A_{m+1}(A_m, \mathbf{S}_{\text{right}}^{m+1}). \quad (35)$$

This suggests that, to obtain the transition function $F(A_m)$, we need to determine all possible $\mathbf{S}_{\text{right}}^{m+1}$ given A_m :

$$\mathcal{S}_{\text{right}}^{m+1}(A_m) = \{\mathbf{S}_{\text{right}}^{m+1}|A_m\} \equiv \{\mathbf{S}_{\text{right}}^{m+1}(\mathbf{Q})|A_m = A_m(\mathbf{Q}), \mathbf{Q} \in \mathcal{S}(\mathbf{P})\}. \quad (36)$$

Thus, the transition function $F(A_m)$ can be written as

$$F(A_m) = \{A_{m+1}(A_m, \mathbf{S}_{\text{right}}^{m+1})|\mathbf{S}_{\text{right}}^{m+1} \in \mathcal{S}_{\text{right}}^{m+1}(A_m)\}. \quad (37)$$

However, the exact computation of $\mathcal{S}_{\text{right}}^{m+1}(A_m)$ is still exponentially scaled. A solution to this issue is proposed by relaxing the definition of state machines and transition functions as follows:

Definition 8. (Relaxed state machine and transition function) Let A_m be a state machine defined on \mathbf{D} with transition function F , and $\mathcal{A}_m = \{A_m(\mathbf{s})|\mathbf{s} \in \mathbf{D}\}$. For an enlarged space $\tilde{\mathcal{A}}_m \supseteq \mathcal{A}_m$, we say $A_m \in \tilde{\mathcal{A}}_m$ is a **relaxed state machine**, and $\tilde{F}(A_m \in \tilde{\mathcal{A}}_m)$ is a **relaxed transition function** if

1. $\tilde{F}(A_m \in \mathcal{A}_m) \cap \mathcal{A}_{m+1} = F(A_m)$, i.e. \tilde{F} behaves the same with F in the “valid region” \mathcal{A}_m .
2. $\tilde{F}(A_m \in (\tilde{\mathcal{A}}_m - \mathcal{A}_m)) \subseteq \tilde{\mathcal{A}}_{m+1} - \mathcal{A}_{m+1}$, i.e. if $A_{m+1} \in \tilde{\mathcal{A}}_{m+1}$, then $A_m \in \tilde{\mathcal{A}}_m$

According to this definition, once some path $\{A_1, A_2, \dots\}$ enters into the “invalid region” at some A_m , i.e., $A_m \in \tilde{\mathcal{A}}_m - \mathcal{A}_m$, all the following $\{A_{m+1}, \dots\}$ will stay in the invalid region and the path could even be early terminated at step $t < n$ when $\tilde{F}(A_t) = \emptyset$. To assure each full path $\{A_1, \dots, A_n\}$ always staying in the valid region, the condition of $\tilde{\mathcal{A}}_n - \mathcal{A}_n = \emptyset$ is additionally required. With this additional condition, the replacement of F to the relaxed definitions, \tilde{F} , in Theorem 2 should still result in the ground state. We refer to this replaced algorithm as the relaxed state machine algorithm, whose schematic diagram is shown in Fig. 3.

Corollary 4. (Relaxed state machine algorithm of constrained 1D local classical ground state) Following the notations in Definition 8, we replace F by \tilde{F} and replace the initial \mathcal{A}_1 by some $\tilde{\mathcal{A}}_1 \supseteq \mathcal{A}_1$ in Theorem 2, and generate $\tilde{\mathcal{A}}_m$, $m = 1, 2, \dots, n$ with the same procedure. If we additionally have $\tilde{\mathcal{A}}_n = \mathcal{A}_n$, then the modified algorithm still gives the correct ground state.

We now revisit the stabilizer ground state problem, where an enlarged space $\tilde{\mathcal{S}}_{\text{right}}^{m+1}(A_m) \supseteq \mathcal{S}_{\text{right}}^{m+1}(A_m)$ needs to be created. By implying $\tilde{\mathcal{A}}_m \supseteq \mathcal{A}_m$ for each m , the corresponding construction (Eq. (38)) automatically satisfies first condition of Definition 8.

$$\tilde{F}(A_m) = \{A_{m+1}(A_m, \mathbf{S}_{\text{right}}^{m+1})|\mathbf{S}_{\text{right}}^{m+1} \in \tilde{\mathcal{S}}_{\text{right}}^{m+1}(A_m)\}. \quad (38)$$

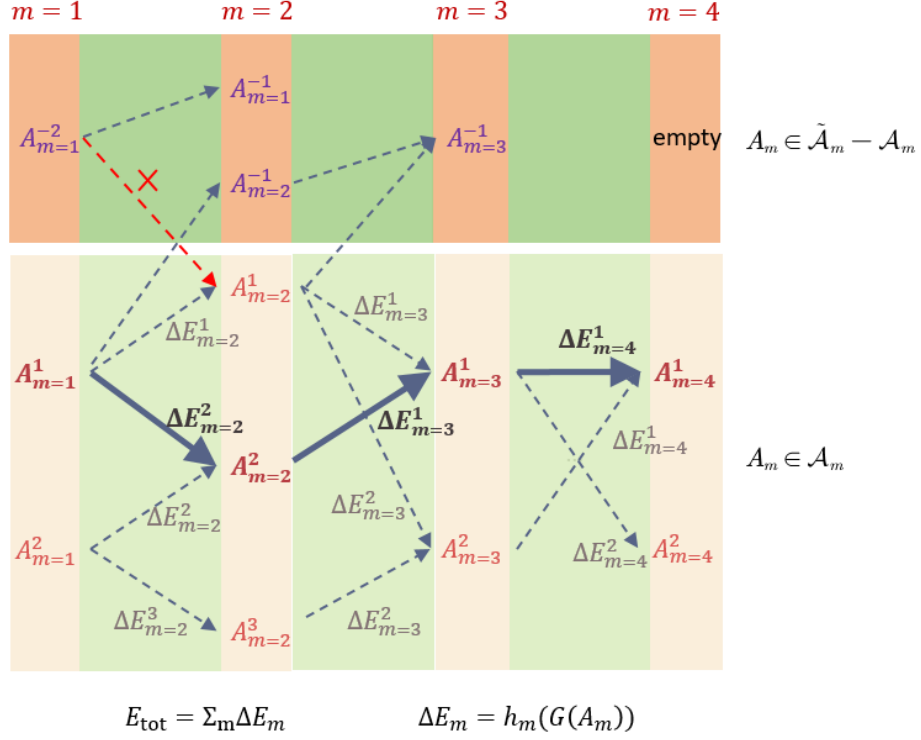


FIG. 3. Schematic diagram of the relaxed state machine algorithm to obtain the ground state of constrained 1D local classical Hamiltonians in Corollary 4. Given a relaxed state machine A_m and a relaxed transition function \tilde{F} defined in Definition 8, the full space of the relaxed state machine \tilde{A}_m is divided to a valid part \mathcal{A}_m and a non-valid part $\tilde{\mathcal{A}}_m - \mathcal{A}_m$. \tilde{F} can connect $A_m \in \tilde{\mathcal{A}}_m$ with $A_{m+1} \in \tilde{\mathcal{A}}_{m+1}$, $A_m \in \tilde{\mathcal{A}}_m$ with $A_{m+1} \notin \tilde{\mathcal{A}}_{m+1}$, $A_m \notin \mathcal{A}_m$ with $A_{m+1} \notin \tilde{\mathcal{A}}_{m+1}$, but not $A_m \notin \tilde{\mathcal{A}}_m$ with $A_{m+1} \in \tilde{\mathcal{A}}_{m+1}$ (red dashed line with a “ \times ” sign). In the valid part \mathcal{A}_m , the behavior of \tilde{F} should be the same as the original transition function F . (the bottom part is the same as Fig. 2. If there’s no invalid state machine at $m = n$, i.e. $\tilde{\mathcal{A}}_m = \mathcal{A}_m$, then the ground state can be obtained by the same approach in Theorem 2 with the relaxed transition function \tilde{F} . (once the path A_1, A_2, \dots enters into the top part is never reaches $m = n$ so does not affect the result) With the mapping of the stabilizer ground problem to the constrained classical ground state problem in Sec. II C 2, and the constructed relaxed state machine A_m , relaxed transition function \tilde{F} , and state function G , one can obtain the stabilizer ground state of 1D local Hamiltonians with a linear scaling. (See Corollary 6)

In Appendix V D, we show that the second condition of Definition 8 can be achieved if each $S_{\text{right}}^{m+1} \in \tilde{\mathcal{S}}_{\text{right}}^{m+1}(A_m)$ satisfies

$$\begin{aligned}
 -I &\notin \langle \mathbf{Q}_{m+1} \rangle, \\
 \mathbf{Q}_{m+1} \cap \tilde{\mathbf{P}}_{\text{invalid}}^m(\mathbf{Q}_{\leq m}) &= \emptyset, \\
 \langle \mathbb{P}_{\leq m}(S_{\text{right}}^{m+1}), \mathbf{Q}_m \rangle &= S_{\text{right}}^m, \\
 S_{\text{proj}}^{m+1} \cap S_{\text{right}}^{m+1} &= \mathbf{Q}_{m+1},
 \end{aligned} \tag{39}$$

where we used $\mathbf{Q}_m = S_{\text{right}}^m \cap \mathbf{P}_m$, $\mathbf{Q}_{m+1} = S_{\text{right}}^{m+1} \cap \mathbf{P}_{m+1}$, and $S_{\text{proj}}^{m+1} = S_{\text{proj}}^{m+1}(S_{\text{proj}}^m, \mathbf{Q}_{m+1})$ defined in Eq. (33). Thus, $\tilde{\mathcal{S}}_{\text{right}}^{m+1}(A_m)$ could be constructed by looping over all stabilizer groups between qubit $m - k + 2$ and $m + 1$, and keeping only the terms satisfying Eq. (39). However, this approach has a non-ideal upper bound $|\tilde{\mathcal{S}}_{\text{right}}^m| \leq \mathcal{S}(k) \sim 2^{\frac{1}{2}(k+1)(k+2)}$. We note that if \tilde{F} on $\tilde{\mathcal{A}}_m \supseteq \mathcal{A}_m$ is a relaxed transition function, \tilde{F} on any $\tilde{\mathcal{A}}'_m$ with $\tilde{\mathcal{A}}_m \supseteq \tilde{\mathcal{A}}'_m \supseteq \mathcal{A}_m$ is automatically a relaxed transition function (Fig. 3). Thanks to this fact, a better solution can be obtained with the truncation operation defined as follows:

Definition 9. (Truncation) Let $P \in \mathcal{P}_n$ be a Pauli operator, and $P = \pm p_1 \otimes p_2 \otimes \dots \otimes p_n$, where $p_i \in \{I_i, X_i, Y_i, Z_i\}$. The **truncation** of P to qubits I is $\mathbb{T}_I(P) = \otimes_{i \in I} p_i$. Similarly, the truncation of a set of Pauli operators \mathbf{P} is $\mathbb{T}_I(\mathbf{P}) = \{\mathbb{T}_I(P) | P \in \mathbf{P}\}$.

A tighter constraint is $\mathcal{S}_{\text{right}}^m(\mathbf{Q} \in \mathcal{S}(\mathbf{P})) \in \mathcal{T}_{\text{right}}^m$, where

$$\mathcal{T}_{\text{right}}^m = \{\langle \mathbf{Q} \rangle \mid \mathbf{Q} \in \mathcal{S}(\mathbb{T}_{\leq m}(\mathbf{P}_{\geq m}))\}, \quad (40)$$

which are stabilizer groups generated by elements in $\pm \mathbb{T}_{\leq m}(\mathbf{P}_{\geq m})$. For example, if a stabilizer group \mathbf{S} is generated by elements in $\mathbf{P} = \{X_1X_2, Z_1Z_2, Z_2\}$, $\mathbf{S}_1 = \mathbb{P}_1(\mathbf{S})$ is generated by elements in $\mathbb{T}_1(\mathbf{P}) = \{X_1, Z_1\}$. Note that the converse statement is not true, i.e. \mathbf{S}_1 generated by $\mathbb{T}_1(\mathbf{P})$ is not necessarily some $\mathbb{P}_1(\mathbf{S})$. Clearly the number of elements in $\mathbb{T}_{\leq m}(\mathbf{P}_{\geq m})$ is up to the number of elements in $\mathbf{P}_{m, m+k-1}$. This leads to a $O(\exp(Ck \log k))$ scaling for some constant C given the Hamiltonian is sparse, which will be shown in Theorem 3.

Finally, we define

$$\tilde{\mathcal{S}}_{\text{right}}^{m+1}(A_m) = \{\mathbf{S}_{\text{right}}^m \in \mathcal{T}_{\text{right}}^m \mid \mathbf{S}_{\text{right}}^m \text{ satisfies Eq. (39)}\}. \quad (41)$$

The corresponding relaxed transition function $\tilde{F}(A_m)$ is now given by

Corollary 5. (Relaxed transition function of the stabilizer ground state problem) $\tilde{F}(A_m)$ defined in Eq. (38) with $\tilde{\mathcal{S}}_{\text{right}}^{m+1}(A_m)$ defined in Eq. (41) is a relaxed transition function of the state machine A_m defined in Corollary 3.

The last component we missed is an approach to determine the initial values $\tilde{\mathcal{A}}_1$. A clever construction is $\tilde{\mathcal{A}}_1 = \cup_{A_0 \in \tilde{\mathcal{A}}_0} F(A_0)$ from $\tilde{\mathcal{A}}_0$ by adding an ancillary site 0 with $\mathbf{Q}_0 = \mathbf{P}_0 = \emptyset$. With this ancillary site, we can derive $\mathbf{S}_{\text{proj}}^0 = \mathbb{P}_{>-k}(\langle \mathbf{Q}_{\leq 0} \rangle) = \langle \emptyset \rangle$, $\tilde{\mathbf{P}}_{\text{invalid}}^0 = \{P \in \tilde{\mathbf{P}}_{>0} \mid [P, \mathbf{Q}_{\leq 0}] \neq 0\} = \emptyset$, $\mathbf{S}_{\text{right}}^0 = \mathbb{P}_{\leq 0}(\langle \mathbf{Q}_{\geq 0} \rangle) = \langle \emptyset \rangle$, and thus $\tilde{\mathcal{A}}_0 = \{A_0\}$, where $A_0 = (\langle \emptyset \rangle, \emptyset, \langle \emptyset \rangle)$. This naturally gives $\tilde{\mathcal{A}}_1 = \tilde{F}(A_0 = (\langle \emptyset \rangle, \emptyset, \langle \emptyset \rangle))$. According to Corollary 4, the final exact 1D local algorithm is given by:

Corollary 6. (Exact 1D local algorithm of the stabilizer ground state problem) With the state machine A_m , relaxed transition function \tilde{F} , and state function G defined in Corollary 3, Corollary 5 and Eq. (32), starting from $\tilde{\mathcal{A}}_1 = \tilde{F}(A_0 = (\langle \emptyset \rangle, \emptyset, \langle \emptyset \rangle))$, the stabilizer ground state of 1D local Hamiltonians can be determined by Corollary 4.

5. Computational complexity

We estimate the computational scaling of the exact 1D local algorithm, which is controlled by $|\tilde{\mathcal{A}}_m|$. For the similar reason mentioned in Sec. II B, it does not have a simple expression. A loose upper bound is provided in the following and its detailed proof is given in Appendix V E.

Theorem 3. (Upper bound of $|\tilde{\mathcal{A}}_m|$) Let $H = \sum_{P \in \mathbf{P}} w_P P$ be a k -local Hamiltonian, and there exists M such that $|\mathbf{P}_m| \leq M$ for each m . Then for any m , we can construct candidate values of A_m as $\tilde{\mathcal{A}}'_m \supseteq \tilde{\mathcal{A}}_m$ solely from $\mathbb{T}_{m-2k+1, m}(\tilde{\mathbf{P}})$, such that $|\tilde{\mathcal{A}}'_m| < N_A = (4kM)^{3k} = \exp(3k \log 4kM)$.

We rewrite $|\tilde{\mathcal{A}}_m| \sim O(\exp(Ck \log kM))$ for simplicity and further analysis. The total cost spent on each site m is bounded by the product of (1) $|\tilde{\mathcal{A}}_m|$, (2) $|\tilde{\mathcal{A}}_{m+1}|$, and (3) time to compute a single $A_{m+1} \in \tilde{\mathcal{A}}_{m+1}$ from a single $A_m \in \tilde{\mathcal{A}}_m$. Since all stabilizer state operations used in the algorithm can be realized in polynomial scaling of k , the total cost scales as

$$\begin{aligned} T &\sim n \times O(\exp(Ck \log kM)) \times O(\exp(Ck \log kM)) \times O(\text{poly}(k)) \\ &\sim O(n \exp(C'k \log kM)) \end{aligned}$$

for some constant C' . Similar to Definition 4, we consider the 1D local and sparse Hamiltonians defined as follows:

Definition 10. (local sparse Hamiltonians) For a 1D k -local Pauli Hamiltonian $H = \sum_{P \in \mathbf{P}} w_P P$, we say that it is sparse if $|\mathbf{P}_m| \sim O(\text{poly}(k))$.

The conclusions $T \sim O(n \exp(C'k \log kM))$ and $M \sim O(\text{poly}(k))$ lead to the final computation complexity as:

Corollary 7. (Computational complexity of the exact 1D local algorithm) The computational cost T to obtain the stabilizer ground state of a n -qubit, k -local sparse Hamiltonian is $T \sim O(n \exp(Ck \log k))$ for some constant C .

D. Stabilizer ground states of infinite periodic Hamiltonians

In this section, the stabilizer ground state problem of infinite periodic Hamiltonians (referred to as periodic Hamiltonians) is discussed. We will show that, for any 1D periodic local Hamiltonian, the stabilizer ground state also has periodic stabilizers in some supercells. We also show that, the stabilizer ground states of 1D periodic local Hamiltonians can be similarly obtained by the state machine solution in the exact 1D algorithm with an additional periodic boundary condition of state machines in a supercell. This algorithm is referred as the exact 1D periodic local algorithm. For general periodic Hamiltonians in higher dimensions, we conjecture that the stabilizer ground states should still have periodic stabilizers. With this assumption, the formalism in Sec. II B is extended to general periodic Hamiltonians.

We first review the properties of the eigenstates of periodic Hamiltonians on an infinitely long 1D lattice. Let T be an operator to translate a given $|\psi\rangle$ by some fixed number of sites, and H be a Hamiltonian satisfying $[H, T] = 0$. Bloch's theorem [66] states that the eigenstates $|\psi\rangle$ of H can be classified by the eigenvalue of T via $T|\psi\rangle = e^{i\phi}|\psi\rangle$ since H and T can be simultaneously diagonalized. In numerical treatments, a supercell with size L is usually introduced and ϕ can take discrete values $\phi = 2\pi\frac{j}{L}$ for integers $0 \leq j < L$ [67, 68].

Now we consider stabilizer states in the qubit space. Let T_l be the operator to translate qubit q to $q + l$ for any q . A Hamiltonian $H = \sum_{P \in \mathbf{P}} w_P P$ is defined to be invariant under T_l if $P' = T_l^\dagger P T_l$ satisfies $P' \in \mathbf{P}$ and $w_{P'} = w_P$ for any $P \in \mathbf{P}$. However, the stabilizer ground state $|\psi\rangle$ of H might not be an eigenstate of T_l , i.e., $T_l|\psi\rangle = \lambda|\psi\rangle$ for some λ . An example is $H = H_0 + \epsilon H_I$, where $H_0 = -\sum_n (X_{3n}X_{3n+1}X_{3n+2} + Z_{3n}Z_{3n+1}Z_{3n+2})$ and $H_I = -\sum_n (Z_{3n-1}X_{3n} + X_{3n-1}Z_{3n})$, and H thus has a period of 3. At $\epsilon = 0$, H can be divided into independent subsystems $\{3n, 3n+1, 3n+2\}$ for each n , and each subsystem has degenerate stabilizer ground states with stabilizers $X_{3n}X_{3n+1}X_{3n+2}$ and $Z_{3n}Z_{3n+1}Z_{3n+2}$, respectively. At $0 < \epsilon \ll 1$, the interaction term H_I breaks the degeneracy, and the stabilizers of the stabilizer ground state become alternating $X_{3n}X_{3n+1}X_{3n+2}$ and $Z_{3n}Z_{3n+1}Z_{3n+2}$. This system has a period of 6 and thus does not satisfy $T_{l=3}|\psi\rangle = \lambda|\psi\rangle$.

Now let us treat the infinite periodic Hamiltonians as n -qubit Hamiltonians with $n = \infty$. According to Sec. II C, we can efficiently determine the ground state by constructing the state machines $\{A_m\}$ from the relaxed transition function \tilde{F} , so we get an infinitely long state machine chain $\{A_{m=-\infty}^\infty\}$. We introduce an equivalence condition $A \simeq B$, if A and B differ only by translation of some cl lattices, where $c \in \mathbb{Z}$, e.g. $\langle Z_1, Z_2 \rangle \simeq \langle Z_7, Z_8 \rangle$ with $l = 3$. The following theorem presents that the state machine chain $\{A_{m=-\infty}^\infty\}$ corresponding to the stabilizer ground state is periodic with some period cl , $c \in \mathbb{Z}$. The proof is given in Appendix V F.

Theorem 4. (State machines of CMCS of infinitely periodic Hamiltonians are periodic) *Let $H = \sum_{P \in \mathbf{P}} w_P P$ be an infinitely periodic 1D local sparse Hamiltonian with period l , and $\mathbf{Q}^* \in \mathcal{S}(\mathbf{P})$ be the CMCS of H . Let $A_m = A_m(\mathbf{Q}^*)$, there exists some $c < N_A$ such that $A_{m+cl} \simeq A_m$ for any m , where N_A is given in Theorem 3. Furthermore, the stabilizer ground state energy per site is*

$$E_{gs}^{\text{periodic}} = \min_{c \leq N_A} \min_{\{A_m^{cl} \mid A_{i+1} \in \tilde{F}(A_i), A_0 \simeq A_{cl}\}} \frac{1}{cl} \sum_{m=1}^{cl} h_m(G(A_m)), \quad (42)$$

which involves a periodic boundary condition $A_0 \simeq A_{cl}$, and the boundary state machine must be one of the candidate values in Theorem 3.

For a fixed supercell size c and boundary state machine A_0 , one can perform the algorithm in Theorem 2 with an additional final state restriction of $A_{cl} \simeq A_0$ to obtain the chain $\{A_0, A_1, \dots, A_{cl}\}$ with the lowest energy. With additional loops over c and the boundary state machine A_0 , one can find the stabilizer ground state with a linear scaling of l . This algorithm is referred to as the **exact 1D periodic local algorithm**. Besides, Theorem 4 implies that the CMCS \mathbf{Q}^* is also periodic, and thus the stabilizer ground state $|\psi\rangle$ is also periodic, i.e. $T_{cl}|\psi\rangle = |\psi\rangle$.

We then move on to discuss higher-dimensional Hamiltonians. Although we are not able to theoretically prove that the stabilizer ground state $|\psi\rangle$ satisfies $T_{cl}|\psi\rangle = |\psi\rangle$ for translation operators T_{cl} in each dimension, we speculate that at least some approximated (if not exact) stabilizer ground state satisfies such condition due to its similarity to the supercell treatments of exact eigenstates.

With the assumption of $T_{cl}|\psi\rangle = |\psi\rangle$, we present the stabilizer ground state theory for general infinite periodic Hamiltonians. For any stabilizer P with $P|\psi\rangle = |\psi\rangle$, let $P' = T_{cl}^\dagger P T_{cl}$, we have $P'|\psi\rangle = |\psi\rangle$, and thus P' is also a stabilizer of $|\psi\rangle$. We only need to consider those $\mathbf{Q} \in \mathcal{S}(\mathbf{P})$ such that $\mathbf{Q} = T_{cl}^\dagger \mathbf{Q} T_{cl}$. (Roughly speaking, we only need to determine the stabilizers \mathbf{Q} in a single supercell and then copy it to others) Strictly, we define the **closed commuting periodic subsets** (CCPS) as

$$\mathcal{S}_c(\mathbf{P}) = \{\mathbf{Q} \subseteq \tilde{\mathbf{P}} \mid \mathbf{Q} = \langle \mathbf{Q} \rangle \cap \tilde{\mathbf{P}}, -I \notin \langle \mathbf{Q} \rangle, \mathbf{Q} = T_{cl}^\dagger \mathbf{Q} T_{cl}\}. \quad (43)$$

Since $[Q, T_{cl}^\dagger Q T_{cl}] = 0$ for any $Q \in \mathbf{Q}$, $\mathbf{Q} \in \mathcal{S}_c(\mathbf{P})$, a naïve but useful simplification of $\mathcal{S}_c(\mathbf{P})$ is

$$\mathcal{S}_c(\mathbf{P}) = \mathcal{S}_c(\mathbf{P}'), \quad (44)$$

where $\mathbf{P}' = \{P \in \mathbf{P} | [P, T_{cl}^\dagger P T_{cl}] = 0\}$. Consider the example $H = \sum_i Z_i X_{i+1}$ which has period $l = 1$. If the supercell size is $c = 1$, then according to $\{Z_i X_{i+1}, Z_{i+1} X_{i+2}\} = 0$, we have $\mathbf{P}' = \emptyset$ and thus $\mathcal{S}_{c=1}(\mathbf{P}) = \{\emptyset\}$. This indicates that $c = 1$ is not a good choice. If the supercell size is $c = 2$, we could, for example have $\mathbf{Q} = \{Z_{2i} X_{2i+1} | i \in \mathbb{Z}\}$. Finally, the stabilizer ground state is given by

$$E_{\text{gs}} = \min_{c, \mathbf{Q} \in \mathcal{S}_c(\mathbf{P})} E_{\text{stab}}(H, \langle \mathbf{Q} \rangle). \quad (45)$$

The $\mathbf{Q} \in \mathcal{S}_c(\mathbf{P})$ minimizing Eq. (45) is referred as the **closed maximally-commuting periodic subset** (CMCPS) of $\tilde{\mathbf{P}}$ (or H). For physically reasonable Hamiltonians, it might be enough to search for the minimum stabilizer ground state energy by checking a few small c .

E. Applications analysis of stabilizer ground states

In the following, we discuss the potential applications of the concept and algorithms of stabilizer ground states in simulating many-body physics problems from the aspects of both quantum and classical algorithms. The stabilizer ground states are also compared with other common ground states ansatzes, e.g. the mean-field state, and matrix product states (MPS). Since the concept of "mean-field" has different definitions in different situations, we only consider the product states, which is a typical example of mean-field states in the qubit space. However, a similar analysis also works for many other cases.

Stabilizer ground states could serve as good candidates for initial states in terms of quantum algorithms. Specifically, we consider two quantum algorithms for many-body ground state problems, i.e., the variational quantum eigensolver (VQE) [9, 10] and quantum phase estimation (QPE) [69, 70], which are the most widely studied algorithms in the noisy intermediate-scale quantum (NISQ) [71] and fault-tolerant quantum computation (FTQC) [72] era, respectively. For VQE, a notorious issue is the barren plateau problem [73–75], implying that the energy gradients with respect to the circuit parameters are exponentially small except in an exponentially small region, and such behavior resulting in the failure of classical optimizations [74]. Thus, starting from a physically valid state, such as an approximated ground state in the case of stabilizer ground state, serves as the easiest and the most straightforward solution to mitigate the barren plateau problem. In terms of the QPE algorithm, the output is a random eigenstate. Let the initial state be $|\psi\rangle_{\text{init}}$, the probability of getting each eigenstate $|\psi_k\rangle$ follows Born rule $|\langle\psi_{\text{init}}|\psi_k\rangle|^2$. For randomly chosen $|\psi_{\text{init}}\rangle$, $|\langle\psi_{\text{init}}|\psi_k\rangle|^2$ also decays exponentially with the system size [6]. Thus, an initial state having a large overlap with the exact ground state is also vital for the success of QPE. In summary, for both VQE and QPE, an initial state close to the ground state is desired, where stabilizer ground states and the corresponding efficient algorithms serve as good candidates.

One of the main advantages of the stabilizer states for initial states on quantum computers is its ability to be efficiently prepared on quantum circuits with up to $O(n^2 / \log n)$ single-qubit and double-qubit Clifford gates [39]. Such advantage is further magnified on fault-tolerant quantum computers, where the computational cost is dominated by non-Clifford operations via, e.g., magic state distillation [40]. Besides, we prove in the following that, the gate count number can be further reduced to $O(nk / \log k)$ for the preparation of stabilizer ground states of 1D k -local Hamiltonians (assuming the stabilizer ground state is not highly degenerate).

Theorem 5. (Decomposed Clifford transformations of local stabilizer groups) *Given a n -qubit stabilizer group \mathbf{S} , if there exists independent generators $\mathbf{P} = \{P_1, \dots, P_n\}$ (i.e. $\mathbf{S} = \langle \mathbf{P} \rangle$) that each P_i is k -local, then we can find up to $L \sim O(nk / \log k)$ single-qubit and double-qubit Clifford transformations U_1, \dots, U_L , such that the combined Clifford transformation $U = \prod_{i=1}^L U_i$ satisfies $U^\dagger \mathbf{S} U = \langle Z_1, Z_2, \dots, Z_n \rangle$. Furthermore, if there are up to s elements in $\{P_i\}$ that are not k -local, the above conclusion still holds with $L \sim O(nk' / \log k')$, where $k' = k + s$.*

Proof. See Appendix V G. The corresponding algorithm is given in Algorithm 1. \square

Corollary 8. (Quantum state preparation of stabilizer ground states of 1D local Hamiltonians) *Let $H = \sum_{P \in \mathbf{P}} w_P P$ be a n -qubit, k -local 1D local Hamiltonian, and the corresponding CMCS is $\mathbf{Q}^* \in \mathcal{S}(\mathbf{P})$. According to Theorem 1 the stabilizer ground states are those stabilizer states stabilized by $\langle \mathbf{Q}^* \rangle$. If $\langle \mathbf{Q}^* \rangle$ has $n - s$ independent generators, then each of the corresponding ground states can be prepared on quantum circuits with up to $L \sim O(nk' / \log k')$ single-qubit and double-qubit Clifford operations, where $k' = k + s$. Specifically, if the stabilizer ground state is non-degenerate, one needs $L \sim O(nk / \log k)$ operations.*

Proof. Since each $Q \in \mathbf{Q}^*$ is k -local, $\mathbf{S} = \langle \mathbf{Q}^* \rangle$ has $n - s$ k -local and independent generators, thus it meets the requirement of Theorem 5, and the conclusion applies. Since each (degenerate) stabilizer ground state satisfies $P|\psi\rangle = |\psi\rangle$ for $P \in \mathbf{S}$, we have $U^\dagger PU(U^\dagger|\psi\rangle) = (U^\dagger|\psi\rangle)$. Since $U^\dagger \mathbf{S}U = \langle Z_1, Z_2, \dots, Z_n \rangle$, we have $|\psi'\rangle = U^\dagger|\psi\rangle = |0\rangle^{\otimes n}$, or $|\psi\rangle = U|0\rangle^{\otimes n}$, i.e. $|\psi\rangle$ can be prepared by U , which contains L single and double-qubit Clifford operations. When and only when $s = 0$, the stabilizer ground state is unique, thus the non-degenerate stabilizer ground state implies $L \sim O(nk/\log k)$. \square

As a comparison, product states [76, 77] are effectively classical states (i.e., 0/1 string in the qubit case) with single-site rotations, and classical states are a subset of the stabilizer states without entanglements. By similarly applying single-site rotations to stabilizer states (which is further discussed in Sec. III D), product states are a subset of such extended stabilizer states. The relations between classical states, stabilizer states, product states, and extended stabilizer states are shown in Fig. 4. MPS is another powerful common ground state ansatz, while its power is limited to 1D local and gapped systems, in which case the ground state satisfies the area-law entanglement. It has also been shown that a n -site MPS with bond dimension χ can be prepared on quantum computers with n numbers of $(\log_2 \chi + 1)$ -qubit unitaries [44, 78]. Since m -qubit gate can be decomposed to $O(4^m)$ single-qubit and double-qubit gates [79], this gives a total number of $O(n\chi^2)$ single-qubit and double-qubit gates. This number is much larger than $O(nk/\log k)$, i.e. the gate count for the 1D local stabilizer ground states. In the worst case, MPS requires bond dimension $\chi = 2^k$ to describe a $(k + 1)$ -local stabilizer state, e.g. the rainbow state $|\psi\rangle = \sum_{i_1 \dots i_k} |i_1 \dots i_k i_1 \dots i_k\rangle$, which is essentially the product of k bell pairs on qubits $(i, k + i)$, $i = 1, \dots, k$. Additionally, the decomposed circuit of MPS is generally non-Clifford, which implies the situation is even worse in the FTQC era considering the large error correction overhead for T gates.

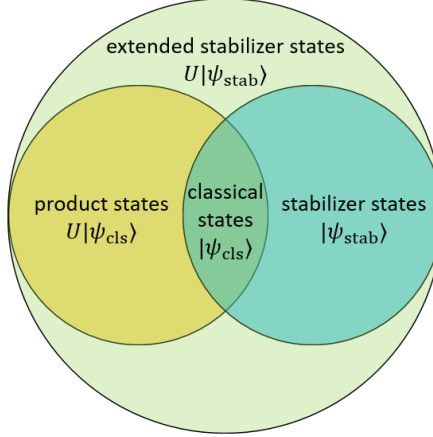


FIG. 4. Relations between classical states, stabilizer states, product states, and extended stabilizer states. Classical states $|\psi_{\text{cls}}\rangle$ are 0/1 bitstrings. The four states are the 2×2 combinations of the following two approaches to extending the classical states, i.e. (1) applying single-site rotations $U = \otimes_i R_i$, and (2) extending $|\psi_{\text{cls}}\rangle$ to stabilizer states $|\psi_{\text{stab}}\rangle$. It gives the product states, stabilizer states, or extended stabilizer states if we employ only the former one, only the latter one, or both, respectively.

Besides serving as initial states, stabilizer states are also closely related to the Clifford operations, which are commonly used to transform the Hamiltonians to improve classical/quantum algorithms [59, 61, 80] or reduce the entanglements of the Hamiltonians [60]. With the stabilizer ground states efficiently obtained from the algorithms introduced in this work, one can immediately find a Clifford operation U_C such that the stabilizer ground state of the transformed Hamiltonian $H' = U_C^\dagger H U_C$ is simply $|0\rangle^{\otimes n}$, indicating that the exact ground state of the transformed Hamiltonian might have small entanglements. The desired U_C can be easily obtained by solving $|\psi_{\text{stab}}\rangle = U_C|0\rangle^{\otimes n}$, which can be performed classically in polynomial time.

In terms of classical algorithms, we discuss two important types of methods, i.e. variational methods and perturbative methods. Variational-based methods approximate ground states by constructing parameterized quantum state ansatz $|\psi(\theta)\rangle$ and minimizing the energy expectation value. A necessary condition of such ansatzes is the ability to evaluate the expectation energy in a polynomial time either deterministically (e.g. MPS) or stochastically (e.g. variational quantum Monte Carlo), otherwise the numerical optimization is infeasible. Most of the current classical algorithms can be viewed as methods based on classical states basis, which support efficient computations of $\langle \psi' | H | \psi \rangle$ for a wide range of Hamiltonians. For example, product states are essentially classical states with single-site rotations; tensors of MPS are in the form of superpositions of classical states, i.e. $A_{ij}^\alpha |\alpha\rangle$, where α is the physical index; and i, j are bond indices, and the variational monte carlo (VMC) anastz can generally be written as $|\psi\rangle = \sum \psi_{i_1 \dots i_n}(\theta) |i_1 \dots i_n\rangle$, where

the coefficients $\psi_{i_1 \dots i_n}(\boldsymbol{\theta})$ are parameterized by some physically-inspired [81] or neural-network ansatz [82]. Similar to classical states, stabilizer states themselves might not be a good ground state ansatz in general. A related evidence is that there exist local Hamiltonians without any low-energy stabilizer states [83]. Nonetheless, since $\langle \psi' | H | \psi \rangle$ can be efficiently computed for stabilizer states and Pauli Hamiltonians, one can similarly construct ansatzes based on stabilizer states and stabilizer ground states. In Sec. III D, we introduced the extended stabilizer ground state as a direct extension of product states; a “stabilizer tensor network” method [84] is also recently proposed to construct MPS on top of the stabilizer basis; and the VMC ansatz can be similarly extended to the stabilizer basis with properly designed coefficient ansatzes, i.e. $|\psi\rangle = \sum_{\psi_{\text{stab}}} C(\psi_{\text{stab}}) |\psi_{\text{stab}}\rangle$, where the summation is over all or a subset of n -qubit stabilizer states. These numerical methods are more expressive than the original classical-state-based ansatzes (since classical states are a subset of stabilizer states), and might be especially suitable to capture strong entanglement or long-range entanglement due to the nature of stabilizer states.

We also consider the combination of perturbation methods and stabilizer states. Such methods require a division of the full Hamiltonian H into an exactly solvable part H_0 and the perturbative part H_1 , and the accuracy typically depends on the relative strength between H_0 and H_1 . As shown in Sec. II B, one can determine the stabilizer ground state by finding the CMCS \mathbf{Q}^* of $H = \sum_{P \in \mathbf{P}} w_P P$, which gives a natural choice of $H_0 = \sum_{P \in \mathbf{P} \cap \pm \mathbf{Q}^*} w_P P$, and the stabilizer ground state is exactly the ground state of H_0 . Thus, stabilizer ground state algorithms can also be used to determine the division of H_0 and H_1 . A related recent work is the doped stabilizer states [85], which utilizes the stabilizer nullity of the Hamiltonian for efficient simulation.

III. RESULTS

In this section, we first perform a few benchmarks on the exact 1D local algorithm, including the computational cost in Sec. III A and the comparison with numerically optimized approximated stabilizer ground states in Sec. III B. Furthermore, we demonstrate a few potential applications for stabilizer ground states and the corresponding algorithms on (1) simple qualitative analysis of phase transitions in Sec. III C, (2) serving as the cornerstone of developing advanced ground state ansatzes in Sec. III D, and (3) generation of initial states for VQE problems for better performance in Sec. III E.

All algorithms introduced in this work are implemented in both Python and C++ in https://github.com/SUSYUSTC/stabilizer_gs. The Python code is presented for concept illustration and readability, and the C++ code is used for optimal performance with a simple parallelization.

A. Computational cost of the exact 1D local algorithm

The scaling of the computation time for this exact 1D local algorithm only has a loose theoretical upper bound (Theorem 3 and Corollary 7) and lacks an exact analytical formula. Therefore, we implement the algorithm in C++ and numerically benchmark the computational time. All corresponding timings are collected on an 8-core i7-9700K Intel CPU.

We consider the following stochastic k -nearest Heisenberg model as the example Hamiltonian:

$$H = \sum_{i=1}^n \sum_{j=i+1}^{i+k-1} J_{ij}^{xx} S_i^x S_j^x + J_{ij}^{yy} S_i^y S_j^y + J_{ij}^{zz} S_i^z S_j^z \quad (46)$$

with each $J_{ij}^{xx}, J_{ij}^{yy}, J_{ij}^{zz} \sim \mathcal{N}(0, 1)$, i.e. all these coupling coefficients independently follow the normal distribution. We also consider the case of $J_{ij}^{zz} = 0$, $J_{ij}^{xx}, J_{ij}^{yy} \sim \mathcal{N}(0, 1)$ for comparisons. The two models are referred to as {XX,YY,ZZ} and {XX,YY}, respectively.

Following the procedure of the exact 1D local algorithm, all the possible values of $\{A_m\}$ with $m = 1, 2, \dots, n+1$ are generated sequentially. In Figure 5(a), the computational time of generating $\{A_{m+1}\}$ from $\{A_m\}$ are plotted as a function of site m for both the {XX,YY,ZZ} and {XX,YY} models with $n = 25$ and $k = 5$. Except for a few sites near the boundaries, the wall-clock time spent at each site is almost a constant for both models. This verifies that the computational cost of the 1D local algorithm scales as $O(n)$, as proved in Theorem 3. Due to the smaller number of Pauli terms in the Hamiltonian, the computational cost of the {XX,YY} model is systematically lower than the {XX,YY,ZZ} model.

After showing that the time spent at each site is a constant except for the sites near the boundaries, we further discuss the scaling of the maximum single-site running time as a function of the locality parameter k for different types of Hamiltonians. Figure 5(b) displays the maximum wall-clock time of a single site as a function of k for both

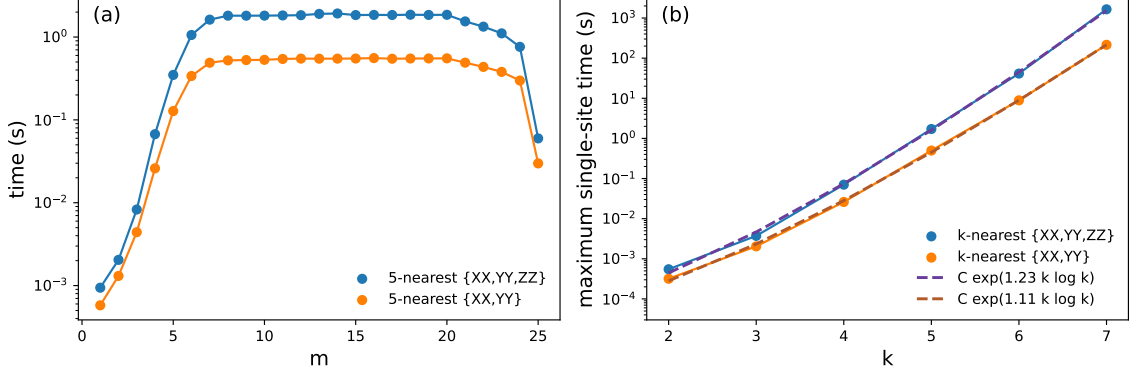


FIG. 5. Wall-clock time of the 1D local algorithm on the $\{\text{XX,YY,ZZ}\}$ and $\{\text{XX,YY}\}$ model (see the main text). (a) Computational time spent on each site m for the two models. (b) Maximum single-site computational time (solid lines) as a function of k for the two models, and fitted curves (dashed lines) with the form of $C \exp(C' k \log k)$.

models. We assume that the form of the scaling function is $C \exp(C' k \log k)$ according to Corollary 7. The numerical scaling functions are fitted independently for two models in Figure 5(b). The resulting fitted scaling curves have the parameters $C' = 1.23$ and $C' = 1.11$ for the $\{\text{XX,YY,ZZ}\}$ and $\{\text{XX,YY}\}$ models, respectively, and match the true timing data well. This indicates that the computation time of different Hamiltonians within the same class scales similarly.

B. Comparison with numerical discrete optimizations of stabilizer ground states

We demonstrate that numerical optimizations of stabilizer ground states are not scalable and lead to unacceptable energy errors with an increasing number of qubits. The numerical optimization of stabilizer ground states can be performed by discrete optimizations of the Clifford circuits representing stabilizer states [62].

Here, we still use the stochastic k -nearest Heisenberg Hamiltonian in Eq. (46) (the $\{\text{XX,YY,ZZ}\}$ model) as an example. The Clifford ansatz employed here modifies the hardware-efficient Clifford ansatz in Ref. [62] by generalizing the single-qubit Clifford rotations to all single-qubit Clifford operations (24 unique choices in total) [86]. The simulated annealing algorithm is used in the discrete optimization with an exponential decay of temperature from 5 to 0.05 in 2500 steps. In each step of the simulated annealing, one of the single-qubit Clifford operations is randomly selected and replaced with one of the 24 operations, and the move is accepted with a probability of $\min(\exp(-\Delta E/T), 1)$, where ΔE is the energy difference.

Figure 6(a) compares the stabilizer ground state energies obtained from the exact 1D local algorithm (E_{exact}^s) and the numerical optimization algorithm (E_{opt}^s). For each n , 100 random Hamiltonians are tested. For every single test, the numerically optimized ground state energy is either equal to or higher than the exact stabilizer ground state energy. With increasing n , the success probability of numerical optimization that results in accurate stabilizer ground state energies decreases and E_{opt}^s approaches zero. This indicates that the numerical discrete optimization cannot correctly obtain the stabilizer ground state due to the exponential scaling of the number of stabilizer states and the number of possible Clifford circuits. Figure 6(b) displays the quantitative statistics of the performance degradation speed of numerical optimization by plotting the averaged relative stabilizer ground state energy $\langle E_{\text{opt}}^s / E_{\text{exact}}^s \rangle$ versus the number of sites n with $k = 4$. A rapid decay of the energy ratio is observed from 97.4% at $n = 4$ to 0.4% at $n = 20$. Therefore, the optimization method fails to bootstrap large-scale variational quantum algorithms via stabilizer initializations as claimed in Ref. [62] and the challenge is fully solved by our new algorithm at least in the 1D case.

C. Qualitative analysis of phase transitions

Similar to the mean-field states, stabilizer ground states can also qualitatively capture the phases and phase transitions in many interesting systems. Specifically, stabilizer ground states are good at capturing topological phases with long-range entanglements. This capability is demonstrated using an infinite 1D generalized cluster model [87] as an

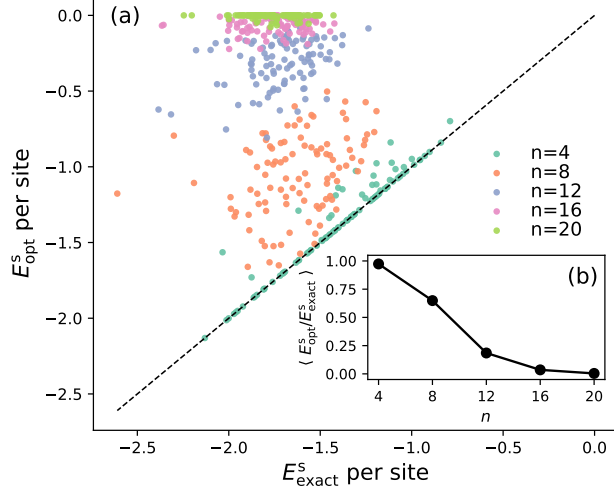


FIG. 6. Stabilizer ground state energies of the stochastic k -nearest Heisenberg model obtained by the exact 1D local algorithm (E_{exact}^s) and the numerical simulated annealing optimization algorithm (E_{opt}^s). (a) E_{exact}^s per site versus E_{opt}^s per site with $n = 4, 8, 12, 16, 20$ and $k = 4$. The black dashed line corresponds to $E_{\text{exact}}^s = E_{\text{opt}}^s$. (b) The mean relative energy error of stabilizer ground state energy captured by the numerical optimization algorithm ($\langle E_{\text{opt}}^s / E_{\text{exact}}^s \rangle$) versus n with locality $k = 4$.

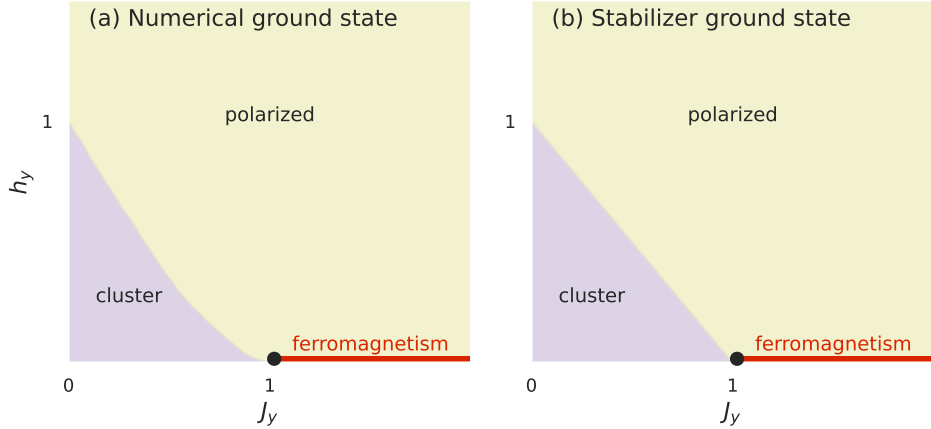


FIG. 7. Ground state phase diagram of the Hamiltonian in Eq. (47) obtained by (a) numerical DMRG calculations in Ref. [87] and (b) stabilizer ground state calculations via the exact 1D periodic local algorithm. There are three phases, including the cluster phase, the polarized phase, and the ferromagnetic phase, for both cases.

example, whose Hamiltonian is

$$H = \sum_{n=-\infty}^{\infty} -X_{n-1}Z_nX_{n+1} - J_yY_nY_{n+1} + h_yY_n. \quad (47)$$

This model is equivalent to the free fermion model at $h_y = 0$, while it is not dual to any free fermion model at $h_y \neq 0$ due to the lack of Z_2 symmetry. This Hamiltonian has been studied by numerical density matrix renormalization group (DMRG) calculations in Ref. [87], and the corresponding phase diagram is replotted in Figure 7(a). Three phases are observed in this phase diagram, including the symmetry-protected topological phase at small but positive J_y and h_y , the polarized phase at $J_y \rightarrow \infty$, $h_y \rightarrow \infty$, and the ferromagnetic phase at $h_y = 0, J_y > 1$.

We apply the exact 1D periodic local algorithm to the Hamiltonian to obtain the stabilizer ground states of this model using different parameters (J_y, h_y). Calculations are performed with candidate supercell sizes $c \leq 6$, and the minimum energy is selected as the stabilizer ground state energy. All possible types of distinct stabilizer ground states are listed in Table I, and the corresponding phase diagram is plotted in Figure 7(b). When comparing Figure 7 (a) and

TABLE I. Stabilizer ground states of the Hamiltonian in Eq. (47) in different phases. Note that the conditions of (J_y, h_y) do not strictly contradict each other, which indicates degeneracies of stabilizer ground states in the overlap regions (borders between phases or the tricritical point).

Stabilizers	(J_y, h_y)	Phase
$\{X_{n-1}Z_nX_{n+1}\}$	$J_y + h_y \leq 1$	Cluster
$\{-Y_n\}$	$J_y + h_y \geq 1, h_y > 0$	Polarized
$\{Y_nY_{n+1}\}$	$J_y \geq 1, h_y = 0$	Ferromagnetism
$\{X_{3n-1}Z_{3n}X_{3n+1}, Y_{3n-1}Y_{3n}, Y_{3n}Y_{3n+1}\}$	$J_y = 1, h_y = 0$	Tricritical point
$\{X_{3n-1}Z_{3n}X_{3n+1}, X_{3n}Z_{3n+1}X_{3n+2}, Y_{3n}Y_{3n+1}\}$	$J_y = 1, h_y = 0$	Tricritical point

(b), the stabilizer ground state phase diagram matches the numerical ground state phase diagram well except for the shape of the boundary between the cluster phase and the polarized phase. The boundary predicted by stabilizer ground states is a straight line, while the numerical boundary is slightly curved. These agreements indicate that stabilizer ground states are useful to qualitatively understand phase transitions in quantum many-body systems and provide a new perspective compared to conventional mean-field approaches. The stabilizer ground state at the tricritical point $J_y = 1, h_y = 0$ is observed to have two new degenerate stabilizer ground states besides the stabilizer ground states in other phases. These two new stabilizer ground states have stabilizers $\{X_{3n-1}Z_{3n}X_{3n+1}, Y_{3n-1}Y_{3n}, Y_{3n}Y_{3n+1}\}$ and $\{X_{3n-1}Z_{3n}X_{3n+1}, X_{3n}Z_{3n+1}X_{3n+2}, Y_{3n}Y_{3n+1}\}$, respectively.

D. Extended stabilizer ground states

Stabilizer ground states can be used as a starting point to develop advanced numerical methods or quantum state ansatz for classical simulation. As an illustration, we introduce the extended stabilizer ground state and demonstrate its capability of characterizing phase transitions of a 2D generalized toric code model. The relation between classical states, stabilizer states, product states, and extended stabilizer states are discussed in Sec. II E and Fig. 4. We first introduce a quantum state ansatz expressed as applying single-qubit rotations on some stabilizer states, i.e.

$$|\psi\rangle = U(\{\theta_j\})|\psi_{\text{stab}}\rangle = \prod_j e^{i\theta_j \cdot \mathbf{S}_j} |\psi_{\text{stab}}\rangle, \quad (48)$$

where \mathbf{S}_j is the vector spin operator on the j th qubit. We then define the extended stabilizer ground state by the state $|\psi\rangle$ with the lowest energy among all possible combinations of $\{\theta_j\}$ and $|\psi_{\text{stab}}\rangle$. Instead of directly finding the value of $\{\theta_j\}$ and $|\psi_{\text{stab}}\rangle$ that minimizes the energy, which requires expensive discrete optimizations, we can effectively transform the Hamiltonian by

$$H \rightarrow H'(\{\theta_j\}) = U^\dagger(\{\theta_j\}) H U(\{\theta_j\}). \quad (49)$$

The stabilizer ground state of the Hamiltonian $H'(\{\theta_j\})$ is thus a function of $\{\theta_j\}$. Since local Hamiltonians after single-site rotations remain local with the same localities k , such an extended stabilizer ground state formalism increases the expressive power without significantly complicating the problem, especially when each Pauli operator only nontrivially acts on a limited number of sites.

As a demonstration, we consider a 2D generalized toric code model with external magnetic fields. The Hamiltonian is

$$H = - \left(\sum_v A_v + \sum_p B_p \right) - h_x \sum_j X_j - h_z \sum_j Z_j, \quad (50)$$

which is defined on a torus, where $A_v = \prod_{j \in v} X_j$ and $B_p = \prod_{j \in p} Z_j$ represent the product of spin operators on bonds incident to the vertex v and surrounding plaquette p , respectively. The geometry of the vertices and plaquettes is shown in Figure 8(a). This Hamiltonian is studied by continuous-time Monte Carlo simulation in Ref. [88] and the phase diagram is reproduced in Figure 8(b). At $h_x \rightarrow \infty$ with fixed h_z or $h_z \rightarrow \infty$ with fixed h_x , each spin is polarized in the x or z direction, and gives the phase A or B, respectively. A phase transition happens between the phase A and B at the first-order transition line $h_x = h_z$, which begins at $h_x = h_z = 0.34$ and ends at $h_x = h_z = 0.418$. In the limit of $h_x \rightarrow \infty$ and $h_z \rightarrow \infty$, the polarization of the system varies continuously between phases A and B, thus no phase transition occurs.

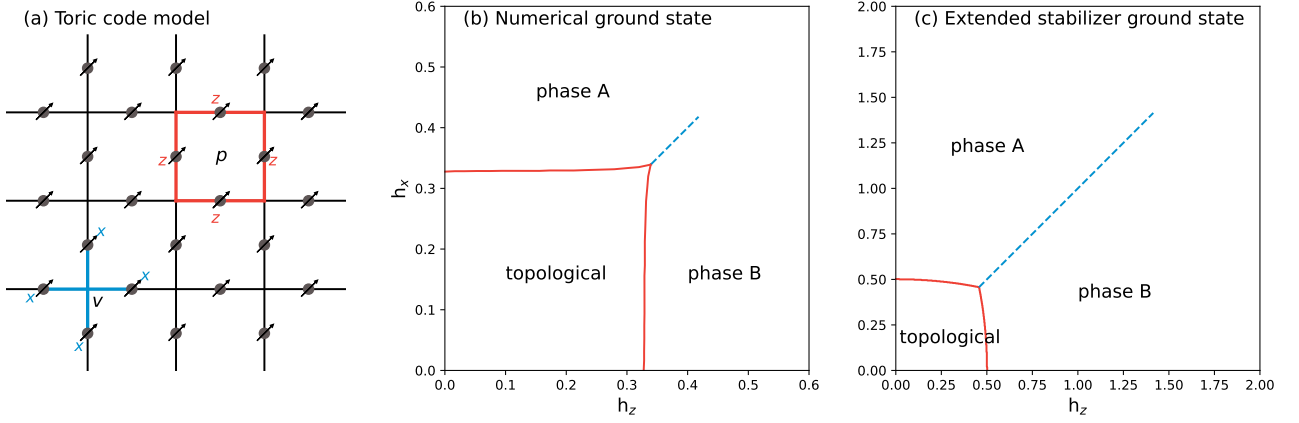


FIG. 8. Geometry and phase diagrams of the 2D generalized toric code. (a) The geometry of the 2D generalized toric code model in Eq. (50). (b) Numerical ground state phase diagram obtained by continuous-time Monte Carlo calculations in Ref. [88]. (c) Extended stabilizer ground state phase diagram. For both (b) and (c), three phases are found, including the topological phase, phase A, and phase B. The first-order transition line (dashed blue line) at $h_x = h_z$ begins at $h_x = h_z = 0.34$ and ends at $h_x = h_z = 0.418$ in (b), while it begins at $h_x = h_z = 0.46$ and ends at $h_x = h_z = 1.414$ in (c)

Now we consider the extended stabilizer ground state of this Hamiltonian. Since the Hamiltonian only contains X and Z, the single-qubit rotations can be restricted to the form of $U(\{\theta_j\}) = \prod_j e^{\frac{1}{2}i\theta_j Y_j}$. As stated previously, we need to transform the Hamiltonian in Eq. (50) by $U(\{\theta_j\})$ and then determine the stabilizer ground state. As discussed in Sec. II D, the stabilizer ground state of a periodic local Hamiltonian should be periodic over supercells with some size c . For simplification, the stabilizer ground state is assumed to have period 1. We set $\theta_j = \alpha$ and $\theta_j = \beta$ for sites j on vertical bonds and horizontal bonds, respectively, and thus the total rotation operator can be written as $U(\alpha, \beta)$.

With fixed supercell size $c = 1$, the stabilizer ground state of the rotated Hamiltonian $U(\alpha, \beta)^\dagger H U(\alpha, \beta)$ can be found via Eq. (45) for each set of rotation angles α, β . The corresponding stabilizer ground state energy per site is written as $E(h_x, h_z, \alpha, \beta)$. The extended stabilizer ground state energy per site is then given by $E(h_x, h_z) = \min_{\alpha, \beta} E(h_x, h_z, \alpha, \beta)$. In the following analysis, we apply the simplification process in Eq. (44) for convenience, which allows us to exclude Pauli terms like $P = X_l Z_r X_u Z_d$, where the subscripts l, r, u, d stand for the left, right, up, and down site of either a vertex or a plaquette. The valid Pauli terms of the rotated Hamiltonians include (1) X and Z on each site; and (2) $X_l X_r X_u X_d, X_l X_r Z_u Z_d, Z_l Z_r X_u X_d$, and $Z_l Z_r Z_u Z_d$ on each vertex or plaquette.

The resulting extended stabilizer ground state phase diagram is plotted in Figure 8(c) and it matches the exact phase diagram qualitatively. In the topologically ordered phase, the stabilizers are the set of all $X_l X_r X_u X_d, X_l X_r Z_u Z_d, Z_l Z_r X_u X_d, Z_l Z_r Z_u Z_d$ on all vertices and plaquettes. We find that the corresponding $E(h_x, h_z, \alpha, \beta)$ is a constant with respect to α and β , attributed to the fact that $U(\alpha, \beta)$ is a symmetry operation of this stabilizer state. In phase A and B, the stabilizers are simply X on each site and $X_l X_r X_u X_d$ on each vertex and plaquette, which corresponds to the product of single-site polarized states in the picture of the unrotated Hamiltonian. We consider $h_x = h_z$, in which case the extended stabilizer ground state is always found at $\alpha = \beta$. The corresponding per-site energy function $E(h, \alpha) = E(h_x = h, h_z = h, \alpha, \beta = \alpha)$ is given by

$$E(h, \alpha) = -\frac{1}{2}(\cos^4 \alpha + \sin^4 \alpha) - h(\cos \alpha + \sin \alpha), \quad (51)$$

which is symmetric under $\alpha \rightarrow \frac{\pi}{2} - \alpha$. No phase transition happens for large h since only one minimum $\alpha = \frac{\pi}{4}$, while two minimums can be found for small h . The behavior could be better understood by Taylor expansion around $\alpha = \frac{\pi}{4}$, which gives

$$E(h, \alpha = \frac{\pi}{4} + \theta) = \text{const} + \left(\frac{h}{\sqrt{2}} - 1\right)\theta^2 + \frac{32 - \sqrt{2}h}{24}\theta^4 + O(\theta^6). \quad (52)$$

This indicates that the first-order transition ends at $h = \sqrt{2}$, where a second-order phase transition happens due to the change of sign of the quadratic term. Furthermore, at $h < h_c \approx 0.46$, $E(h, \alpha)$ is higher than the energy of the topologically ordered state for all α . Thus, we claim that the corresponding first-order transition line begins at $h_x = h_z \approx 0.46$ and ends at $h_x = h_z = \sqrt{2} \approx 1.414$. Although the exact transition values are different, the qualitative picture captured by the extended stabilizer ground state is consistent with the ground truth.

E. Initial state for VQE problems

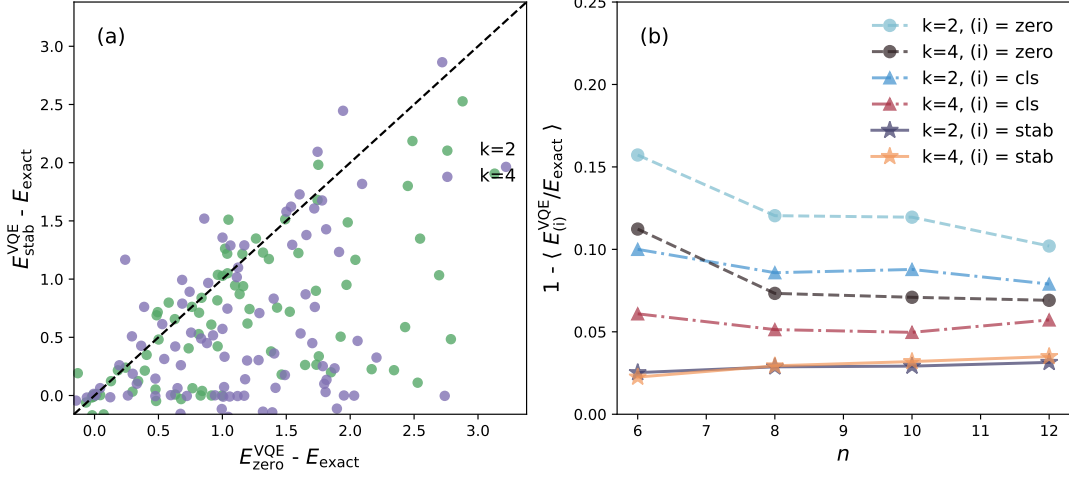


FIG. 9. Errors of optimized VQE energies computed using the stochastic k -nearest Heisenberg model. E_{exact} represents the exact ground state energy, and $E_{(i)}^{\text{VQE}}$ is the optimized VQE energy, where (i) is the employed initialization scheme. Three initialization schemes, i.e. zero state, classical ground state, and stabilizer ground state, are compared. They are abbreviated as $(i) = \text{zero}$, $(i) = \text{cls}$, $(i) = \text{stab}$, respectively. (a) $E_{\text{stab}}^{\text{VQE}} - E_{\text{exact}}$ plots versus $E_{\text{zero}}^{\text{VQE}} - E_{\text{exact}}$ for $N = 100$ random Hamiltonians with $n = 6$ and $k = 2, 4$. (b) Mean relative errors of energies $(1 - \langle E_{(i)}^{\text{VQE}} / E_{\text{exact}} \rangle)$ versus the number of sites n for the three initializations with $k = 2, 4$.

Stabilizer states have been recently used as initial states [62, 63] for VQE problems to mitigate the notorious barren plateau issue [73–75]. The stabilizer initial states can be prepared on quantum circuits by efficient decomposition to up to $O(n^2 / \log n)$ single-qubit and double-qubit Clifford gates [39], or even fewer gates for stabilizer ground states of 1D local Hamiltonians (see Corollary 8). The effective VQE ansatz is

$$|\psi(\boldsymbol{\theta})\rangle = U(\boldsymbol{\theta})|\psi_{\text{stab}}\rangle = U(\boldsymbol{\theta})U_C|0\rangle^{\otimes n}, \quad (53)$$

where the stabilizer initial state $|\psi_{\text{stab}}\rangle$ is decomposed to $U_C|0\rangle^{\otimes n}$. Another approach is to employ the quantum state ansatz as follows:

$$|\psi(\boldsymbol{\theta})\rangle = U_C U(\boldsymbol{\theta})|0\rangle^{\otimes n}. \quad (54)$$

The advantage of the latter approach is that one can equivalently transform the Hamiltonian by $H \rightarrow H' = U_C^\dagger H U_C$ classically, and thus only the $U(\boldsymbol{\theta})$ part needs to be performed on the quantum circuit [58, 59, 89]. However, its disadvantage is that it might break the locality of the Hamiltonian and cause additional overhead on the hardware that cannot support nonlocal operations [90, 91]. Therefore, we adopt the former strategy in Eq. (53) for the following benchmark.

The $\{\text{XX}, \text{YY}, \text{ZZ}\}$ model in Eq. (46) still serves as the example Hamiltonian, and the variational Hamiltonian ansatz [92] is used as the example VQE circuit for ground state optimization. By rewriting the Hamiltonian as $H = \sum_P w_P P$ with $P = S_i^x S_j^x, S_i^y S_j^y, S_i^z S_j^z$, the corresponding quantum circuit ansatz is as follows:

$$|\psi(\boldsymbol{\theta})\rangle = \prod_P e^{i\theta_P P} |\psi_{\text{init}}\rangle. \quad (55)$$

We compare three choices of the initial state $|\psi_{\text{init}}\rangle$, including the $|0\rangle^{\otimes n}$ state (referred to as zero state), the classical ground state, and the stabilizer ground state obtained by the exact 1D local algorithm. The relations between classical ground states, stabilizer ground states, and product states are discussed in Sec. II C 2. The quantum circuit simulations are conducted via the *TensorCircuit* software [93]. The optimization of parameters $\boldsymbol{\theta}$ is performed by the default L-BFGS-B [94] optimizer in *SciPy* [95] with zero initial values.

Figure 9(a) displays the distributions of optimized energy errors of the zero state and stabilizer ground state initialization strategies tested on 100 random Hamiltonians with $n = 6$. Stabilizer state initializations result in lower VQE errors compared with those via the zero state in 82% and 92% of the 100 tests for $k = 2$ and $k = 4$, respectively.

There are few points in the region of $E_{\text{zero}}^{\text{VQE}} < E_{\text{stab}}^{\text{VQE}}$, which is attributed to the fact that an initialization state with a lower energy does not guarantee a lower final energy after VQE optimizations. Figure 9(b) also shows the mean relative errors of energies $1 - \langle E_{(i)}^{\text{VQE}} / E_{\text{exact}} \rangle$ for increasing n and $k = 2, 4$, where (i) represents each of the three initialization strategies. Initializations via stabilizer ground states are observed to systematically provide better energy estimations for both $k = 2$ and $k = 4$.

IV. CONCLUSIONS AND OUTLOOK

In this work, we introduce stabilizer ground states as a versatile toolkit of both qualitative analysis of quantum systems and cornerstone of developing advanced quantum state anstazes on classical or quantum computers. For general Hamiltonians, we establish the equivalence between the stabilizer ground state and the closed maximally-commuting Pauli subset. For 1D local Hamiltonians, we additionally develop an exact and efficient algorithm to obtain the exact stabilizer ground state with linear scaling. Besides, we prove that the stabilizer ground state of 1D local Hamiltonians can be prepared on quantum circuits with a linear scaled circuit depth. Furthermore, both the equivalence formalism for general Hamiltonians and the linear-scaled algorithm for 1D local Hamiltonians can be extended to infinite periodic systems. We also compare stabilizer ground states, mean-field ground states, and MPS ground states in terms of the applications for constructing quantum and classical ansatzes. By benchmarking on example Hamiltonians, we verified the computational scaling of the exact 1D local algorithm and demonstrated the substantial performance gain over the traditional discrete optimization strategies. We also illustrate that stabilizer ground states are promising tools for various applications, including qualitative analysis of phase transitions, generating better heuristics for VQE problems, and developing more expressive classical ground state ansatzes.

Looking forward, future studies can fruitfully branch into three major directions. The first avenue is to develop algorithms for stabilizer ground states of other types of Hamiltonians, including Hamiltonians with other quasi-1D structures and local Hamiltonians in higher dimensions. For the latter, finding the exact stabilizer ground state is NP-hard, evidenced by the NP-hardness of one of its simplified cases, i.e., the ground state problem of 2D classical spin models with random magnetic fields [96, 97]. However, approximate or heuristic algorithms [98–100] for stabilizer ground states may still be practically useful for higher-dimensional systems. The second avenue extends the concept of stabilizer ground states to other physically interesting properties, such as excited states, mixed states, and thermal state sampling. These extensions are plausible, as the automaton structure of the 1D algorithm shares similarities with an ensemble of quantum states. The third avenue involves the exploration of more downstream applications for stabilizer ground states, especially via combining with other well-established quantum state ansatzes, such as tensor network [84], perturbation theory [56, 85], variational quantum Monte Carlo, or low-rank (or low-energy) stabilizer decomposition [54].

ACKNOWLEDGEMENT

J.S. gratefully acknowledges the support of the Hongyan Scholarship.

V. APPENDIX

A. Proof of Theorem 1

Let $\mathbf{S} = \langle \mathbf{Q} \rangle$, $\mathbf{Q} \in \mathcal{S}(\mathbf{P})$ be one of the stabilizer group such that $E_{\text{stab}}(H, \mathbf{S}) = E_{\text{gs}}$, and $|\psi\rangle$ is any stabilizer state stabilized by \mathbf{S} . Let $\mathbf{S}_\psi = \langle \text{Stab}(|\psi\rangle) \cap \tilde{\mathbf{P}} \rangle$, obviously we have $\mathbf{S} \subseteq \mathbf{S}_\psi$. Let $\mathbf{S}_\psi = \langle \mathbf{S}, P_1, P_2, \dots, P_k \rangle$ where each $P_i \in \tilde{\mathbf{P}}$, $1 \leq i \leq k$. We consider the sequence $\mathbf{S}_i = \langle \mathbf{S}, P_1, P_2, \dots, P_i \rangle$ with $i = 0, 1, \dots, k$. Clearly we have $\mathbf{S}_i \cap \tilde{\mathbf{P}} \in \mathcal{S}(\mathbf{P})$ for each \mathbf{S}_i .

First we prove that $E_{\text{stab}}(H, \mathbf{S}_i) = E_{\text{gs}}$ for each \mathbf{S}_i . Obviously, it is true for $i = 0$. Given it is true for \mathbf{S}_i , we then consider $\mathbf{S}_{i+1} = \langle \mathbf{S}_i, P_{i+1} \rangle$. If $P_{i+1} \in \mathbf{S}_i$, then $\mathbf{S}_{i+1} = \mathbf{S}_i$ so $E_{\text{stab}}(H, \mathbf{S}_{i+1}) = E_{\text{gs}}$. Otherwise we consider $E_i = E_{\text{stab}}(H, \mathbf{S}_i)$, $E_+ = E_{\text{stab}}(H, \langle \mathbf{S}_i, P_{i+1} \rangle)$ and $E_- = E_{\text{stab}}(H, \langle \mathbf{S}_i, -P_{i+1} \rangle)$. For each $P \in \mathbf{P}$, it falls into one of the following situations: (1) $P \in \pm \mathbf{S}_i$ so it contributes equally to E_+ and E_- , (2) $P \notin \pm \mathbf{S}_i$ but $P \in \pm \langle \mathbf{S}_i, P_{i+1} \rangle$ so it contributes no energy to E_i and opposite energy to E_+ and E_- , (3) $P \notin \pm \langle \mathbf{S}_i, P_{i+1} \rangle$ so it contributes no energy to

E_i , E_+ and E_- . Thus we have $2E_i = E_+ + E_-$. However E_i is already the minimum of $E_{\text{stab}}(H, \mathbf{S})$ for $\mathbf{S} \in \mathcal{S}(\mathbf{P})$, thus $E_+ = E_- = E_i = E_{\text{gs}}$, i.e. $E_{\text{stab}}(H, \mathbf{S}_{i+1}) = E_{\text{gs}}$. Now we can conclude that $E_{\text{stab}}(H, \mathbf{S}_i) = E_{\text{gs}}$ for each \mathbf{S}_i , which implies $E_{\text{stab}}(H, \mathbf{S}_\psi) = E_{\text{gs}}$.

Next we prove $|\psi\rangle$ is a (degenerate) stabilizer ground state. According to Corollary 1, we have $\langle\psi|H|\psi\rangle = E_{\text{stab}}(H, \mathbf{S}_\psi) = E_{\text{gs}}$. If there exists stabilizer state $|\psi'\rangle$ such that $\langle\psi'|H|\psi'\rangle < \langle\psi|H|\psi\rangle = E_{\text{gs}}$, we should have $E_{\text{stab}}(H, \langle\text{Stab}(|\psi'\rangle) \cap \tilde{\mathbf{P}}\rangle) = \langle\psi'|H|\psi'\rangle < E_{\text{gs}}$, which conflicts with the definition of E_{gs} . Thus we conclude that $|\psi\rangle$ is a (degenerate) stabilizer ground state.

B. Proof of Eq. 16 from Eq. 19

We first introduce an important fact $\mathbf{s} \leftrightarrow \{A_1, \dots, A_n\}$, where \leftrightarrow means bijective mapping. This is because (1) $G(A_m) = s_m$ gives the mapping from the latter one to the former one, and (2) $A_m(\mathbf{s})$ itself is the function that maps from the former one to the latter one. Based on this, we have

$$\begin{aligned} \{\mathbf{s}|A_m\} &\leftrightarrow \{A_1, \dots, A_n|A_m\} \\ &= \{A_1, \dots, A_m|A_m\} \otimes \{A_{m+1}, \dots, A_n|A_m\} \\ &\rightarrow \{\mathbf{s}_{\leq m}|A_m\} \otimes \{\mathbf{s}_{>m}|A_m\} \\ &\supseteq \{\mathbf{s}|A_m\}, \end{aligned} \quad (56)$$

where in the first line used $\mathbf{s} \leftrightarrow \{A_1, \dots, A_n\}$, the second line used Eq. 19, the third line used the mapping $G(A_m) = s_m$, and \rightarrow means the surjective mapping. Thus Eq. 56 gives a four-step way to map $\{\mathbf{s}|A_m\}$ to itself. Therefore the mapping in each step must be bijective. Specifically, the mapping from the third line to the fourth line is bijective, which exactly gives Eq. 16, i.e.

$$\{\mathbf{s}|A_m\} = \{\mathbf{s}_{\leq m}|A_m\} \otimes \{\mathbf{s}_{>m}|A_m\}. \quad (57)$$

C. Derivation of the state machine

We first introduce the following lemma related to the projection operations, which will be frequently used:

Lemma 3. *If $\mathbf{B} \subseteq \mathcal{P}_I$, then $\mathbb{P}_I(\langle\mathbf{A}, \mathbf{B}\rangle) = \langle\mathbb{P}_I(\langle\mathbf{A}\rangle), \mathbf{B}\rangle$.*

Proof. We only need to prove $\langle\mathbf{A}, \mathbf{B}\rangle \cap \mathcal{P}_I = \langle\mathbf{A} \cap \mathcal{P}_I, \mathbf{B}\rangle$. This can be seen by (1) $\langle\mathbf{A} \cap \mathcal{P}_I, \mathbf{B}\rangle \subseteq \langle\mathbf{A}, \mathbf{B}\rangle$, (2) $\langle\mathbf{A} \cap \mathcal{P}_I, \mathbf{B}\rangle \subseteq \mathcal{P}_I$ since $\mathbf{A} \cap \mathcal{P}_I \subseteq \mathcal{P}_I$ and $\mathbf{B} \subseteq \mathcal{P}_I$, and (3) for any $P = \langle\mathbf{A}, \mathbf{B}\rangle \cap \mathcal{P}_I$ we can write $P = AB$ where $A \in \mathbf{A}$ and $B \in \mathbf{B}$. Since $B \in \mathcal{P}_I$, $P \in \mathcal{P}_I$ we also have $A \in \mathcal{P}_I$. Thus $P = AB \in \langle\mathbb{P}_I(\langle\mathbf{A}\rangle), \mathbf{B}\rangle$. \square

We have already proved that Eq. 16 is a necessary condition of Eq. 19. In fact, if we additionally have

$$\begin{aligned} \{\mathbf{s}_{\leq m}, A_m\} &\leftrightarrow \{A_1, \dots, A_m\}, \\ \{\mathbf{s}_{>m}, A_m\} &\leftrightarrow \{A_m, \dots, A_n\} \end{aligned} \quad (58)$$

they are equivalent. With the mapping $\mathbf{s} \rightarrow \mathbf{Q}$ given in Sec. II C 2, Eq. 58 becomes

$$\begin{aligned} \{\mathbf{Q}_{\leq m}, A_m\} &\leftrightarrow \{A_1, \dots, A_m\}, \\ \{\mathbf{Q}_{>m}, A_m\} &\leftrightarrow \{A_m, \dots, A_n\}, \end{aligned} \quad (59)$$

and Eq. 16 becomes

$$\{\mathbf{Q}|A_m\} = \{\mathbf{Q}_{\leq m}|A_m\} \otimes \{\mathbf{Q}_{>m}|A_m\}, \quad (60)$$

i.e. $\mathbf{Q}_{\leq m}$ must be decoupled from $\mathbf{Q}_{>m}$ given A_m . The coupling between $\mathbf{Q}_{\leq m}$ and $\mathbf{Q}_{>m}$ is given in the following two lemmas:

Lemma 4. *If $\mathbf{Q} \in \mathcal{S}(\mathbf{P})$, then $\mathbf{Q}_{\leq m} \in \mathcal{S}(\mathbf{P}_{\leq m})$ for each m .*

Proof. We recall that $\mathcal{S}(\mathbf{P}) = \{\mathbf{Q}|\mathbf{Q} = \langle\mathbf{Q}\rangle \cap \tilde{\mathbf{P}}, -I \notin \langle\mathbf{Q}\rangle\}$. Then $-I \notin \langle\mathbf{Q}_{\leq m}\rangle$ is obvious because $\mathbf{Q}_{\leq m} \subseteq \mathbf{Q}$. Given that $\mathbf{Q} = \langle\mathbf{Q}\rangle \cap \tilde{\mathbf{P}}$, we have $\langle\mathbf{Q}_{\leq m}\rangle \cap \tilde{\mathbf{P}}_{\leq m} \subseteq \langle\mathbf{Q}\rangle \cap \tilde{\mathbf{P}}_{\leq m} = \langle\mathbf{Q}\rangle \cap \tilde{\mathbf{P}} \cap \tilde{\mathbf{P}}_{\leq m} = \mathbf{Q} \cap \tilde{\mathbf{P}}_{\leq m} = \mathbf{Q}_{\leq m}$. On the other hand, we must have $\mathbf{Q}_{\leq m} \subseteq \langle\mathbf{Q}_{\leq m}\rangle \cap \tilde{\mathbf{P}}_{\leq m}$. Thus $\langle\mathbf{Q}_{\leq m}\rangle \cap \tilde{\mathbf{P}}_{\leq m} = \mathbf{Q}_{\leq m}$, i.e. $\mathbf{Q}_{\leq m} \in \mathcal{S}(\mathbf{P}_{\leq m})$. \square

For simplicity, given $\mathbf{Q}_{\leq m} \in \mathcal{S}(\mathbf{P}_{\leq m})$, we say $\mathbf{Q}_{>m} \subseteq \tilde{\mathbf{P}}_{>m}$ is valid if $\mathbf{Q} = \mathbf{Q}_{\leq m} \cup \mathbf{Q}_{>m} \in \mathcal{S}(\mathbf{P})$. The requirement of $\mathbf{Q}_{>m}$ can be rewritten as follows:

Corollary 9. Given $\mathbf{Q}_{\leq m} \in \mathcal{S}(\mathbf{P}_{\leq m})$, $\mathbf{Q}_{>m} \subseteq \tilde{\mathbf{P}}_{>m}$ is valid if and only if

1. $-I \notin \langle \mathbf{Q}_{>m} \rangle$, i.e. $\langle \mathbf{Q}_{>m} \rangle$ is a stabilizer group
2. $[\mathbf{Q}_{>m}, \mathbf{Q}_{\leq m}] = 0$
3. $\langle \mathbf{Q}_{\leq m}, \mathbf{Q}_{>m} \rangle \cap \tilde{\mathbf{P}}_{>m} = \mathbf{Q}_{>m}$
4. $\langle \mathbf{Q}_{\leq m}, \mathbf{Q}_{>m} \rangle \cap \tilde{\mathbf{P}}_{\leq m} = \mathbf{Q}_{\leq m}$

Condition 1 is only dependent on $\mathbf{Q}_{>m}$ itself so it does not couple $\mathbf{Q}_{>m}$ with $\mathbf{Q}_{\leq m}$. Condition 2 requires that the added stabilizers $\mathbf{Q}_{>m}$ should commute with all previous stabilizers $\mathbf{Q}_{\leq m}$. Conditions 3 and 4 require that group multiplication operations between $\mathbf{Q}_{\leq m}$ and $\mathbf{Q}_{>m}$ does not generate new elements in $\tilde{\mathbf{P}}$, which can be further decomposed to $\tilde{\mathbf{P}}_{>m}$ and $\tilde{\mathbf{P}}_{\leq m}$. Thus conditions 2, 3, 4 give the coupling between $\mathbf{Q}_{>m}$ and $\mathbf{Q}_{\leq m}$. Now we want to construct A_m to decouple them. With

$$\tilde{\mathbf{P}}_{\text{invalid}}^m = \tilde{\mathbf{P}}_{\text{invalid}}^m(\mathbf{Q}_{\leq m}) = \{P \in \tilde{\mathbf{P}}_{>m} \mid [P, \mathbf{Q}_{\leq m}] \neq 0\} \quad (61)$$

(i.e. Eq. 28), condition 2 can be rewritten as

$$\begin{aligned} & [\mathbf{Q}_{\leq m}, \mathbf{Q}_{>m}] = 0 \\ & \Leftrightarrow \mathbf{Q}_{>m} \cap \{P \in \tilde{\mathbf{P}}_{>m} \mid [P, \mathbf{Q}_{\leq m}] \neq 0\} = \emptyset \\ & \Leftrightarrow \mathbf{Q}_{>m} \cap \tilde{\mathbf{P}}_{\text{invalid}}^m = \emptyset \end{aligned} \quad (62)$$

which is only dependent on $\mathbf{Q}_{>m}$. With

$$\mathbf{S}_{\text{proj}}^m = \mathbf{S}_{\text{proj}}^m(\mathbf{Q}_{\leq m}) = \mathbb{P}_{>m-k}(\langle \mathbf{Q}_{\leq m} \rangle) \quad (63)$$

(i.e. Eq. 29), condition 3 can be rewritten as

$$\begin{aligned} \mathbf{Q}_{>m} &= \langle \mathbf{Q}_{\leq m}, \mathbf{Q}_{>m} \rangle \cap \tilde{\mathbf{P}}_{>m} \\ &= \mathbb{P}_{>m-k}(\langle \mathbf{Q}_{\leq m}, \mathbf{Q}_{>m} \rangle) \cap \tilde{\mathbf{P}}_{>m} \\ &= \langle \mathbb{P}_{>m-k}(\langle \mathbf{Q}_{\leq m} \rangle), \mathbf{Q}_{>m} \rangle \cap \tilde{\mathbf{P}}_{>m} \\ &= \langle \mathbf{S}_{\text{proj}}^m, \mathbf{Q}_{>m} \rangle \cap \tilde{\mathbf{P}}_{>m}, \end{aligned} \quad (64)$$

which is only dependent on $\mathbf{Q}_{>m}$. Here we used $\mathbf{Q}_{>m} \subseteq \mathcal{P}_{>m-k}$ and Lemma 3 in the third line. With

$$\mathbf{S}_{\text{right}}^m = \mathbf{S}_{\text{right}}^m(\mathbf{Q}_{\geq m}) = \mathbb{P}_{\leq m}(\langle \mathbf{Q}_{\geq m} \rangle) \quad (65)$$

(i.e. Eq. 30), condition 4 can be rewritten as

$$\begin{aligned} \mathbf{Q}_{\leq m} &= \langle \mathbf{Q}_{\leq m}, \mathbf{Q}_{>m} \rangle \cap \tilde{\mathbf{P}}_{\leq m} \\ &= \langle \mathbf{Q}_{\leq m}, \mathbf{Q}_{\geq m} \rangle \cap \tilde{\mathbf{P}}_{\leq m} \\ &= \mathbb{P}_{\leq m}(\langle \mathbf{Q}_{\leq m}, \mathbf{Q}_{\geq m} \rangle) \cap \tilde{\mathbf{P}}_{\leq m} \\ &= \langle \mathbf{Q}_{\leq m}, \mathbb{P}_{\leq m}(\langle \mathbf{Q}_{\geq m} \rangle) \rangle \cap \tilde{\mathbf{P}}_{\leq m} \\ &= \langle \mathbf{Q}_{\leq m}, \mathbf{S}_{\text{right}}^m \rangle \cap \tilde{\mathbf{P}}_{\leq m}, \end{aligned} \quad (66)$$

which is only dependent on $\mathbf{Q}_{\leq m}$. Here we used $\mathbf{Q}_{\leq m} \subseteq \mathcal{P}_{\leq m}$ and Lemma 3 in the fourth line. As a summary, given

$$A_m(\mathbf{Q}) = (\mathbf{S}_{\text{proj}}^m(\mathbf{Q}_{\leq m}), \tilde{\mathbf{P}}_{\text{invalid}}^m(\mathbf{Q}_{\leq m}), \mathbf{S}_{\text{right}}^m(\mathbf{Q}_{\geq m})), \quad (67)$$

the four conditions are now

$$\begin{aligned} & -I \notin \langle \mathbf{Q}_{>m} \rangle \\ & \mathbf{Q}_{>m} \cap \tilde{\mathbf{P}}_{\text{invalid}}^m = \emptyset \\ & \langle \mathbf{S}_{\text{proj}}^m, \mathbf{Q}_{>m} \rangle \cap \tilde{\mathbf{P}}_{>m} = \mathbf{Q}_{>m}. \end{aligned} \quad (68)$$

for conditions 1, 2, 3, which depend on $\mathbf{Q}_{>m}$, and

$$\langle \mathbf{Q}_{\leq m}, \mathbf{S}_{\text{right}}^m \rangle \cap \tilde{\mathbf{P}}_{\leq m} = \mathbf{Q}_{\leq m}. \quad (69)$$

for condition 4, which depends on $\mathbf{Q}_{\leq m}$. Recalling that Corollary 9 additionally requires $\mathbf{Q}_{\leq m} \in \mathcal{S}(\mathbf{P}_{\leq m})$, we conclude that Eq. 60 holds with

$$\{\mathbf{Q}_{\leq m} | A_m\} = \{\mathbf{Q}_{\leq m} \in \mathcal{S}(\mathbf{P}_{\leq m}) \text{ satisfying Eq. 69}\} \quad (70)$$

and

$$\{\mathbf{Q}_{>m} | A_m\} = \{\mathbf{Q}_{>m} \subseteq \tilde{\mathbf{P}}_{>m} \text{ satisfying Eq. 68}\}. \quad (71)$$

Now we show that A_m is a state machine. The existence of the state function G is already given in Eq. 32. Therefore we just need to prove Eq. 59. The “ \leftarrow ” part is trivial due to the state function G . For the “ \rightarrow ” part, $\{\mathbf{Q}_{\leq m}, A_m\} \rightarrow \{A_1, \dots, A_m\}$ can be obtained by $A_i = (\mathbf{S}_{\text{proj}}^i(\mathbf{Q}_{\leq i}), \tilde{\mathbf{P}}_{\text{invalid}}^i(\mathbf{Q}_{\leq i}), \mathbf{S}_{\text{right}}^i = \mathbb{P}_{\leq i}(\mathbf{Q}_{\geq i}) = \mathbb{P}_{\leq i}(\mathbf{S}_{\text{right}}^m))$ for $i \leq m$. To prove $\{\mathbf{Q}_{>m}, A_m\} \rightarrow \{A_m, \dots, A_n\}$, we show that A_{m+1} can be obtained by A_m and $\mathbf{S}_{\text{right}}^{m+1}$, i.e

$$A_{m+1} = A_{m+1}(A_m, \mathbf{S}_{\text{right}}^{m+1}). \quad (72)$$

Once it is true, $\{A_m, \dots, A_n\}$ can be obtained by applying $A_{i+1} = A_{i+1}(A_i, \mathbf{S}_{\text{right}}^{i+1}(\mathbf{Q}_{\geq i+1}))$ for $i = m, \dots, n-1$. To construct $A_{m+1}(A_i, \mathbf{S}_{\text{right}}^{m+1})$, we only need to derive $\mathbf{S}_{\text{proj}}^{m+1}$ and $\tilde{\mathbf{P}}_{\text{invalid}}^{m+1}$. Specifically, we have:

$$\begin{aligned} \mathbf{S}_{\text{proj}}^{m+1}(\mathbf{Q}_{\leq m+1}) &= \mathbb{P}_{>m-k+1}(\langle \mathbf{Q}_{\leq m}, \mathbf{Q}_{m+1} \rangle) \\ &= \langle \mathbb{P}_{>m-k+1}(\langle \mathbf{Q}_{\leq m} \rangle), \mathbf{Q}_{m+1} \rangle \\ &= \langle \mathbb{P}_{>m-k+1}(\mathbf{S}_{\text{proj}}^m(\mathbf{Q}_{\leq m})), \mathbf{Q}_{m+1} \rangle \\ &:= \mathbf{S}_{\text{proj}}^{m+1}(\mathbf{S}_{\text{proj}}^m, \mathbf{Q}_{m+1}), \end{aligned} \quad (73)$$

where the second line used $\mathbf{Q}_{m+1} \subseteq \mathcal{P}_{>m-k+1}$ and Lemma 3, and

$$\begin{aligned} \tilde{\mathbf{P}}_{\text{invalid}}^{m+1}(\mathbf{Q}_{\leq m+1}) &= \{P \in \tilde{\mathbf{P}}_{>m+1} | [P, \mathbf{Q}_{\geq m+1}] \neq 0\} \\ &= \{P \in \tilde{\mathbf{P}}_{\geq m+1} | P \in \tilde{\mathbf{P}}_{\text{invalid}}^m(\mathbf{Q}_{\leq m}) \text{ or } [P, \mathbf{Q}_{m+1}] \neq 0\} \\ &:= \tilde{\mathbf{P}}_{\text{invalid}}^{m+1}(\tilde{\mathbf{P}}_{\text{invalid}}^m, \mathbf{Q}_{m+1}), \end{aligned} \quad (74)$$

which are the same with Eq. 33 and Eq. 34. Finally, \mathbf{Q}_{m+1} is given by $\mathbf{S}_{\text{right}}^{m+1} \cap \tilde{\mathbf{P}}_{m+1}$ according to Eq. 32, thus we conclude that A_{m+1} can indeed be rewritten as a function of A_m and $\mathbf{S}_{\text{right}}^{m+1}$.

D. Derivation of Eq. 39

Definition 8 requires that, for any path $\{A_1, \dots, A_{m+1} | A_{i+1} \in \tilde{F}(A_i)\}$, if $A_{m+1} \in \mathcal{A}_{m+1}$, then $A_m \in \mathcal{A}_m$. We require a stronger version: if $A_{m+1} = A_{m+1}(\mathbf{Q})$ for some $\mathbf{Q} \in \mathcal{S}(\mathbf{P})$, then $A_m = A_m(\mathbf{Q}')$, where $\mathbf{Q}' = \mathbf{Q}_{>m+1} \cup \mathbf{Q}'_{\leq m}$, $\mathbf{Q}'_{\leq m} = \cup_{i=1}^m G(A_i)$. Clearly it implies $A_m \in \mathcal{A}_m$ given $A_{m+1} \in \mathcal{A}_{m+1}$. Additionally, we require that $\mathbf{Q}'_{\leq m} \in \{\mathbf{Q}_{\leq m} | A_m\}$. As shown in Eq. 70, it is equivalent to

$$\begin{aligned} \mathbf{Q}'_{\leq m} &\in \mathcal{S}(\mathbf{P}_{\leq m}), \\ \langle \mathbf{Q}'_{\leq m}, \mathbf{S}_{\text{right}}^m \rangle \cap \tilde{\mathbf{P}}_{\leq m} &= \mathbf{Q}'_{\leq m}. \end{aligned} \quad (75)$$

Now we construct $\tilde{F}(A_m)$ to satisfy the above two requirements. Following the logic of Sec. II C 4, we essentially need to construct $\tilde{\mathcal{S}}_{\text{right}}^{m+1}(A_m)$, and $\tilde{F}(A_m)$ is then given in Eq. 38. The latter requirement $\mathbf{Q}'_{\leq m} \in \{\mathbf{Q}_{\leq m} | A_m\}$ is equivalent to say that, if Eq. 75 holds for m , it also holds for $m+1$. Given $\mathbf{Q}'_{\leq m} = \cup_{i=1}^m G(A_i) \in \mathcal{S}(\mathbf{P}_{\leq m})$, we want to construct $\mathbf{Q}'_{m+1} = \mathbf{S}_{\text{right}}^{m+1} \cap \tilde{\mathbf{P}}_{m+1}$ such that $\mathbf{Q}'_{\leq m+1} = \mathbf{Q}'_{\leq m} \cup \mathbf{Q}'_{m+1} \in \mathcal{S}(\mathbf{P}_{\leq m+1})$. We can derive it by replacing

all subscripts $> m$ to $m+1$ in Corollary 9 and the following derivations. With such replacements, we require \mathbf{Q}'_{m+1} to satisfy

$$\begin{aligned} -I &\notin \langle \mathbf{Q}'_{m+1} \rangle \\ \mathbf{Q}'_{m+1} \cap \tilde{\mathbf{P}}_{\text{invalid}}^m &= \emptyset \\ \langle \mathbf{S}_{\text{proj}}^m, \mathbf{Q}'_{m+1} \rangle \cap \tilde{\mathbf{P}}_{m+1} &= \mathbf{Q}'_{m+1} \end{aligned} \quad (76)$$

for the first three conditions, and

$$\langle \mathbf{Q}'_{\leq m}, \mathbf{Q}'_{m+1} \rangle \cap \tilde{\mathbf{P}}_{\leq m} = \mathbf{Q}'_{\leq m} \quad (77)$$

for the last condition. Similarly, given $\langle \mathbf{Q}'_{\leq m}, \mathbf{S}_{\text{right}}^m \rangle \cap \tilde{\mathbf{P}}_{\leq m} = \mathbf{Q}'_{\leq m}$, we require $\langle \mathbf{Q}'_{\leq m+1}, \mathbf{S}_{\text{right}}^{m+1} \rangle \cap \tilde{\mathbf{P}}_{\leq m+1} = \mathbf{Q}'_{\leq m+1}$, which can be decomposed to the $\tilde{\mathbf{P}}_{\leq m}$ part and $\tilde{\mathbf{P}}_{\leq m}$ part as:

$$\begin{aligned} \mathbf{Q}'_{m+1} &= \langle \mathbf{Q}'_{\leq m+1}, \mathbf{S}_{\text{right}}^{m+1} \rangle \cap \tilde{\mathbf{P}}_{m+1} \\ &= \langle \mathbb{P}_{\leq m+1}(\mathbf{Q}'_{\leq m+1}), \mathbf{S}_{\text{right}}^{m+1} \rangle \cap \tilde{\mathbf{P}}_{m+1} \\ &= \langle \mathbf{S}_{\text{proj}}^{m+1}(\mathbf{Q}'_{\leq m+1}), \mathbf{S}_{\text{right}}^{m+1} \rangle \cap \tilde{\mathbf{P}}_{m+1} \\ &= \langle \mathbf{S}_{\text{proj}}^{m+1}(\mathbf{S}_{\text{proj}}^m, \mathbf{Q}'_{m+1}), \mathbf{S}_{\text{right}}^{m+1} \rangle \cap \tilde{\mathbf{P}}_{m+1} \end{aligned} \quad (78)$$

where $\mathbf{S}_{\text{proj}}^{m+1}(\mathbf{S}_{\text{proj}}^m, \mathbf{Q}'_{m+1})$ is given in Eq. 64, and

$$\begin{aligned} \mathbf{Q}'_{\leq m} &= \langle \mathbf{Q}'_{\leq m+1}, \mathbf{S}_{\text{right}}^{m+1} \rangle \cap \tilde{\mathbf{P}}_{\leq m} \\ &= \langle \mathbf{Q}'_{\leq m}, \mathbf{S}_{\text{right}}^{m+1} \rangle \cap \tilde{\mathbf{P}}_{\leq m} \\ &= \langle \mathbf{Q}'_{\leq m}, \langle \mathbb{P}_{\leq m}(\mathbf{S}_{\text{right}}^{m+1}), \mathbf{Q}'_m \rangle \rangle \cap \tilde{\mathbf{P}}_{\leq m}, \end{aligned} \quad (79)$$

where in the second line we used $\mathbf{Q}'_{m+1} = \mathbf{S}_{\text{right}}^{m+1} \cap \tilde{\mathbf{P}}_{m+1} \subseteq \mathbf{S}_{\text{right}}^{m+1}$. By comparing with $\langle \mathbf{Q}'_{\leq m}, \mathbf{S}_{\text{right}}^m \rangle \cap \tilde{\mathbf{P}}_{\leq m} = \mathbf{Q}'_{\leq m}$, Eq. 79 is satisfied if

$$\langle \mathbb{P}_{\leq m}(\mathbf{S}_{\text{right}}^{m+1}), \mathbf{Q}'_m \rangle = \mathbf{S}_{\text{right}}^m. \quad (80)$$

Now we consider the former requirement $A_m = A_m(\mathbf{Q}')$, which is equivalent to $\mathbf{S}_{\text{proj}}^m = \mathbf{S}_{\text{proj}}^m(\mathbf{Q}'_{\leq m})$, $\tilde{\mathbf{P}}_{\text{invalid}}^m = \tilde{\mathbf{P}}_{\text{invalid}}^m(\mathbf{Q}'_{\leq m})$, and $\mathbf{S}_{\text{right}}^m = \mathbf{S}_{\text{right}}^m(\mathbf{Q}'_{\geq m} = \mathbf{Q}_{>m+1} \cup G(A_{m+1}))$ given $A_{m+1} = A_{m+1}(\mathbf{Q})$, where $\mathbf{Q}' = \mathbf{Q}_{>m+1} \cup \mathbf{Q}'_{\leq m}$, $\mathbf{Q}'_{\leq m} = \cup_{i=1}^m G(A_i)$. The first two are trivial since $\mathbf{S}_{\text{proj}}^m$ and $\tilde{\mathbf{P}}_{\text{invalid}}^m$ are recursively constructed by $\mathbf{S}_{\text{proj}}^{i+1} = \mathbf{S}_{\text{proj}}^{i+1}(\mathbf{S}_{\text{proj}}^i, \mathbf{Q}'_{i+1})$ and $\tilde{\mathbf{P}}_{\text{invalid}}^{i+1}(\tilde{\mathbf{P}}_{\text{invalid}}^i, \mathbf{Q}'_{i+1})$. Combined with Eq. 73 and Eq. 74, we can recursive derive $\mathbf{S}_{\text{proj}}^{i+1} = \mathbf{S}_{\text{proj}}^{i+1}(\mathbf{Q}'_{\leq i+1})$ from $\mathbf{S}_{\text{proj}}^i = \mathbf{S}_{\text{proj}}^{i+1}(\mathbf{Q}'_{\leq i})$, $\tilde{\mathbf{P}}_{\text{invalid}}^{i+1} = \tilde{\mathbf{P}}_{\text{invalid}}^{i+1}(\mathbf{Q}'_{\leq i+1})$ from $\tilde{\mathbf{P}}_{\text{invalid}}^i = \tilde{\mathbf{P}}_{\text{invalid}}^i(\mathbf{Q}'_{\leq i})$. We show that $\mathbf{S}_{\text{right}}^m = \mathbf{S}_{\text{right}}^m(\mathbf{Q}'_{\geq m} = \mathbf{Q}_{>m+1} \cup G(A_{m+1}))$ can be derived from Eq. 80 as

$$\begin{aligned} \mathbf{S}_{\text{right}}^m(\mathbf{Q}'_{\geq m}) &= \mathbb{P}_{\leq m}(\langle \mathbf{Q}'_{\geq m} \rangle) \\ &= \langle \mathbb{P}_{\leq m}(\langle \mathbf{Q}'_{\geq m+1} \rangle), \mathbf{Q}'_m \rangle \\ &= \langle \mathbb{P}_{\leq m}(\mathbb{P}_{\leq m+1}(\langle \mathbf{Q}'_{\geq m+1} \rangle)), \mathbf{Q}'_m \rangle \\ &= \langle \mathbb{P}_{\leq m}(\mathbf{S}_{\text{right}}^{m+1}(\mathbf{Q}'_{\geq m+1})), \mathbf{Q}'_m \rangle \\ &= \langle \mathbb{P}_{\leq m}(\mathbf{S}_{\text{right}}^{m+1}), \mathbf{Q}'_m \rangle \\ &= \mathbf{S}_{\text{right}}^m, \end{aligned} \quad (81)$$

where in the last line we used Eq. 80.

Until now, we have shown that $A_{m+1} \in \mathcal{A}_{m+1}$ implies $A_m \in \mathcal{A}_m$ if Eq. 76, Eq. 77, Eq. 78, and Eq. 80 are satisfied. We now simplify these conditions as follows. First we show that Eq. 77 can be derived from Eq. 80 and

$\langle \mathbf{Q}'_{\leq m}, \mathbf{S}_{\text{right}}^m \rangle \cap \tilde{\mathbf{P}}_{\leq m} = \mathbf{Q}'_{\leq m}$ by observing

$$\begin{aligned}
\mathbf{Q}'_{\leq m} &= \langle \mathbf{Q}'_{\leq m} \rangle \cap \tilde{\mathbf{P}}_{\leq m} \\
&\subseteq \langle \mathbf{Q}'_{\leq m}, \mathbf{Q}'_{m+1} \rangle \cap \tilde{\mathbf{P}}_{\leq m} \\
&\subseteq \langle \mathbf{Q}'_{\leq m}, \mathbf{S}_{\text{right}}^{m+1} \rangle \cap \tilde{\mathbf{P}}_{\leq m} \\
&= \langle \mathbf{Q}'_{\leq m}, \mathbb{P}_{\leq m}(\mathbf{S}_{\text{right}}^{m+1}) \rangle \cap \tilde{\mathbf{P}}_{\leq m} \\
&= \langle \mathbf{Q}'_{\leq m}, \mathbf{S}_{\text{right}}^m \rangle \cap \tilde{\mathbf{P}}_{\leq m} \\
&= \mathbf{Q}'_{\leq m},
\end{aligned} \tag{82}$$

which implies that all the \subseteq relations must be $=$. Similarly, the third line in Eq. 76 can be derived from Eq. 78 by observing

$$\begin{aligned}
\mathbf{Q}'_{m+1} &= \langle \mathbf{Q}'_{m+1} \rangle \cap \tilde{\mathbf{P}}_{m+1} \\
&\subseteq \langle \mathbf{S}_{\text{proj}}^m, \mathbf{Q}'_{m+1} \rangle \cap \tilde{\mathbf{P}}_{m+1} \\
&\subseteq \langle \mathbf{S}_{\text{proj}}^{m+1}, \mathbf{S}_{\text{right}}^{m+1} \rangle \cap \tilde{\mathbf{P}}_{m+1} \\
&= \mathbf{Q}'_{m+1}.
\end{aligned} \tag{83}$$

Thus it simplifies to the four conditions in Eq. 39, i.e.

$$\begin{aligned}
-I &\notin \langle \mathbf{Q}'_{m+1} \rangle, \\
\mathbf{Q}'_{m+1} \cap \tilde{\mathbf{P}}_{\text{invalid}}^m &= \emptyset, \\
\langle \mathbb{P}_{\leq m}(\mathbf{S}_{\text{right}}^{m+1}), \mathbf{Q}'_m \rangle &= \mathbf{S}_{\text{right}}^m, \\
\mathbf{S}_{\text{proj}}^{m+1} \cap \mathbf{S}_{\text{right}}^{m+1} &= \mathbf{Q}'_{m+1},
\end{aligned} \tag{84}$$

where $\mathbf{S}_{\text{proj}}^{m+1} = \mathbf{S}_{\text{proj}}^{m+1}(\mathbf{S}_{\text{proj}}^m, \mathbf{Q}'_{m+1} = \mathbf{S}_{\text{right}}^{m+1} \cap \tilde{\mathbf{P}}_{m+1})$ is a function of $\mathbf{S}_{\text{right}}^{m+1}$. This expression is the same with Eq. 39.

Besides, one can easily verify that Eq. 39 is satisfied for $A_m(\mathbf{Q})$ and $A_{m+1}(\mathbf{Q})$ if $\mathbf{Q} \in \mathcal{S}(\mathbf{P})$. This means that \tilde{F} defined by Eq. 38 and Eq. 41 has the same behavior with F in the valid region \mathcal{A}_m , which is the first requirement of Definition 8. Finally, we can conclude that such \tilde{F} is a relaxed transition function according to Definition 8.

E. Proof of Theorem 3

Proof. Following Sec. II C 4, and especially Eq. 75, for each (partial) path $\{A_{i=1}^m | A_{i+1} \in \tilde{F}(A_i)\}$, let $\mathbf{Q}_{\leq m} = \cup_{i \leq m} \mathbf{Q}_i = \cup_{i \leq m} \mathbf{S}_{\text{right}}^i \cap \tilde{\mathbf{P}}_i$, we always have $\mathbf{Q}_{\leq m} \in \mathcal{S}(\mathbf{P}_{\leq m})$, $\mathbf{S}_{\text{proj}}^m = \mathbf{S}_{\text{proj}}^m(\mathbf{Q}_{\leq m})$ and $\tilde{\mathbf{P}}_{\text{invalid}}^m = \tilde{\mathbf{P}}_{\text{invalid}}^m(\mathbf{Q}_{\leq m})$. In the following we give the upper bound of the number of pairs $(\mathbf{S}_{\text{proj}}^m, \tilde{\mathbf{P}}_{\text{invalid}}^m)$ and the number of $\mathbf{S}_{\text{right}}^m$, respectively.

First, we can prove that the pair $(\mathbf{S}_{\text{proj}}^m, \tilde{\mathbf{P}}_{\text{invalid}}^m)$ can be determined from

$$\mathbf{S}' = \mathbb{P}_{>m-2k+2}(\langle \mathbf{Q}_{\leq m} \rangle). \tag{85}$$

For $\mathbf{S}_{\text{proj}}^m$ we have

$$\mathbf{S}_{\text{proj}}^m = \mathbb{P}_{>m-k}(\langle \mathbf{Q}_{\leq m} \rangle) \tag{86}$$

$$= \mathbb{P}_{>m-k}(\mathbf{S}'). \tag{87}$$

For $\tilde{\mathbf{P}}_{\text{invalid}}^m$, since $P \in \tilde{\mathbf{P}}_{>m}$ has $q_P^{\text{begin}} > m - k + 1$, any $Q \in \mathbf{Q}_{<m}$ with $\{P, Q\} = 0$ must have $q_P^{\text{last}} > m - k + 1$ and thus $q_P^{\text{begin}} > m - 2k + 2$, so we have $Q \in \mathbf{S}'$. Thus

$$\tilde{\mathbf{P}}_{\text{invalid}}^m = \{P \in \tilde{\mathbf{P}}_{>m} | [P, \mathbf{Q}_{\leq m}] \neq 0\} \tag{88}$$

$$= \{P \in \tilde{\mathbf{P}}_{>m} | [P, \mathbf{S}'] \neq 0\}. \tag{89}$$

For simplify we use $\mathbf{S}_{\text{proj}}^m(\mathbf{S}')$ and $\tilde{\mathbf{P}}_{\text{invalid}}^m(\mathbf{S}')$ as the shorthands of the above two formulas.

Next, we have

$$\mathbf{S}' \in \{\langle \mathbf{Q} \rangle | \mathbf{Q} \in \mathcal{S}(\mathbb{T}_{>m-2k+2}(\tilde{\mathbf{P}}_{\leq m}))\} \quad (90)$$

Since any $P \in \mathbf{P}_{\leq m}$ with $\mathbb{T}_{>m-2k+2} \neq I$ must have $q_P^{\text{last}} > m - 2k + 2$, thus $\mathbb{T}_{>m-2k+2}(\tilde{\mathbf{P}}_{\leq m})$ has at most $(2k-2)M$ non-identity elements. Also \mathbf{S}' is a $2k-2$ qubit stabilizer group. According to Lemma 2, there are at most $(2(2k-2)M)^{2k-1}$ choices of \mathbf{S}' .

Finally, according to Eq. 41, we have

$$\mathbf{S}_{\text{right}}^m \in \mathcal{T}_{\text{right}}^m \equiv \{\langle \mathbf{Q} \rangle | \mathbf{Q} \in \mathcal{S}(\mathbb{T}_{\leq m}(\mathbf{P}_{\geq m}))\} \quad (91)$$

For the similar reason, there are at most kM non-identity elements in $\mathbb{T}_{\leq m}(\tilde{\mathbf{P}}_{\geq m})$. Thus there are at most $(2kM)^{k+1}$ choices of $\mathbf{S}_{\text{right}}^m$.

Combining the above results, we can construct

$$\tilde{\mathcal{A}}'_m = \{(\mathbf{S}_{\text{proj}}^m(\mathbf{S}'), \tilde{\mathbf{P}}_{\text{invalid}}^m(\mathbf{S}'), \mathbf{S}_{\text{right}}^m) | \mathbf{S}', \mathbf{S}_{\text{right}}^m \text{ satisfy Eq. 90 and Eq. 91}\}. \quad (92)$$

Clearly we have $\tilde{\mathcal{A}}'_m \supseteq \tilde{\mathcal{A}}_m$ and $|\tilde{\mathcal{A}}'_m| \leq (2(2k-2)M)^{2k-1} \cdot (2kM)^{k+1} < (4kM)^{3k}$. Also both $\mathbb{T}_{\leq m}(\tilde{\mathbf{P}}_{\geq m})$ and $\mathbb{T}_{>m-2k+2}(\tilde{\mathbf{P}}_{<m})$ can be determined by $\mathbb{T}_{m-2k+1,m}(\tilde{\mathbf{P}})$. Thus $\tilde{\mathcal{A}}'_m$ can be determined by $\mathbb{T}_{m-2k+1,m}(\tilde{\mathbf{P}})$. \square

F. Proof of Theorem 4

We prove that the stabilizer ground state per site of an infinite periodic local and sparse Hamiltonian with period l is given by:

$$E_{\text{gs}}^{\text{periodic}} = \min_{c, A, \{A_{m=0}^{cl} | A_{i+1} \in F(A_i), A_0 \simeq A_{cl} \simeq A\}} \frac{1}{cl} \sum_{m=1}^{cl} h_m(G(A_m)). \quad (93)$$

Strictly speaking, let H_n be the n -qubit Hamiltonian truncated from the infinite Hamiltonian (with arbitrary truncation strategy at edges), $E_{\text{gs}}^{\text{periodic}}$ above is defined by the minimum per-site stabilizer ground state of H_n in the limit of $n \rightarrow \infty$.

$$E_{\text{gs}}^{\text{periodic}} = \lim_{n \rightarrow \infty} \frac{1}{n} \min_{n\text{-qubit stabilizer state} |\psi\rangle} \langle \psi | H_n | \psi \rangle. \quad (94)$$

We first prove that, for any chain of state machine A_0, A_1, \dots, A_n such that $A_{m+1} \in F(A_m)$ for each m , if $n \geq N_{Al}$ we can always find c_1 and c_2 that $A_{c_1 l} \simeq A_{c_2 l}$, and $|c_1 - c_2| \leq N_A$, where N_A is defined in Theorem 3. According to Theorem 3, each possible A_m is taken from candidate values $\tilde{\mathcal{A}}'_m \supseteq \tilde{\mathcal{A}}_m$, and $\tilde{\mathcal{A}}'_m$ is periodic with period l , i.e. $\tilde{\mathcal{A}}'_m \simeq \tilde{\mathcal{A}}'_{m+l}$, since it is determined by local terms $\mathbb{T}_{m-2k+1,m}(\tilde{\mathbf{P}})$ in the Hamiltonian. Now we consider the equivalence set $\{A_{cl} | c \in \mathbb{Z}\}$. Since each $A_{cl} \in \tilde{\mathcal{A}}_{cl} \simeq \tilde{\mathcal{A}}_0$ for each c , and $\tilde{\mathcal{A}}_0$ has up to N_A values according to Theorem 3, we can find some $A_{c_1 l} \simeq A_{c_2 l}$ with $|c_1 - c_2| \leq N_A$.

If $E_{\text{gs}}^{\text{periodic}}$ is not the stabilizer ground state energy per site, then for sufficiently large n , the stabilizer ground state energy $E_{\text{min}}^{(n)}$ of $H_n = \sum_{P \in \mathbf{P}} w_P P$ can be lower than $n E_{\text{gs}}^{\text{periodic}}$ by arbitrary amount of energy E_C , i.e. $E_{\text{min}}^{(n)} \leq n E_{\text{gs}}^{\text{periodic}} - E_C$. Let the stabilizer group of the corresponding n -qubit stabilizer state be $\mathbf{S} = \langle \mathbf{Q}^* \rangle$, $\mathbf{Q}^* \in \mathcal{S}(\mathbf{P})$, and let $A_m = A_m(\mathbf{Q}^*)$ for each m . The expectation energy is given by $E = \sum_{m=1}^n h_m(G(A_m))$. If $n > N_{Al}$, we can find $0 \leq c_1 \leq c_2 \leq n$ such that $A_{c_1 l} \simeq A_{c_2 l} \simeq A$. Then we have $\Delta E = \sum_{m=c_1 l+1}^{c_2 l} h_m(G(A_m)) \geq (c_2 - c_1)l E_{\text{gs}}^{\text{periodic}}$ according to the definition of $E_{\text{gs}}^{\text{periodic}}$. Now we remove $\{A_{i=c_1 l+1}^{c_2 l}\}$ from the path $\{A_{m=1}^n\}$, and consider the new path $\{A'_i | 0 \leq i \leq n'\}$, such that $A'_i = A_i$ for $i \leq c_1 l$ and $A'_i \simeq A_{i+(c_2 - c_1)l}$ for $i > c_1 l$, where $n' = n - (c_2 - c_1)l$. Obviously, it still satisfies $A'_{m+1} \in F(A'_m)$ for each m , thus it maps to some n' -qubit stabilizer state with energy $E^{(n')} = E_{\text{min}}^{(n)} - \Delta E \leq E_{\text{min}}^{(n)} - (c_2 - c_1)\tilde{E}_{\text{min}} \leq n'\tilde{E}_{\text{min}} - E_C$. We can then continue the above deleting process and create $\{A''_i | 0 \leq i \leq n''\}$, $\{A'''_i | 0 \leq i \leq n'''\}$, ..., until we end up with some $n^* \leq N_{Al}$ and the corresponding path $\{A_i^* | 0 \leq i \leq n^*\}$. Such path can map to some n^* -qubit stabilizer state $|\psi^*\rangle$ with energy $\langle \psi^* | H_{n^*} | \psi^* \rangle = E^{(n^*)} \leq n^* \tilde{E}_{\text{min}} - E_C$. However $\langle \psi^* | H_{n^*} | \psi^* \rangle$ should have a finite lower bound in the order of $O(N_{Al})$, which is independent of n . Thus E_C cannot be arbitrarily large, which conflicts with the assumption. Thus we conclude that $E_{\text{gs}}^{\text{periodic}}$ is the stabilizer ground state energy per site.

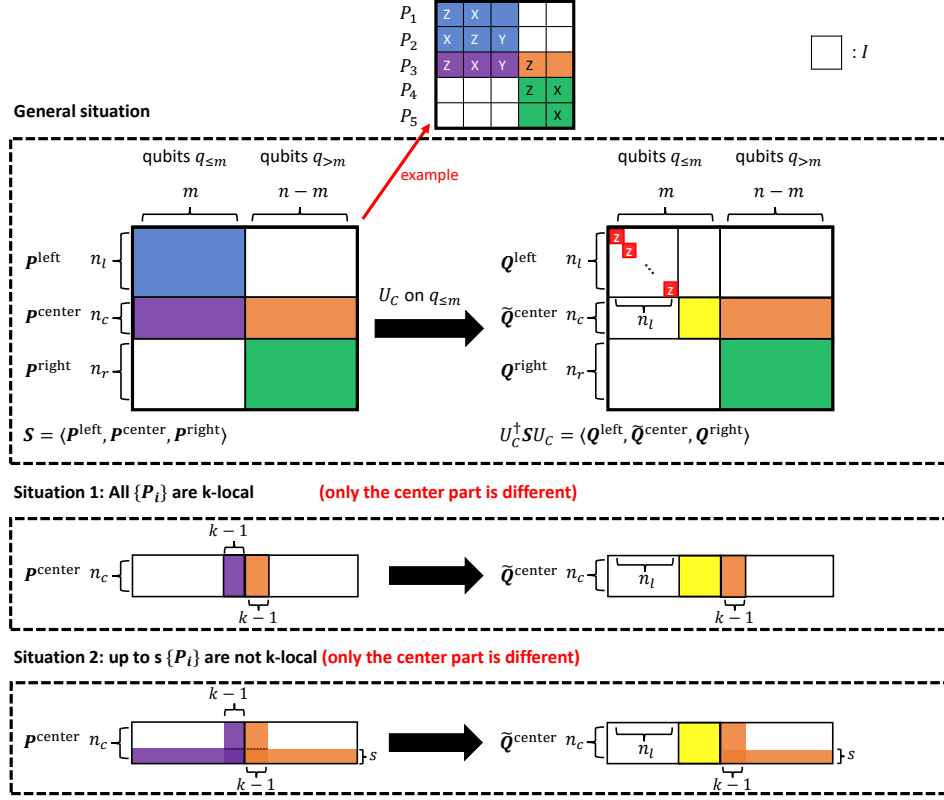


FIG. 10. Schematic diagram of a single iteration of the algorithm for Theorem 4. Blocks in the same color indicate the same values. Three situations are discussed, including (1) the general situation that all $\{P_i\}$ have no locality, (2) all $\{P_i\}$ are k -local, and (3) up to s elements in $\{P_i\}$ are not k -local. The performed operation is the same for these three situations (i.e. simply the same algorithm with different types of inputs) except the choice of m in these cases is different. For a given m , the qubits are divided into the left part $q_{\leq m}$ and the right part $q_{>m}$, and $\{P_i\}$ are divided to \mathbf{P}^{left} , $\mathbf{P}^{\text{center}}$, and $\mathbf{P}^{\text{right}}$ by the part that each P_i acts on. A Clifford U_C is applied on $q_{\leq m}$ to transform \mathbf{P}^{left} to $\{Z_1, Z_2, \dots, Z_{n_l}\}$. One can prove that the other generators of the stabilizer groups are effectively transformed to qubits $q_{>n_l}$, i.e. the generators become two decoupled parts. In the general situation that $\{P_i\}$ are non-local, we cannot guarantee that $n_l > 0$. If there are up to s elements in $\{P_i\}$ that are not k -local, then for any $m \geq 3k - 3$, one can guarantee that $n_l \geq m - 2k + 2 - s$. Thus we can let $m = 4(k + s)$, which gives $n_l \geq 2k + 3s + 2 \sim O(k + s)$. Thus with $O(n/(k + s))$ numbers of $O(k + s)$ -qubit Clifford transformations we transform $\langle \mathbf{P} \rangle$ to $\langle Z_1, \dots, Z_n \rangle$.

G. Proof of Theorem 5

Let q_I be a shorthand of qubits in the index set I with the same convention of $\tilde{\mathbf{P}}_I$ in Sec. II C 2. We first consider a general situation that $\mathbf{P} = \{P_i\}$ are nonlocal, and we introduce a procedure to transform the stabilizers S and the generators \mathbf{P} . (see Fig 10, general situation) Let m be some arbitrary integer, divide $\mathbf{P} = \{P_1, \dots, P_n\}$ to three parts $\mathbf{P}^{\text{left}} = \{P_1^{\text{left}}, \dots, P_{n_l}^{\text{left}}\}$, $\mathbf{P}^{\text{center}} = \{P_1^{\text{center}}, \dots, P_{n_c}^{\text{center}}\}$, and $\mathbf{P}^{\text{right}} = \{P_1^{\text{right}}, \dots, P_{n_r}^{\text{right}}\}$ such that, each P_i^{left} only acts on qubits $q_{\leq m}$ (the blue block), each P_i^{right} only acts on qubits $q_{>m}$ (the green block), and each P_i^{center} acts on both qubits $q_{\leq m}$ (the purple block) and $q_{>m}$ (the orange block), where n_l, n_c, n_r are number of elements in $\mathbf{P}^{\text{left}}, \mathbf{P}^{\text{center}}, \mathbf{P}^{\text{right}}$ respectively. For each P_i^{center} , we can uniquely decompose it to the left and right part, i.e. $P_i^{\text{center}} = P_{l,i}^{\text{center}} P_{r,i}^{\text{center}}$ (up to a choice of ± 1 sign), where $P_{l,i}^{\text{center}}$ (the purple block) only acts on $q_{\leq m}$, and $P_{r,i}^{\text{center}}$ (the orange block) only acts on qubits $q_{>m}$. Next, we construct a Clifford transformation U_C on $q_{\leq m}$ such that $U_C^\dagger P_i^{\text{left}} U_C = Z_i$ (small red blocks) for each P_i^{left} . The existence of such U_C comes from the fact that elements in \mathbf{P}^{left} commute with each other and are independent. Now we consider the elements in $U_C^\dagger \mathbf{P} U_C$, which are generators of the transformed stabilizer group $U_C^\dagger S U_C$. We keep the above conventions but use symbol Q to denote the transformed

Pauli operators, i.e. $\mathbf{Q} = U_C^\dagger \mathbf{P} U_C$, $\mathbf{Q}^\mu = U_C^\dagger \mathbf{P}^\mu U_C$ and $Q_i^\mu = U_C^\dagger P_i^\mu U_C$ for $\mu = \text{left, center, right}$. Thus we have $Q_i^{\text{left}} = Z_i$ according to the definition, and $Q_i^{\text{right}} = P_i^{\text{right}}$ since U_C acts on $q_{\leq m}$. For $Q_i^{\text{center}} = Q_{l,i}^{\text{center}} Q_{r,i}^{\text{center}}$, we have $Q_{r,i}^{\text{center}} = P_{r,i}^{\text{center}}$. We then focus on $Q_{l,i}^{\text{center}}$. Since elements of a stabilizer group commute with each other, we have

$$\begin{aligned} [Q_{l,i}^{\text{center}}, Z_j^{\text{left}}] &= [Q_{l,i}^{\text{center}}, Q_j^{\text{left}}] \\ &= [P_{l,i}^{\text{center}}, P_j^{\text{left}}] \\ &= [P_i^{\text{center}}, P_j^{\text{left}}] \\ &= 0 \end{aligned} \tag{95}$$

for each i, j , where the first line uses $Q_j^{\text{left}} = Z_j^{\text{left}}$, the second line uses the fact that Clifford transformation does not change commutation relation, the third line uses the fact that $P_{r,i}^{\text{center}}$ is on $q_{>m}$ so commutes with P_j^{left} , and the last line use the fact that generators of a stabilizer group commute. Thus we can write

$$Q_{l,i}^{\text{center}} = \left(\prod_{k=1}^{n_l} (Q_k^{\text{left}})^{s_k} \right) \tilde{Q}_{l,i}^{\text{center}} \tag{96}$$

such that $s_k \in \{0, 1\}$, and $\tilde{Q}_{l,i}^{\text{center}}$ (the yellow block) acts on qubits $q_{n_l+1, m}$ (i.e. between qubit $n_l + 1$ and m). Since $\langle P, PQ \rangle = \langle P, Q \rangle$, for the transformed stabilizer group $\langle \mathbf{Q} \rangle = \{Q^{\text{left}}, Q^{\text{center}}, Q^{\text{right}}\}$, we can now remove the $\prod_{k=1}^{n_l} (Q_k^{\text{left}})^{s_k}$ part in each $Q_i^{\text{center}} = \prod_{k=1}^{n_l} (Q_k^{\text{left}})^{s_k} \tilde{Q}_{l,i}^{\text{center}} Q_{r,i}$. Rigorously, let $\tilde{Q}_i^{\text{center}} = \tilde{Q}_{l,i}^{\text{center}} P_{r,i}^{\text{center}}$ and $\tilde{\mathbf{Q}}^{\text{center}} = \{\tilde{Q}_i^{\text{center}}\}$, we have $\langle \mathbf{Q} \rangle = \langle Q^{\text{left}}, \tilde{\mathbf{Q}}^{\text{center}}, Q^{\text{right}} \rangle$ as well, where elements in $\tilde{\mathbf{Q}}^{\text{center}}$ acts on $q_{>n_l}$ and elements in Q^{right} acts on $q_{>m}$. Thus the first n_l sites are decoupled from the other sites in the transformed stabilizer group $\langle \mathbf{Q} \rangle$, i.e. $\langle \mathbf{Q} \rangle = \langle Z_1, \dots, Z_{n_l} \rangle \otimes \langle \tilde{\mathbf{Q}}^{\text{center}}, Q^{\text{right}} \rangle$, where $\langle \tilde{\mathbf{Q}}^{\text{center}}, Q^{\text{right}} \rangle$ is on qubits $q_{>n_l}$. Therefore, we have successfully reduced the n -qubit problem to a $n - n_l$ qubit problem on $q_{>n_l}$. All we do until now is some Clifford operation on $q_{\leq m}$. Since $\tilde{Q}_{l,i}^{\text{center}}$ can be viewed as a truncation of $Q_{l,i}^{\text{center}}$ with the global sign kept, we write it as

$$\tilde{\mathbf{Q}}^{\text{center}} = \mathbb{T}_{>n_l}^*(U_C^\dagger \mathbf{P}^{\text{center}} U_C), \tag{97}$$

where \mathbb{T}_I^* indicates the truncation operation to qubits I with signs kept (similar to Definition 9).

For general stabilizer groups and generators, there is no guarantee that $n_l > 0$, so the above procedure may eventually do nothing. Now we consider the situation that P_1, \dots, P_n are all k -local (see Fig. 10, situation 1), and we hope to construct some $m \sim O(k)$, so that when we can iteratively execute the above procedure, we can reduce the problem size by some $n_l > 0$ in each iteration until $n = 0$. When we execute the above procedure for the first time, each P_i^{center} (the purple and orange block) is between qubit $m - k + 2$ to $m + k - 1$ (totally $2k - 2$) due to the k -local condition, so $n_c \leq 2k - 2$, where we used the fact that a n -qubit stabilizer group has up to n independent generators. For the same reason, we have $n_l \leq m$ and $n_r \leq n - m$. Since $n_c + n_l + n_r = n$, we should have $n_l = n - n_c - n_r \geq n - (2k - 2) - (n - m) = m - 2k + 2$. Thus we just need to let $m > 2k - 2$, so that we have $n_l > 0$ in the first iteration. When it comes to later iterations, the situation becomes slightly different. As explained above, the “right” part is unchanged (i.e. $Q^{\text{right}} = \mathbf{P}^{\text{right}}$), so each Q_i^{right} is still k -local. However, for each $\tilde{Q}_i^{\text{center}} = \tilde{Q}_{l,i}^{\text{center}} P_{r,i}^{\text{center}}$, $\tilde{Q}_{l,i}^{\text{center}}$ (the yellow block) is on $q_{n_l+1, m}$ and $P_{r,i}^{\text{center}}$ (the orange block) is on $q_{m+1, m+k-1}$, so we can only ensure that Q_i^{center} is on $q_{n_l+1, m+k-1}$. In the reduced $n - n_l$ qubit problem (i.e. the first n_l qubits are removed), it is between qubit 1 and $m + k - n_l - 1 \leq 3k - 3$, so it is $3k - 3$ local. Fortunately, in the above analysis to derive $n_l \geq m - 2k + 2$, we only require each $P \in \mathbf{P}^{\text{center}}$ to be k -local, but we don't require it for \mathbf{P}^{left} and $\mathbf{P}^{\text{right}}$. Therefore we want to additionally ensure that all $\tilde{Q}_i^{\text{center}}$ in the previous iteration enter into \mathbf{P}^{left} in the next iteration, so $\mathbf{P}^{\text{center}}$ in the next iteration are all taken from $\mathbf{Q}^{\text{right}} = \mathbf{P}^{\text{right}}$ in the previous iteration, which are k -local. Recall that \mathbf{P}^{left} are elements of \mathbf{P} on $q_{\leq m}$ only, so we just need to have $m \geq 3k - 3$. To summarize, with $m \geq 3k - 3$, we can iteratively apply a m -qubit Clifford transformation to reduce the problem size by $n_l \geq m - 2k + 2$. Thus we could, for example, let $m = 4k$, so each time we reduce the problem size by $O(k)$. Finally, with $O(n/k)$ number of $O(k)$ -qubit Clifford transformations, we can transform the original stabilizer group to $\langle Z_1, Z_2, \dots, Z_n \rangle$. Since $O(k)$ -qubit Clifford transformation can decompose to $O(k^2 / \log k)$ single-qubit and double-qubit Clifford transformations [39], the total number of single-qubit and double-qubit Clifford transformations we need is $O(n/k) \times O(k^2 / \log k) = O(nk / \log k)$.

Finally, we consider the situation that there are up to s elements in $\{P_1, \dots, P_n\}$ that are not k -local. (see Fig. 10, situation 2) In fact, we can use the same procedure with $m = 4(k + s)$ and no other modifications. To see the reason, in the first iteration, we have all these s elements classified into $\mathbf{P}^{\text{center}}$ (the wide purple and orange blocks at the bottom), so we have $n_c = |\mathbf{P}^{\text{center}}| \leq 2k - 2 + s$ ($2k - 2$ local elements and s non-local elements). After the

Clifford transformation, for those k -local P_i^{center} (the narrow purple block), the corresponding Q_i^{center} (the narrow orange block) are still $3k - 3$ local, and for those non-local P_i^{center} (the wide purple block), the corresponding Q_i^{center} (the wide orange block) are still generally nonlocal (can also accidentally be local). Thus in the next iteration, those local Q_i^{center} enter into \mathbf{P}^{left} (including the nonlocal ones that accidentally become local), and those non-local Q_i^{center} enter into $\mathbf{P}^{\text{center}}$. So we still have $n_c \leq 2k - 2 + s$ in the next iteration. Thus, with $m \geq 3k - 3$, we can iteratively apply m -qubit Clifford transformation to reduce the problem size by $n_l \geq m - n_c = m - 2k + 2 - s$. By choosing, for example, $m = 4(k + s)$, we achieve the same conclusion with $L \sim O(nk'/\log k')$, where $k' = k + s$. In fact, when $s = 0$, this algorithm reduces to the previous situation. A pseudo-code of this algorithm is shown in Algorithm 1.

Algorithm 1 Algorithm to find Clifford operations for Theorem 5

```

1:  $m = 4(k + s)$ 
2: Initiate an empty list of single-qubit and double-qubit Clifford operations  $\mathbf{U}$ 
3: while  $n = |\mathbf{P}| > 0$  do
4:   Classify each  $P \in \mathbf{P}$  to  $\mathbf{P}^{\text{left}}$ ,  $\mathbf{P}^{\text{right}}$ ,  $\mathbf{P}^{\text{center}}$  if  $P$  acts on only  $q_{\leq m}$ , only  $q_{>m}$ , or both parts, respectively
5:    $n_l = |\mathbf{P}^{\text{left}}|$ 
6:   Construct Clifford transformation  $U_C$  such that  $U_C^\dagger \mathbf{P}^{\text{left}} U_C = \{Z_1, \dots, Z_{n_l}\}$ 
7:   Decompose  $U_C$  to single-qubit and double-qubit Clifford operations  $U_C = U_1 U_2 \cdots U_N$  with the standard method [39]
8:   Append  $\{U_1, U_2, \dots, U_N\}$  (the order matters) to the end of  $\mathbf{U}$ 
9:    $\mathbf{P} \rightarrow \mathbb{T}_{>n_l}^*(U_C^\dagger \mathbf{P}^{\text{center}} U_C) \cup \mathbf{P}^{\text{right}}$ 
10: end while
11: Output  $\mathbf{U}$ 

```

- [1] A. Kitaev, A. H. Shen, and M. N. Vyalyi, *Classical and Quantum Computation*, 47 (American Mathematical Soc., Providence, 2002).
- [2] D. Aharonov and T. Naveh, Quantum NP - A Survey, arXiv:quant-ph/0210077 (2002), [arXiv:quant-ph/0210077](https://arxiv.org/abs/quant-ph/0210077).
- [3] J. Kempe, A. Kitaev, and O. Regev, The complexity of the local Hamiltonian problem, *SIAM J. Comput.* **35**, 1070 (2006).
- [4] N. Schuch and F. Verstraete, Computational complexity of interacting electrons and fundamental limitations of density functional theory, *Nat. Phys.* **5**, 732 (2009).
- [5] Y. Huang, Two-dimensional local Hamiltonian problem with area laws is QMA-complete, *J. Comput. Phys.* **443**, 110534 (2021).
- [6] S. Lee, J. Lee, H. Zhai, Y. Tong, A. M. Dalzell, A. Kumar, P. Helms, J. Gray, Z.-H. Cui, W. Liu, *et al.*, Evaluating the evidence for exponential quantum advantage in ground-state quantum chemistry, *Nat. Commun.* **14**, 1952 (2023).
- [7] R. Shankar, *Principles of quantum mechanics* (Springer Science & Business Media, 2012).
- [8] A. Kandala, A. Mezzacapo, K. Temme, M. Takita, M. Brink, J. M. Chow, and J. M. Gambetta, Hardware-efficient variational quantum eigensolver for small molecules and quantum magnets, *nature* **549**, 242 (2017).
- [9] M. Cerezo, K. Sharma, A. Arrasmith, and P. J. Coles, Variational quantum state eigensolver, *npj Quantum Information* **8**, 113 (2022).
- [10] J. Tilly, H. Chen, S. Cao, D. Picozzi, K. Setia, Y. Li, E. Grant, L. Wossnig, I. Rungger, G. H. Booth, *et al.*, The variational quantum eigensolver: a review of methods and best practices, *Physics Reports* **986**, 1 (2022).
- [11] F. Verstraete, V. Murg, and J. Cirac, Matrix product states, projected entangled pair states, and variational renormalization group methods for quantum spin systems, *Adv. Phys.* **57**, 143 (2008).
- [12] U. Schollwöck, The density-matrix renormalization group in the age of matrix product states, *Ann. Phys.* **326**, 96 (2011).
- [13] H.-J. Liao, J.-G. Liu, L. Wang, and T. Xiang, Differentiable programming tensor networks, *Phys. Rev. X* **9**, 31041 (2019).
- [14] G. Carleo and M. Troyer, Solving the quantum many-body problem with artificial neural networks, *Science* **355**, 602 (2017).
- [15] D.-L. Deng, X. Li, and S. Das Sarma, Quantum entanglement in neural network states, *Phys. Rev. X* **7**, 021021 (2017).
- [16] I. Glasser, N. Pancotti, M. August, I. D. Rodriguez, and J. I. Cirac, Neural-network quantum states, string-bond states, and chiral topological states, *Phys. Rev. X* **8**, 11006 (2018).
- [17] J. Chen, S. Cheng, H. Xie, L. Wang, and T. Xiang, Equivalence of restricted Boltzmann machines and tensor network states, *Phys. Rev. B* **97**, 085104 (2018).
- [18] S.-X. Zhang, Z.-Q. Wan, and H. Yao, Automatic differentiable Monte Carlo: Theory and application, *Phys. Rev. Res.* **5**, 033041 (2023).
- [19] X.-Q. Sun, T. Nebabu, X. Han, M. O. Flynn, and X.-L. Qi, Entanglement features of random neural network quantum states, *Phys. Rev. B* **106**, 115138 (2022).
- [20] J. Romero, R. Babbush, J. R. McClean, C. Hempel, P. J. Love, and A. Aspuru-Guzik, Strategies for quantum computing molecular energies using the unitary coupled cluster ansatz, *Quantum Science and Technology* **4**, 014008 (2018).

[21] J. Lee, W. J. Huggins, M. Head-Gordon, and K. B. Whaley, Generalized unitary coupled cluster wave functions for quantum computation, *Journal of chemical theory and computation* **15**, 311 (2018).

[22] A. Anand, P. Schleich, S. Alperin-Lea, P. W. Jensen, S. Sim, M. Díaz-Tinoco, J. S. Kottmann, M. Degroote, A. F. Izmaylov, and A. Aspuru-Guzik, A quantum computing view on unitary coupled cluster theory, *Chemical Society Reviews* **51**, 1659 (2022).

[23] P. M. Chaikin, T. C. Lubensky, and T. A. Witten, *Principles of condensed matter physics*, Vol. 10 (Cambridge university press Cambridge, 1995).

[24] L. P. Kadanoff, More is the same; phase transitions and mean field theories, *Journal of Statistical Physics* **137**, 777 (2009).

[25] J. W. Negele, The mean-field theory of nuclear structure and dynamics, *Reviews of Modern Physics* **54**, 913 (1982).

[26] P. Lykos and G. Pratt, Discussion on the hartree-fock approximation, *Reviews of Modern Physics* **35**, 496 (1963).

[27] I. N. Levine, D. H. Busch, and H. Shull, *Quantum chemistry*, Vol. 6 (Pearson Prentice Hall Upper Saddle River, NJ, 2009).

[28] A. Szabo and N. S. Ostlund, *Modern quantum chemistry: Introduction to advanced electronic structure theory* (Courier Corporation, 2012).

[29] C. Møller and M. S. Plesset, Note on an approximation treatment for many-electron systems, *Phys. Rev.* **46**, 618 (1934).

[30] I. Shavitt and R. J. Bartlett, *Many-body methods in chemistry and physics: MBPT and coupled-cluster theory* (Cambridge university press, 2009).

[31] R. J. Bartlett and M. Musiał, Coupled-cluster theory in quantum chemistry, *Rev. Mod. Phys.* **79**, 291 (2007).

[32] A. Kitaev, Anyons in an exactly solved model and beyond, *Annals of Physics* **321**, 2 (2006).

[33] X. Chen, Z.-C. Gu, Z.-X. Liu, and X.-G. Wen, Symmetry-protected topological orders in interacting bosonic systems, *Science* **338**, 1604 (2012).

[34] D. I. Lyakh, M. Musiał, V. F. Lotrich, and R. J. Bartlett, Multireference nature of chemistry: The coupled-cluster view, *Chemical reviews* **112**, 182 (2012).

[35] H. Lischka, D. Nachtigalova, A. J. Aquino, P. G. Szalay, F. Plasser, F. B. Machado, and M. Barbatti, Multireference approaches for excited states of molecules, *Chemical reviews* **118**, 7293 (2018).

[36] M. A. Nielsen and I. L. Chuang, Quantum computation and quantum information, *Phys. Today* **54**, 60 (2001).

[37] D. Gottesman, Theory of fault-tolerant quantum computation, *Phys. Rev. A* **57**, 127 (1998).

[38] D. Gottesman, The Heisenberg representation of quantum computers, arXiv preprint quant-ph/9807006 (1998).

[39] S. Aaronson and D. Gottesman, Improved simulation of stabilizer circuits, *Phys. Rev. A* **70**, 052328 (2004).

[40] E. T. Campbell, B. M. Terhal, and C. Vuillot, Roads towards fault-tolerant universal quantum computation, *Nature* **549**, 172 (2017).

[41] M. Howard and E. Campbell, Application of a resource theory for magic states to fault-tolerant quantum computing, *Physical review letters* **118**, 090501 (2017).

[42] C. Chamberland and A. W. Cross, Fault-tolerant magic state preparation with flag qubits, *Quantum* **3**, 143 (2019).

[43] B. Zeng, X. Chen, D.-L. Zhou, and X.-G. Wen, *Quantum Information Meets Quantum Matter*, Quantum Science and Technology (Springer New York, New York, NY, 2019).

[44] D. Perez-Garcia, F. Verstraete, M. M. Wolf, and J. I. Cirac, Matrix product state representations, arXiv preprint quant-ph/0608197 (2006).

[45] D. Fattal, T. S. Cubitt, Y. Yamamoto, S. Bravyi, and I. L. Chuang, Entanglement in the stabilizer formalism, arXiv preprint quant-ph/0406168 (2004).

[46] Z. Webb, The Clifford group forms a unitary 3-design, *Quantum Info. Comput.* **16**, 1379–1400 (2016).

[47] H. Y. Huang, R. Kueng, and J. Preskill, Predicting many properties of a quantum system from very few measurements, *Nat. Phys.* **16**, 1050 (2020).

[48] A. Nahum, J. Ruhman, S. Vijay, and J. Haah, Quantum entanglement growth under random unitary dynamics, *Phys. Rev. X* **7**, 031016 (2017).

[49] C. W. von Keyserlingk, T. Rakovszky, F. Pollmann, and S. L. Sondhi, Operator hydrodynamics, OTOCs, and entanglement growth in systems without conservation laws, *Phys. Rev. X* **8**, 021013 (2018).

[50] A. Nahum, S. Vijay, and J. Haah, Operator spreading in random unitary circuits, *Phys. Rev. X* **8**, 021014 (2018).

[51] D. Gottesman, Stabilizer codes and quantum error correction, arXiv preprint quant-ph/9705052 (1997).

[52] A. G. Fowler, M. Mariantoni, J. M. Martinis, and A. N. Cleland, Surface codes: Towards practical large-scale quantum computation, *Phys. Rev. A* **86**, 032324 (2012).

[53] C. Nayak, S. H. Simon, A. Stern, M. Freedman, and S. Das Sarma, Non-Abelian anyons and topological quantum computation, *Rev. Mod. Phys.* **80**, 1083 (2008).

[54] S. Bravyi, D. Browne, P. Calpin, E. Campbell, D. Gosset, and M. Howard, Simulation of quantum circuits by low-rank stabilizer decompositions, *Quantum* **3**, 181 (2019).

[55] S. Bravyi and D. Gosset, Improved classical simulation of quantum circuits dominated by Clifford gates, *Phys. Rev. Lett.* **116**, 250501 (2016).

[56] T. Begušić, K. Hejazi, and G. K. Chan, Simulating quantum circuit expectation values by clifford perturbation theory, arXiv preprint arXiv:2306.04797 (2023).

[57] M. Cheng, K. Khosla, C. Self, M. Lin, B. Li, A. Medina, and M. Kim, Clifford circuit initialisation for variational quantum algorithms, arXiv preprint arXiv:2207.01539 (2022).

[58] S. Zhang, Z.-Q. Wan, C.-Y. Hsieh, H. Yao, and S. Zhang, Variational quantum-neural hybrid error mitigation, *Adv. Quantum Technol.* **6** (2023).

[59] J. Sun, L. Cheng, and W. Li, Toward chemical accuracy with shallow quantum circuits: A Clifford-based Hamiltonian

engineering approach, *J. Chem. Theory Comput.* **20**, 695 (2024).

[60] R. V. Mishmash, T. P. Gujarati, M. Motta, H. Zhai, G. K.-L. Chan, and A. Mezzacapo, Hierarchical Clifford transformations to reduce entanglement in quantum chemistry wave functions, *J. Chem. Theory Comput.* (2023).

[61] P. Schleich, J. Boen, L. Cincio, A. Anand, J. S. Kottmann, S. Tretiak, P. A. Dub, and A. Aspuru-Guzik, Partitioning quantum chemistry simulations with clifford circuits, arXiv preprint arXiv:2303.01221 (2023).

[62] G. S. Ravi, P. Gokhale, Y. Ding, W. Kirby, K. Smith, J. M. Baker, P. J. Love, H. Hoffmann, K. R. Brown, and F. T. Chong, Cafqa: A classical simulation bootstrap for variational quantum algorithms, in *Proceedings of the 28th ACM International Conference on Architectural Support for Programming Languages and Operating Systems, Volume 1* (2022) pp. 15–29.

[63] B. Bhattacharyya and G. S. Ravi, Optimal Clifford initial states for Ising Hamiltonians, in *2023 IEEE International Conference on Rebooting Computing (ICRC)* (IEEE, 2023) pp. 1–10.

[64] K. Mitarai, Y. Suzuki, W. Mizukami, Y. O. Nakagawa, and K. Fujii, Quadratic clifford expansion for efficient benchmarking and initialization of variational quantum algorithms, *Physical Review Research* **4**, 033012 (2022).

[65] D. Gross, Hudson’s theorem for finite-dimensional quantum systems, *J. Math. Phys.* **47** (2006).

[66] F. Bloch, Über die quantenmechanik der elektronen in kristallgittern, *Zeitschrift für physik* **52**, 555 (1929).

[67] P. Kratzer and J. Neugebauer, The basics of electronic structure theory for periodic systems, *Front. Chem.* **7**, 106 (2019).

[68] R. M. Martin, *Electronic structure: basic theory and practical methods* (Cambridge university press, 2020).

[69] A. Y. Kitaev, Quantum measurements and the abelian stabilizer problem, arXiv preprint quant-ph/9511026 (1995).

[70] A. Y. Kitaev, A. Shen, and M. N. Vyalyi, *Classical and quantum computation*, 47 (American Mathematical Soc., 2002).

[71] J. Preskill, Quantum computing in the nisq era and beyond, *Quantum* **2**, 79 (2018).

[72] P. W. Shor, Fault-tolerant quantum computation, in *Proceedings of 37th conference on foundations of computer science* (IEEE, 1996) pp. 56–65.

[73] M. Cerezo, A. Sone, T. Volkoff, L. Cincio, and P. J. Coles, Cost function dependent barren plateaus in shallow parametrized quantum circuits, *Nat. Commun.* **12**, 1791 (2021).

[74] J. R. McClean, S. Boixo, V. N. Smelyanskiy, R. Babbush, and H. Neven, Barren plateaus in quantum neural network training landscapes, *Nat. Commun.* **9**, 4812 (2018).

[75] H.-K. Zhang, S. Liu, and S.-X. Zhang, Absence of barren plateaus in finite local-depth circuits with long-range entanglement, arXiv:2311.01393 (2023).

[76] S. Gharibian and J. Kempe, Approximation algorithms for qma-complete problems, *SIAM Journal on Computing* **41**, 1028 (2012).

[77] A. Anshu, D. Gosset, and K. Morenz, Beyond product state approximations for a quantum analogue of max cut, arXiv preprint arXiv:2003.14394 (2020).

[78] C. Schön, E. Solano, F. Verstraete, J. I. Cirac, and M. M. Wolf, Sequential generation of entangled multiqubit states, *Physical review letters* **95**, 110503 (2005).

[79] A. Barenco, C. H. Bennett, R. Cleve, D. P. DiVincenzo, N. Margolus, P. Shor, T. Sleator, J. A. Smolin, and H. Weinfurter, Elementary gates for quantum computation, *Physical review A* **52**, 3457 (1995).

[80] X. Qian, J. Huang, and M. Qin, Augmenting density matrix renormalization group with clifford circuits, arXiv preprint arXiv:2405.09217 (2024).

[81] B. M. Austin, D. Y. Zubarev, and W. A. Lester Jr, Quantum monte carlo and related approaches, *Chemical reviews* **112**, 263 (2012).

[82] G. Carleo and M. Troyer, Solving the quantum many-body problem with artificial neural networks, *Science* **355**, 602 (2017).

[83] N. J. Coble, M. Coudron, J. Nelson, and S. S. Nezhadi, Local hamiltonians with no low-energy stabilizer states, arXiv preprint arXiv:2302.14755 (2023).

[84] S. Masot-Llima and A. Garcia-Saez, Stabilizer tensor networks: universal quantum simulator on a basis of stabilizer states, arXiv preprint arXiv:2403.08724 (2024).

[85] A. Gu, S. F. Oliviero, and L. Leone, Doped stabilizer states in many-body physics and where to find them, arXiv preprint arXiv:2403.14912 (2024).

[86] R. Koenig and J. A. Smolin, How to efficiently select an arbitrary Clifford group element, *J. Math. Phys.* **55** (2014).

[87] R. Verresen, R. Moessner, and F. Pollmann, One-dimensional symmetry protected topological phases and their transitions, *Phys. Rev. B* **96**, 165124 (2017).

[88] F. Wu, Y. Deng, and N. Prokof’ev, Phase diagram of the toric code model in a parallel magnetic field, *Phys. Rev. B* **85**, 195104 (2012).

[89] Z.-X. Shang, M.-C. Chen, X. Yuan, C.-Y. Lu, and J.-W. Pan, Schrödinger-Heisenberg variational quantum algorithms, *Phys. Rev. Lett.* **131**, 060406 (2023).

[90] Y. Kim, A. Eddins, S. Anand, K. X. Wei, E. Van Den Berg, S. Rosenblatt, H. Nayfeh, Y. Wu, M. Zaletel, K. Temme, *et al.*, Evidence for the utility of quantum computing before fault tolerance, *Nature* **618**, 500 (2023).

[91] F. Arute, K. Arya, R. Babbush, D. Bacon, J. C. Bardin, R. Barends, R. Biswas, S. Boixo, F. G. Brandao, D. A. Buell, *et al.*, Quantum supremacy using a programmable superconducting processor, *Nature* **574**, 505 (2019).

[92] R. Wiersemä, C. Zhou, Y. de Sereville, J. F. Carrasquilla, Y. B. Kim, and H. Yuen, Exploring entanglement and optimization within the Hamiltonian variational ansatz, *PRX Quantum* **1**, 020319 (2020).

[93] S.-X. Zhang, J. Allcock, Z.-Q. Wan, S. Liu, J. Sun, H. Yu, X.-H. Yang, J. Qiu, Z. Ye, Y.-Q. Chen, C.-K. Lee, Y.-C. Zheng, S.-K. Jian, H. Yao, C.-Y. Hsieh, and S. Zhang, Tensorcircuit: A quantum software framework for the NISQ era,

Quantum **7**, 912 (2023).

[94] R. H. Byrd, P. Lu, J. Nocedal, and C. Zhu, A limited memory algorithm for bound constrained optimization, *SIAM J. Sci. Comput.* **16**, 1190 (1995).

[95] P. Virtanen, R. Gommers, T. E. Oliphant, M. Haberland, T. Reddy, D. Cournapeau, E. Burovski, P. Peterson, W. Weckesser, J. Bright, S. J. van der Walt, M. Brett, J. Wilson, K. J. Millman, N. Mayorov, A. R. J. Nelson, E. Jones, R. Kern, E. Larson, C. J. Carey, Í. Polat, Y. Feng, E. W. Moore, J. VanderPlas, D. Laxalde, J. Perktold, R. Cimrman, I. Henriksen, E. A. Quintero, C. R. Harris, A. M. Archibald, A. H. Ribeiro, F. Pedregosa, P. van Mulbregt, and SciPy 1.0 Contributors, SciPy 1.0: Fundamental algorithms for scientific computing in Python, *Nat. Methods* **17**, 261 (2020).

[96] F. Barahona, On the computational complexity of Ising spin glass models, *J. Phys. A Math. Gen.* **15**, 3241 (1982).

[97] S.-X. Zhang, Classification on the computational complexity of spin models, arXiv preprint arXiv:1911.04122 (2019).

[98] S.-X. Zhang, C.-Y. Hsieh, S. Zhang, and H. Yao, Differentiable quantum architecture search, *Quantum Sci. Technol.* **7**, 045023 (2022).

[99] A. Gu, H.-Y. Hu, D. Luo, T. L. Patti, N. C. Rubin, and S. F. Yelin, Zero and finite temperature quantum simulations powered by quantum magic, arXiv preprint arXiv:2308.11616 (2023).

[100] M. H. Muñoz-Arias, S. Kourtis, and A. Blais, Low-depth clifford circuits approximately solve maxcut, arXiv preprint arXiv:2310.15022 (2023).